MODULATION OF ISCHEMIA- REPERFUSION INJURY IN MAMMALIAN HIBERNATORS AND NON-HIBERNATORS: A COMPARATIVE STUDY

By

Saurav Bhowmick, M.S.

A Dissertation Submitted in Partial Fulfillment of the Requirements

For the Degree of

Doctor of Philosophy

in

Biochemistry and Neuroscience

University of Alaska Fairbanks

December 2017

APPROVED:

Kelly L Drew, Committee Chair

Thomas B Kuhn, Committee Member

Lawrence K Duffy, Committee Member

Scott R Oliver, Committee Member

Thomas K Green, Chair

Department of Chemistry and Biochemistry

Paul Layer, Dean

College of Natural Science and Mathematics

Michael Castellini, Dean of the Graduate School

Abstract

Events characterized by ischemia/reperfusion (I/R), such as stroke and cardiac arrest, are among the most frequent causes of debilitating neurological injury and death worldwide. During ischemia, the brain experiences oxygen and nutrition deprivation due to lack of blood flow, and tissue damage ensues. Arctic ground squirrel (AGS; *Urocitellus parryii*), a hibernating species has the innate ability to survive profound decreases in blood flow (ischemia) during torpor and return of blood flow (reperfusion) during intermittent euthermic periods without any neurological deficit. However, the mechanisms by which AGS tolerate the extreme fluctuations in blood flow remain unclear.

The main focus of this thesis is to investigate the modulation of I/R injury in mammalian hibernators and non-hibernators. The first study validates the microperfusion approach for studying *in vitro* I/R injury (oxygen glucose deprivation, OGD) modeled in acute hippocampal slices and investigates the complex interactions of glutamate-mediated excitotoxicity with acidosis-mediated acidotoxicity to understand the role of acid-sensing ion channels (ASIC1a) and pH in mediating cellular injury during OGD. Using an ischemic tolerant animal model, AGS, the second and third studies explore if hibernation season or state influences tolerance to I/R injury and tests hypotheses regarding mechanisms involving nitric oxide and superoxide radicals in mediating cellular damage during cerebral I/R.

Together, this dissertation demonstrates that when OGD is combined with acidosis as occurs *in vivo*, acidotoxicity mediated via ASIC1a occurs but low pH abolishes NMDAR mediated excitotoxicity. This dissertation also presents evidence that AGS tolerate OGD injury independent of hibernation season and state. At the tissue level, when tissue

temperature is normalized to 36°C despite ATP depletion, ionic derangement, tissue acidosis, and excitatory neurotransmitter efflux, AGS hippocampus resists OGD injury. Finally, the dissertation shows that AGS resist brain injury caused by $ONOO^-$ generated from NO or $O_2^{\bullet -}$ during OGD while rat brain tissue succumbs to this mechanism of injury.

Table of Contents

List of Figures

Page

List of Tables

List of Appendices

Acknowledgements

I would like to express my sincere gratitude to my advisor Dr. Kelly Drew for her mentoring, her scientific expertise, her support and her availability throughout my time at the University of Alaska Fairbanks (UAF). I would like to thank my current and past committee members Dr. Thomas Kuhn, Dr. Lawrence Duffy, Dr. Ryan Oliver, Dr. Barbara Taylor and Dr. Kristin O'Brien for spending their valuable time and for guiding me through their valuable suggestions. Their support and encouragement helped me a lot in my Ph.D. journey at UAF.

I sincerely thank current and past Drew lab members – Carla Frare, Sarah Rice, Bahareh Barati, Bernard Laughlin, Isaac Bailey Katrina Dowell, Jeanette Moore, Tulasi Jinka, and Lori Bogren for helping me in my research. They have always been supportive and fun to work with. I would also like to thank Jessica Armstrong, Katherine Love, International office: Reija Shnoro and Carol Holz and graduate school for all their support.

I would like to thank the funding sources that supported me through my graduate studies: Department of Chemistry for providing me teaching support, Alaska IDeA Network of Biomedical Research Excellence (INBRE) for providing me research and travel support, UAF Biomedical Learning and Student Training (BLaST) for travel support, UAF Institute of Arctic Biology (IAB) for research support.

I remain grateful to my parents, my brother and my wife for their endless love, support, and encouragement that I relied on throughout my tenure at the University of Alaska Fairbanks. I would certainly like to thank all my friends here at UAF especially Swarup Mitra, Malabika Maulik, Tushar Gupta, Vaibhav Srivastava, Neeraj Mahajan, Aditya Nikam, Bakul Mathur, Arya Narayan who has always been supportive and caring through

the tough and difficult times. Finally, I would like to thank my friend Nirmalya Saha who always inspired and motivated me throughout my Ph.D. journey.

CHAPTER 1: General introduction to ischemia/reperfusion injury and the mechanism of neuroprotection in mammalian hibernators

1.1 Overview

Neurological diseases of diverse etiologies such as stroke, traumatic brain injury and other neuropathies such as Alzheimer's disease have significant effects on the quality of life of patients. The limited self-repairing capacity of the brain is considered to be the origin of the irreversible and progressive nature of many neurological diseases. Therefore, neuroprotection is an important goal shared by many clinical neurologists and neuroscientists. Although pre-clinical findings to combat these etiologies have been promising, not much success has been achieved and requires the need for a novel approach. In the present project, tolerance to ischemia/reperfusion (I/R) injury is investigated in Arctic ground squirrels (AGS; *Urocitellus parryii*).

Here, in ***Chapter 1***, the cascade of events associated with I/R injury and the mechanism of neuroprotection in mammalian hibernators is reviewed. Also, I discuss the rationale for the use of acute hippocampal slices as a model to investigate neuroprotection and the microperfusion approach for studying neuroprotective mechanism in mammalian hibernators. Finally, the scope and aims of the project are described. ***Chapter 2*** addressed two research objectives. First, oxygen-glucose deprivation (OGD) injury via the microperfusion approach was induced in acute hippocampal slices from rats to validate if the *in vitro* microperfusion approach mimics I/R injury that occurs under *in vivo* conditions. Results demonstrate that OGD injury via the microperfusion approach causes disruption in energy homeostasis and excitatory neurotransmitter efflux similar to *in vivo* I/R injury. Second, Chapter 2 also tests the

hypothesis that low pH during OGD blocks NMDA-mediated excitotoxicity but produces acidotoxicity via ASIC1a and helps to resolves the controversy regarding the relative importance of acidotoxicity and NMDAR mediated excitotoxicity in I/R injury. Using the novel microperfusion technique, this study separates the effect of pH and oxygen glucose deprivation and for the first time provides time-resolved observations demonstrating that acidosis abolishes OGD-induced excitotoxicity, but induces acidotoxicity via ASIC1a channels. ***Chapter 3*** challenges the dogma that tolerance to cerebral I/R is conveyed by the hibernation state or season by demonstrating that AGS lack seasonal dependence of ischemic tolerance. This study shows that at the tissue level, hibernation season or the torpid state has no influence on oxygen-glucose deprivation (OGD)-induced cell death in Arctic ground squirrel (AGS). Moreover, AGS are highly tolerant to OGD compared to ischemic susceptible Sprague-Dawley rat despite the loss of ATP, excitatory amino acid release, and acidosis and persists during conditions that mimic acidosis and ischemic shift characteristics of cerebral I/R injury *in vivo*. In ***Chapter 4***, I demonstrate that $ONOO^-$ injures rat hippocampal slices during modeled ischemia and requires both nitric oxide (NO) and superoxide ($O_2^{\bullet -}$); neither species is injurious alone. Rats are prone to this mechanism of injury whereas in AGS this mechanism of injury is absent which explains the profound tolerance AGS have for cerebral I/R. Taken together the findings from this project indicate that elucidation of the neuroprotective mechanisms in mammalian hibernators is promising in the quest for therapeutics for disorders characterized by I/R injury.

1.2 Study of protective mechanisms pertinent to stroke is well warranted

According to the American Heart Association, stroke is the fifth leading cause of death worldwide and has devastating clinical outcomes. Each year, over 800,000 Americans suffer a stroke, causing significant adult disability, with an estimated annual expenditure of $ 36.5 billion. Very few treatment options are available (Go *et al.* 2014). A stroke occurs when the blood to the brain is interrupted or reduced. This causes oxygen and glucose deprivation leading to brain cell death. A stroke may be caused due to ischemia (by a blocked artery) or hemorrhagic stroke (leaking or bursting of a blood vessel). Some individuals may experience only a temporary disruption of blood flow to their brain (transient ischemic attack, or TIA). Ischemic stroke is the most common accounting for 87% of total strokes. Other strokes are intracerebral hemorrhage (9%) and subarachnoid hemorrhage (4%). Ischemic stroke is caused most often by emboli to the middle cerebral artery (MCA) (Soler & Ruiz 2010).

Over the past few decades, our understanding of the pathophysiology of stroke has increased, but greater understanding is required to advance the field of stroke recovery. Tissue plasminogen activator (tPA) is the only drug currently available for ischemic stroke. However, tPA is advised only if administered to patients within 4.5 h after the onset of the stroke, thus benefits only 4% of patients (Del Zoppo *et al.* 2009). (Davis & Donnan 2009)

1.3 Pathogenesis of ischemia-reperfusion injury

Cerebral ischemia causes significant failures in cerebral blood flow. Circulatory failure due to cardiac arrest leads to global cerebral ischemia, while occlusion of a major brain artery triggers focal ischemia. Continued circulatory deficits induce irreversible

changes in the brain tissue perpetrating neuronal damage. I/R injury initiates a cascade of events and ensues cell death through a number of mechanisms including both necrosis, a hallmark of cellular swelling, and apoptosis involving complex signaling mechanisms that leads to cellular death (Hotchkiss *et al.* 2009)

1.3.1 Loss of ion homeostasis and energy status

The most upstream consequences of cerebral ischemia are a disruption in energy and ion homeostasis. The central nervous system (CNS) is extremely susceptible even to small changes in metabolism or availability of substrate. Due to reduced cerebral blood flow during ischemia, ATP consumption continues despite insufficient ATP synthesis (Santos *et al.* 1996). Depletion of ATP affects the normal functioning of the ATP-dependent ion pump, Na^+-K^+-ATPase that is responsible for maintaining ion homeostasis. The Na-K ATPase pump is an electrogenic transmembrane enzyme located in the plasma membrane that catalyzes the active transport of Na^+ ions out and K^+ ions into the cells (Skou 1988). Na^+-K^+-ATPase plays a critical role in maintaining resting membrane potential of neurons, cell volume and transmembrane fluxes of Ca^{2+} and extracellular levels of excitatory neurotransmitters (Albers & Siegel 2012). Failure of the Na^+-K^+-ATPase pump depletes intracellular K^+, accumulation of intracellular free Ca^{2+} by activation of voltage-gated Ca^{2+} channels, and reversal of the Na^+ / Ca^{2+}exchanger (DiPolo & Beauge 1991), and an increase in extracellular levels of glutamate.

1.3.2 Glutamate-mediated excitotoxicity

Excessive release of an excitatory neurotransmitter such as glutamate is thought to play a key role in the excitotoxic neuronal death (Benveniste *et al.* 1984). Under ischemic conditions, an excessive amount of glutamate is released reaching to near-

millimolar concentrations in the extracellular space (Featherstone 2010). This causes overstimulation of N-methyl-d-aspartate (NMDA), alpha-amino-3-hydroxy-5-methyl-4-isoxazolepropionic acid (AMPA), and kainate-type glutamate receptors. The heteromeric NMDA receptor–gated ion channels are highly permeable to Ca^{2+} as well as Na^{+} and K^{+}. This results in a high influx of intracellular Ca^{2+} overload. Previous studies demonstrated that exposure to NMDA for 3-5 min is sufficient to trigger neuronal death (Lee *et al.* 2000) whereas selective blockade of NMDA receptor ameliorate cell death in both in-vitro and *in vivo* models (Albers *et al.* 1989, Choi 1992, Choi 1988) indicating that glutamate-gated NMDAR plays an important role in causing excitotoxicity associated with I/R injury. Although effective in reducing ischemic damage of brain tissue in animal models, glutamate receptor antagonists have not been effective in clinical trials of stroke (Ikonomidou & Turski 2002). In addition to glutamate mediated excitatoxicity, drop in pH, an early events of I/R injury may play a role in cell death. Other targets that are activated due to drop in pH such as acid sensing ion channels (ASICs) has spurred new avenues for stroke therapy from the lesson learned from failures of glutamate receptor antagonists in clinical trails of stroke.

1.3.3 Low pH-mediated acidotoxicity

During ischemia, anaerobic metabolism prevails due to O_2 deprivation. This results in accumulation of lactic acid as a by-product of glycolysis and leading to acidosis. Extracellular and intracellular acidosis occurs following ischemia and has been considered as a primary cause of cell death (Siesjo 1988). Recent studies have shown that increased load of proton due to acidosis (Rehncrona *et al.* 1981, Kalimo *et al.* 1981) activates a distinct family of ligand-gated channels, the acid-sensing ion channels

(ASICs,ENaC/Deg superfamily) (Waldmann *et al.* 1997, Baron *et al.* 2002, Alvarez de la Rosa *et al.* 2003). ASICs are expressed throughout the central and peripheral nervous system (Kweon & Suh 2013). Previous studies demonstrated that activation of ASIC1a increased intracellular Ca^{2+}concentration in hippocampal, cortical, and dorsal root ganglion (DRG) neurons (Yermolaieva *et al.* 2004, Xiong *et al.* 2004) and led to neuronal injury during brain ischemia accompanied by prolonged acidosis (Xiong et al. 2004, Pignataro *et al.* 2007). This points towards targeting ASIC1a as a neuroprotective target for brain ischemia (Yermolaieva et al. 2004, Xiong *et al.* 2008).

1.3.4 Calcium dysregulation

The cytoplasmic concentration of free Ca^{2+} of the resting neuron is extremely low (approximately 100nm) whereas the extracellular concentration is about 1-2 mM. The intraneuronal levels of Ca^{2+} are maintained through (a) the entry of extracellular concentration of ligand -operated receptor or voltage-gated ion channels, (b) the release of Ca^{2+} from endoplasmic reticulum or from the mitochondria through Na^{+}-Ca^{2+} exchanger, (c) the extrusion of Ca^{2+} through Ca^{2+}-ATPase or Na^{+}-Ca^{2+} exchanger in the plasma membrane, (d) the binding of Ca^{2+} to target protein, and (e) Ca^{2+} sequestration into the endoplasmic reticulum through Ca^{2+}-ATPase or mitochondria through uniport mechanism (Gill *et al.* 1989, Carafoli 1991, Gunter & Pfeiffer 1990). During ischemic insult, Ca^{2+} ion reaches critical levels leading to cell death (White *et al.* 1984). The influx of Ca^{2+} through NMDA receptors appears to underlie a major portion of Ca^{2+} overload. Other ion pumps and channels that cause high intracellular Ca^{2+} influx includes acid sensing ion channels (Xiong et al. 2004), the Na^{+}/Ca^{2+} exchanger (Bano *et al.* 2007), TRP channels (Aarts & Tymianski 2005) and hemichannels (Contreras *et al.* 2004). Excess of

Ca^{2+} ion concentrations activate proteases, lipases, phosphatases, and endonucleases. Their over-activation may result in the damage of cell structures and further oxidative stress. Ca^{2+} overload can trigger several downstream lethal reactions, including nitrosative and oxidative stress, lipid peroxidation, and mitochondrial dysfunction culminating in cell death (Orrenius *et al.* 2003). The rapid rise in intracellular Ca^{2+} following ischemia can also lead to both apoptotic and necrotic cell death (Simon *et al.* 1984, Xiong et al. 2004). Therefore, targeting Ca^{2+} influx-efflux mechanisms may be a valuable approach to counteract Ca^{2+} dysregulation associated with I/R injury.

1.3.5 Free radical production during ischemia and reperfusion

Oxidative and nitrosative stress are also potent mediators of ischemic injury. Under the normal physiological condition, the redox environment of cells modulates signal transduction cascades that balance between pro-death and pro-survival pathways (Crack & Taylor 2005). However, during I/R injury, ROS and RNS, such as hydroxyl radical, superoxide, and peroxynitrite, are highly reactive and damaging to multiple cellular components, leading to cell death. In the brain, NO is formed by the NO synthase (NOS) isoforms, a family of enzymes (Guix *et al.* 2005, Calabrese *et al.* 2007). Under physiological conditions, NO contributes to autoregulation of cerebral blood flow (CBF) (Toda *et al.* 2009). However, during ischemia, cerebral NO rapidly increases to 2–4 μM, producing damaging levels of NO (Murphy 1999, Kader *et al.* 1993). Concomitantly, a burst of free radicals such as $O_2^{\bullet-}$ (Cuzzocrea *et al.* 2001, El Kossi & Zakhary 2000, Tang *et al.* 2012, Suh *et al.* 2008) is produced after the ischemic event. This scenario is deleterious because $O_2^{\bullet-}$ anion has a high affinity for NO, higher than for the superoxide dismutase (Huie & Padmaja 1993, Cudd & Fridovich 1982). NO and $O_2^{\bullet-}$ react with each

other in an equimolar stoichiometric ratio forming a potent oxidant, $ONOO^-$ further contributing to injury (Beckman *et al.* 1990, Reiter *et al.* 2000, Zielonka *et al.* 2010).

Accumulating evidence demonstrates that excitotoxicity, acidotoxicity and oxidative stress contribute to hypoxic-ischemic cell death through mutually independent pathways. To date, glutamate antagonists, antioxidants, or ASICs blocker have been examined to treat hypoxic-ischemic brain injury. However, the therapeutic effectiveness of neuroprotective drugs against excitotoxicity, acidotoxicity or oxidative stress are not designed to counter deleterious effects on the other cell death pathways that also participate in the process of hypoxic-ischemic neuronal death. A better understanding of how these pathways impact I/R injury and how they interact during I/R injury is highly warranted for maximal neuroprotection against hypoxic-ischemic injury. Investigations of mammalian hibernators may yield insight into mechanisms that protect against I/R. These mechanisms may then translate to non-hibernators for the development of effective stroke therapies.

1.4 Hibernation and neuroprotection

1.4.1 Hibernation physiology

Mammalian hibernators display an amazing phenotypic switch that involves profound changes in physiology, morphology, and behavior during unfavorable environmental conditions. This unique phenotype is thought to have evolved in response to food shortage and utilize a host of protective mechanisms to survive harsh environmental conditions in which hibernating species live (Wang *et al.* 1988). Various mammalian species, including one species of primate (Dausmann *et al.* 2004), rodents, bats, carnivores, and marsupials (Carey *et al.* 2003) hibernate with similar characteristics.

Arctic ground squirrel (AGS), a species native to the northern slope of the Brooks Range and other regions in Alaska, hibernate for approximately 7-8 months each year (Barnes 1989). During hibernation, AGS and other species of ground squirrel enter a highly regulated and reversible state of prolonged torpor. The period of torpor is characterized by a profound decrease in respiratory rate, heart rate, blood flow, cerebral perfusion, and body temperature (Tb). During torpor, body temperature (Tb) falls to within a few degrees of the ambient temperature (Carey et al. 2003). During torpor, body temperature (Tb) typically ranges from 2 to 10°C for most temperate-zone hibernators; however, in AGS, body temperature can drop to as low as −2.9°C (Barnes 1989) and metabolism can be reduced to 1–2% of resting metabolic rate. Torpor bouts are interrupted by arousal periods in which the AGS enters the state of interbout euthermy (Barnes 1989). During an arousal in AGS, physiological changes that took place during torpor return to normothermic values for approximately 24h periods (Daan *et al.* 1991). Species that hibernate differ in hypothermic basal temperature while in torpor or in the duration of torpor bouts, but when T_b falls below 30°C all have in common the need to undergo periodic arousals between bouts and experience prolonged torpor throughout their hibernation season (Carey et al. 2003, Dausmann et al. 2004).

1.4.2 Hibernating animals as a model to study neuroprotective mechanisms

Hibernating species are a natural model of tolerance to insults, such as ischemia, that would be injurious to non-hibernating species. Tolerance to hypoxia in hibernating species was first documented in the early 1800's (Biorck *et al.* 1956). Although hibernating animals experience prolonged ischemic-like low levels in blood flow during torpor and the reperfusion-like return of blood flow during arousal, no neuronal damage

ensues (Ma *et al.* 2005, Frerichs *et al.* 1994). As early as the 1960's, the mechanisms of hypoxia tolerance in hibernating species were proposed to be attributable to factors other than cold temperature (Bullard & Funkhouser 1962) that includes hypo-metabolism, differential modulation of NMDAR, immunosuppression, anticoagulant properties of the blood and antioxidant defenses (Zhou *et al.* 2001, Drew *et al.* 2001).

Tolerance to traumatic brain injury has been demonstrated in hibernating AGS *in vivo* (Zhou et al. 2001). Previous *in vitro* studies in Thirteen-lined ground squirrel explained that hibernation season (Kurtz *et al.* 2006, Lindell *et al.* 2005) or lowering temperature (Frerichs & Hallenbeck 1998) in brain slices from active animals contributes towards tolerance to I/R injury. Later, *in vivo* studies demonstrated that tolerance is not just attributed to hibernation season or hypothermia, since, AGS and other species of ground squirrel tolerate hypoxia (D'Alecy *et al.* 1990) and ischemic-like conditions even when they are not hibernating (Dave *et al.* 2009, Dave *et al.* 2006). This indicates that resistance to I/R injury in hibernators is not just attributed to hibernating season or hypothermia but could also be due to tissue and circulating factors that persist in summer active hibernators. Investigation of the mechanisms in hibernating species that provide this protection from insults is a promising approach for the quest for effective therapeutics for stroke.

1.4.3 Other anoxia and hypoxia-tolerant model systems

1.4.3.1 Naked mole rat

Naked mole rat (*Heterocephalus glaber*) is a cold-blooded (Buffenstein & Yahav 1991) fossorial animal that experiences chronic environmental hypoxia (low oxygen environment) without any damage (Larson & Park 2009). Naked mole rats have

specialized circulatory (High-O_2-affinity hemoglobin) (Johansen *et al.* 1976) and metabolic functions (low resting metabolism) (Buffenstein & Yahav 1991) that helps them to cope with chronic hypoxic conditions. In addition to chronic environmental hypoxia, naked mole-rats also experience acute hypoxia during certain behaviors such as foraging and tunnel excavation. Previous studies demonstrated that hippocampal slices from adult naked mole-rats manifest extreme tolerance to hypoxia in at least three ways, compared to other mammalian species: maintainance of synaptic transmission under more hypoxic conditions; anoxic depolarization time is delayed after total oxygen deprivation, and slices recover electrophysiological responsiveness after much longer periods of anoxia (Larson & Park 2009).

Arrested brain development has been suggested as a mechanism for naked mole rat adaptation of tolerance to hypoxic insult. This predominant mechanism was proposed based on high expression level of NMDA receptor GluN2D subunit in adult naked mole-rat (Peterson *et al.* 2012). GluN2D has previously been shown to play a role in hypoxia tolerance in neonatal rat brain (Bickler *et al.* 2003). Therefore, high expression of GluN2D subunit in naked mole-rat brain suggests retention of a neonatal feature into adulthood. Recent studies have shown that naked mole rat survive anoxia by switching to anaerobic metabolism fueled by fructose (Park *et al.* 2017).

1.4.3.2 Turtle

Several species of turtle tolerate hypoxia and have been studied in great detail. Fresh water turtle (*Trachemys scripta*) is one of the most robust hypoxia-tolerant vertebrates that can withstand a complete anoxic state for days at room temperature to weeks during winter at colder temperatures (Jackson & Ultsch 2010). Another species,

Western painted turtle (*Chrysemys picta bellii*) can survive anoxia for 5 months at 1-3°C during winter (Bickler *et al.* 2002).

One mechanism of this profound tolerance to anoxia in turtle is accomplished by entering into a state of deep reversible hypo-metabolism. The state of hypo-metabolism, a type of hibernation that like mammalian hibernation causes less demand for ATP (70-80%), helps the turtles to survive on the ATP generated through anaerobic metabolism (Hochachka & Lutz 2001). Hypo-metabolism leads to suppression of energy demanding processes that includes a decrease in excitatory neurotransmitter release (Milton & Lutz 1998, Milton *et al.* 2002, Thompson *et al.* 2007), increased neural inhibition (Nilsson & Lutz 1991) channel arrest (reduced ion permeability) and the suppression of action potentials (spike arrest) (Fernandes *et al.* 1997).

Neurotransmitters such as γ-aminobutyric acid (GABA) and adenosine also modulate anoxia tolerance in turtles by decreasing ionic current gated by glutamatergic receptors (Pamenter *et al.* 2012). Adenosine has also shown to affect channel arrest (Pek & Lutz 1997, Perez-Pinzon *et al.* 1993), dopamine release (Milton & Lutz 2005, Milton et al. 2002), NMDAR currents (Buck & Bickler 1998) and cerebral blood flow (Hylland *et al.* 1994) providing further tolerance to anoxia in turtle. In addition, NMDA receptor activity is reduced by 50-60% in the first few minutes of anoxia by dephosphorylating the receptor, which prevents excess calcium influx that can lead to cellular injury. The suppression of NMDA receptor activity is mediated by phosphatase 1 or 2A, adenosine (Bickler et al. 2002, Buck & Bickler 1998) and δ-opioid receptors (Pamenter & Buck 2008) which are expressed in high density in the turtle brain (Xia & Haddad 2001). A variety of other protective mechanisms are also activated at the

molecular level in anoxic turtle brain and other organs that includes increased levels of heat shock proteins (Krivoruchko & Storey 2010, Prentice *et al.* 2004, Stecyk *et al.* 2012, Kesaraju *et al.* 2009), anti-apoptotic factors, activation of MAP kinases, increased expression of antioxidants and modulation of the p53 pathway (Milton *et al.* 2008, Rider *et al.* 2009, Kesaraju et al. 2009, Nayak *et al.* 2011). These factors not only play a role in providing protection during anoxic insult but also ameliorate oxidative stress during reperfusion (reoxygenation).

1.4.3.3 Diving mammals

Diving mammals such as whales and seals are capable of going on long dives and remaining submerged for up to 2 hours (Hindell *et al.* 1991, Watkins *et al.* 1985). Diving mammals rely on a high concentration of hemoglobin in blood and myoglobin in muscle as an endogenous store of O_2 as a way to cope with hypoxia (Lenfant *et al.* 1970, Burns *et al.* 2007). In diving mammals, during simulated diving, the arterial blood O_2 tension drops to 7–10 mmHg (Elsner *et al.* 1970, Kerem & Elsner 1973) which is well below the critical arterial O_2 tension of 25–40 mmHg, at which impairment has been reported from limitations in ATP (Erecinska & Silver 2001). Brains of diving mammals cope with repeated and extreme hypoxemia during diving. This cerebral tolerance to hypoxia reflects intrinsic properties of the neurons. Both adult hooded seal and mice show similar neuronal membrane potentials of around -60 to -70 mV. However, during ten minutes of hypoxia, mice neurons depolarize at around 65 mV whereas seal neurons depolarize around 13 mV (Folkow *et al.* 2008). This lower threshold for depolarization is an intrinsic property of the seal neurons that contributes to hypoxia tolerance.

Deep diving-hooded seals (*Cystophora cristata*) also exhibit cellular differences in neurons that contributes to their hypoxia tolerance. Previous studies have revealed that neuroglobin (Ngb) facilitates O_2 diffusion to maintain aerobic metabolism (Burmester & Hankeln 2009) and might also play a role in ROS detoxification during and after deep diving (Zenteno-Savin *et al.* 2002). Interestingly, levels of brain Ngb in deep diving seals does not differ from those of rats and mice (Mitz *et al.* 2009). However, in contrast to other terrestrial mammals, seals have an unusual distribution of Ngb with higher levels in astrocytes than in neurons (Mitz *et al.* 2009). Ngb in close association with mitochondria supports O_2 supply and oxidative metabolism (Burmester & Hankeln 2009, Mitz *et al.* 2009). The presence of high levels of Ngb and Cytochrome C (a component of the respiratory chain in the mitochondria) in astrocytes of hooded seals brain (Mitz *et al.* 2009) suggest that there are fundamental differences in the localization of aerobic and anaerobic metabolism between hooded seals and non-diving rodents wherein hooded seals might have a reversed lactate shuttle system compared with non-diving mammals (Mitz *et al.* 2009, Schneuer *et al.* 2012). In contrast to hooded seals, whales have a different Ngb distribution with higher levels in neurons than astrocytes suggesting the possible role of Ngb in facilitating diffusion and storage of O_2 within whale neurons (Schneuer et al. 2012).

1.5 An *in vitro* microperfusion approach to investigate neuroprotection in acute hippocampal slices from AGS

1.5.1 Rationale for use of acute hippocampal slices as a model to investigate neuroprotection

To elucidate the mechanisms associated with AGS tolerance to I/R injury, it is relevant to study a region of the brain that is vulnerable to I/R injury in non-hibernating mammals. For these studies, an *in vitro* approach is appropriate since the state of the animal cannot be maintained while manipulating body temperature *in vivo*. In addition, an *in vitro* approach allows for investigation of intrinsic tissue factors that correspond to tolerance in hibernating animals wherein factors such as cold temperature and circulating factors can be eliminated. In humans, the hippocampus can be affected by various insults such as ischemia, inflammation, hypoglycemia, or excessive metabolic demand during epileptic activity that may result in impairment of functional and structural neuronal integrity. Due to vulnerability of hippocampus to ischemia (Schmidt-Kastner & Freund 1991), *in vitro* slices using the hippocampus have been extensively used for investigating tolerance to ischemia (Mitani *et al.* 1994, Djuricic *et al.* 1994). The major advantage of using hippocampal slices as a model is that it allows the separate study of different mechanism of ischemia-reperfusion injury unattainable *in vivo*. Moreover, this study used acute hippocampal slices rather than organotypic cultures. Organotypic cultures are used to model tissues *in vivo* and organotypic cultures of hippocampus are used commonly to model and study I/R injury. Because adult brain tissue does not live well in culture, organotypic cultures of hippocampus typically are prepared from neonatal brain tissue. Interpretation of organotypic cultures is therefore limited by developmental age of the

tissue (Fukuda *et al.* 1995). Another advantage of acute slices of adult hippocampus is that the pattern of synaptic connections within the slice is minimally altered relative to the *in vivo* patterns at the time of harvest (Coltman *et al.* 1995).

1.5.2 Microperfusion approach: A novel method for inducing ischemia reperfusion injury *in vitro*

The novel microperfusion method developed in our laboratory (Kirschner *et al.* 2009) for study of cell death in acute, adult slices overcomes the limitations of methods used in prior studies where high baseline cell death may have compromised interpretation. The microperfusion approach minimizes background cell death by capturing LDH release from the entire slice. This approach is an improvement over other methods where stains such as propidium iodide show cell death only on the surface of the freshly cut slice (Ross *et al.* 2006, Christian *et al.* 2008). Moreover, the microperfusion approach allows us to study cell death in adult AGS tissue. The ability to study adult tissue is an advantage since access to perinatal tissue is restricted by the seasonal breeding cycle of AGS. The *in vitro* microperfusion approach in our study might not apply to the *in vivo* scenario wherein whole animal mechanisms such as pH buffering capacity and limited inflammatory response contribute to tolerance to ischemia reperfusion injury (Bogren *et al.* 2014a, Bogren *et al.* 2014b).

Nonetheless, the microperfusion approach isolates processes occurring at the tissue level so that interpretation is not confounded by whole animal physiology. Moreover, the microperfusion approach allows for the concentration of each component in the perfusion fluid to be defined and manipulated and cell death quantified in a time-dependent manner. In this way, pH can be decreased without hypoxia and cell death

monitored with temporal resolution relevant to onset and recovery from low pH. Such discrete manipulation of individual components of the extracellular milieu is not possible *in vivo* where, for example, pH decreases following anoxia. Thus, the microperfusion approach gives superior control over the extracellular environment that could not be achieved *in vivo*. We acknowledge that the slice preparation differs from the *in vivo* scenario (Cho *et al.* 2007, Saeidnia *et al.* 2015) and in this way, serves our objective to study processes at the tissue level that do not depend on cold tissue temperatures and confer tolerance to AGS.

1.5.3 Cell death marker: Lactate dehydrogenase

The duration and severity of the ischemic insult may also determine the extent to which cell damage occurs by programmed cell death mechanisms after ischemia *in vivo* (Kalogeris *et al.* 2012). In focal ischemia models, cells in the ischemic core predominantly undergo necrotic features of cell death whereas cells in the penumbra region surrounding the ischemic core demonstrate more apoptotic features. Necrosis is characterized by swelling and rupture of intracellular organelles, eventually leading to the breakdown of the plasma membrane (Moquin & Chan 2010, Challa & Chan 2010). One of the markers for quantifying necrotic cell death is to measure the release of lactate dehydrogenase (LDH). LDH is a soluble cytoplasmic enzyme that is present in almost all cells and is released into extracellular space when the plasma membrane is damaged (Burd & Usategui-Gomez 1973).

In this thesis, LDH release is used to interpret necrotic cell death associated with OGD. The LDH approach of monitoring cell death overcomes the limitations of methods

used in prior studies where high baseline cell death challenged interpretation because of acute damage at the slice surface (Ross et al. 2006, Christian et al. 2008).

1.6 Specific aims

Hibernating mammals are a natural model of tolerance to ischemic and hypoxic insult. The purpose of this research is to explore the mechanisms that allow for ischemia tolerance in the AGS in an *in vitro* acute slice model. The aims of the dissertation were therefore:

1. to validate an *in vitro* microperfusion approach that allowed investigation of modeled I/R injury at the tissue level.
2. to determine the role of acidosis mediated acidotoxicity and its interaction with NMDA mediated excitotoxicity in ischemic/reperfusion injury
3. to assess the influence of hibernating state (i.e., hibernating or not hibernating) and hibernation season (i.e., winter vs. summer) on resistance to OGD in AGS brain tissue.
4. to identify if events such as depletion of ATP, acidosis, and glutamate efflux that are associated with anoxic depolarization are attenuated in AGS.
5. to investigate if AGS tolerate peroxynitrite ($ONOO^-$) mediated cell death modeled in acute hippocampal slices.

1.7 References

Aarts, M. M. and Tymianski, M. (2005) TRPMs and neuronal cell death. *Pflugers Archiv : European journal of physiology,* **451,** 243-249.

Albers, G. W., Goldberg, M. P. and Choi, D. W. (1989) N-methyl-D-aspartate antagonists: ready for clinical trial in brain ischemia? *Ann Neurol,* **25,** 398-403.

Albers, R. and Siegel, G. (2012) Membrane transport. In: *Basic Neurochemistry: Principles of Molecular, Cellular and Medical Neurobiology*, (S. Brady, G. Siegel, R. Albers and D. Price eds.), pp. 41–62. Elsevier Academic Press, Massachusetts, USA.

Alvarez de la Rosa, D., Krueger, S. R., Kolar, A., Shao, D., Fitzsimonds, R. M. and Canessa, C. M. (2003) Distribution, subcellular localization and ontogeny of ASIC1 in the mammalian central nervous system. *The Journal of physiology,* **546,** 77-87.

Bano, D., Munarriz, E., Chen, H. L., Ziviani, E., Lippi, G., Young, K. W. and Nicotera, P. (2007) The plasma membrane Na+/Ca2+ exchanger is cleaved by distinct protease families in neuronal cell death. *Ann N Y Acad Sci,* **1099,** 451-455.

Barnes, B. M. (1989) Freeze avoidance in a mammal: body temperatures below 0 degree C in an Arctic hibernator. *Science,* **244,** 1593-1595.

Baron, A., Waldmann, R. and Lazdunski, M. (2002) ASIC-like, proton-activated currents in rat hippocampal neurons. *The Journal of physiology,* **539,** 485-494.

Beckman, J. S., Beckman, T. W., Chen, J., Marshall, P. A. and Freeman, B. A. (1990) Apparent hydroxyl radical production by peroxynitrite: implications for endothelial injury from nitric oxide and superoxide. *Proceedings of the National Academy of Sciences of the United States of America,* **87,** 1620-1624.

Benveniste, H., Drejer, J., Schousboe, A. and Diemer, N. H. (1984) Elevation of the extracellular concentrations of glutamate and aspartate in rat hippocampus during transient cerebral ischemia monitored by intracerebral microdialysis. *Journal of neurochemistry,* **43,** 1369-1374.

Bickler, P. E., Donohoe, P. H. and Buck, L. T. (2002) Molecular adaptations for survival during anoxia: lessons from lower vertebrates. *Neuroscientist,* **8,** 234-242.

Bickler, P. E., Fahlman, C. S. and Taylor, D. M. (2003) Oxygen sensitivity of NMDA receptors: relationship to NR2 subunit composition and hypoxia tolerance of neonatal neurons. *Neuroscience,* **118,** 25-35.

Biorck, G., Johansson, B. and Veige, S. (1956) Some laboratory date on hidgehogs, hibernating and non-hibernating. *Acta physiologica Scandinavica,* **37,** 281-294.

Bogren, L. K., Murphy, C. J., Johnston, E. L., Sinha, N., Serkova, N. J. and Drew, K. L. (2014a) 1H-NMR metabolomic biomarkers of poor outcome after hemorrhagic shock are absent in hibernators. *PloS one,* **9,** e107493.

Bogren, L. K., Olson, J. M., Carpluk, J., Moore, J. M. and Drew, K. L. (2014b) Resistance to systemic inflammation and multi organ damage after global ischemia/reperfusion in the arctic ground squirrel. *PloS one,* **9,** e94225.

Buck, L. T. and Bickler, P. E. (1998) Adenosine and anoxia reduce N-methyl-D-aspartate receptor open probability in turtle cerebrocortex. *The Journal of experimental biology,* **201,** 289-297.

Buffenstein, R. and Yahav, S. (1991) The effect of diet on microfaunal population and function in the caecum of a subterranean naked mole-rat, Heterocephalus glaber. *Br J Nutr,* **65,** 249-258.

Bullard, R. W. and Funkhouser, G. E. (1962) Estimated regional blood flow by rubidium 86 distribution during arousal from hibernation. *The American journal of physiology,* **203,** 266-270.

Burd, J. F. and Usategui-Gomez, M. (1973) A colorimetric assay for serum lactate dehydrogenase. *Clin Chim Acta,* **46,** 223-227.

Burmester, T. and Hankeln, T. (2009) What is the function of neuroglobin? *The Journal of experimental biology,* **212,** 1423-1428.

Burns, J. M., Lestyk, K. C., Folkow, L. P., Hammill, M. O. and Blix, A. S. (2007) Size and distribution of oxygen stores in harp and hooded seals from birth to maturity. *Journal of comparative physiology. B, Biochemical, systemic, and environmental physiology,* **177,** 687-700.

Calabrese, V., Mancuso, C., Calvani, M., Rizzarelli, E., Butterfield, D. A. and Stella, A. M. (2007) Nitric oxide in the central nervous system: neuroprotection versus neurotoxicity. *Nat Rev Neurosci,* **8,** 766-775.

Carafoli, E. (1991) Calcium pump of the plasma membrane. *Physiological reviews,* **71,** 129-153.

Carey, H. V., Andrews, M. T. and Martin, S. L. (2003) Mammalian hibernation: cellular and molecular responses to depressed metabolism and low temperature. *Physiological reviews,* **83,** 1153-1181.

Challa, S. and Chan, F. K. (2010) Going up in flames: necrotic cell injury and inflammatory diseases. *Cell Mol Life Sci,* **67,** 3241-3253.

Cho, S., Wood, A. and Bowlby, M. R. (2007) Brain slices as models for neurodegenerative disease and screening platforms to identify novel therapeutics. *Current neuropharmacology,* **5,** 19-33.

Choi, D. W. (1988) Glutamate neurotoxicity and diseases of the nervous system. *Neuron,* **1,** 623-634.

Choi, D. W. (1992) Excitotoxic cell death. *Journal of neurobiology,* **23,** 1261-1276.

Christian, S. L., Ross, A. P., Zhao, H. W., Kristenson, H. J., Zhan, X., Rasley, B. T., Bickler, P. E. and Drew, K. L. (2008) Arctic ground squirrel (Spermophilus parryii) hippocampal neurons tolerate prolonged oxygen-glucose deprivation and maintain baseline ERK1/2 and JNK activation despite drastic ATP loss. *Journal of cerebral blood flow and metabolism : official journal of the International Society of Cerebral Blood Flow and Metabolism,* **28,** 1307-1319.

Coltman, B. W., Earley, E. M., Shahar, A., Dudek, F. E. and Ide, C. F. (1995) Factors influencing mossy fiber collateral sprouting in organotypic slice cultures of neonatal mouse hippocampus. *J Comp Neurol,* **362,** 209-222.

Contreras, J. E., Sanchez, H. A., Veliz, L. P., Bukauskas, F. F., Bennett, M. V. and Saez, J. C. (2004) Role of connexin-based gap junction channels and hemichannels in ischemia-induced cell death in nervous tissue. *Brain Res Brain Res Rev,* **47,** 290-303.

Crack, P. J. and Taylor, J. M. (2005) Reactive oxygen species and the modulation of stroke. *Free radical biology & medicine,* **38,** 1433-1444.

Cudd, A. and Fridovich, I. (1982) Electrostatic interactions in the reaction mechanism of bovine erythrocyte superoxide dismutase. *The Journal of biological chemistry,* **257,** 11443-11447.

Cuzzocrea, S., Riley, D. P., Caputi, A. P. and Salvemini, D. (2001) Antioxidant therapy: a new pharmacological approach in shock, inflammation, and ischemia/reperfusion injury. *Pharmacol Rev,* **53,** 135-159.

D'Alecy, L. G., Lundy, E. F., Kluger, M. J., Harker, C. T., LeMay, D. R. and Shlafer, M. (1990) Beta-hydroxybutyrate and response to hypoxia in the ground squirrel, Spermophilus tridecimlineatus. *Comp Biochem Physiol B,* **96,** 189-193.

Daan, S., Barnes, B. M. and Strijkstra, A. M. (1991) Warming up for sleep? Ground squirrels sleep during arousals from hibernation. *Neuroscience letters,* **128,** 265-268.

Dausmann, K. H., Glos, J., Ganzhorn, J. U. and Heldmaier, G. (2004) Physiology: hibernation in a tropical primate. *Nature,* **429,** 825-826.

Dave, K. R., Anthony Defazio, R., Raval, A. P., Dashkin, O., Saul, I., Iceman, K. E., Perez-Pinzon, M. A. and Drew, K. L. (2009) Protein kinase C epsilon activation delays neuronal depolarization during cardiac arrest in the euthermic arctic ground squirrel. *Journal of neurochemistry,* **110,** 1170-1179.

Dave, K. R., Prado, R., Raval, A. P., Drew, K. L. and Perez-Pinzon, M. A. (2006) The arctic ground squirrel brain is resistant to injury from cardiac arrest during euthermia. *Stroke; a journal of cerebral circulation,* **37,** 1261-1265.

Davis, S. M. and Donnan, G. A. (2009) 4.5 hours: the new time window for tissue plasminogen activator in stroke. *Stroke; a journal of cerebral circulation,* **40,** 2266-2267.

Del Zoppo, G. J., Saver, J. L., Jauch, E. C., Adams, H. P., Jr. and American Heart Association Stroke, C. (2009) Expansion of the time window for treatment of acute ischemic stroke with intravenous tissue plasminogen activator: a science advisory from the American Heart Association/American Stroke Association. *Stroke; a journal of cerebral circulation,* **40,** 2945-2948.

DiPolo, R. and Beauge, L. (1991) Regulation of Na-Ca exchange. An overview. *Ann N Y Acad Sci,* **639,** 100-111.

Djuricic, B., Rohn, G., Paschen, W. and Hossmann, K. A. (1994) Protein synthesis in the hippocampal slice: transient inhibition by glutamate and lasting inhibition by ischemia. *Metab Brain Dis,* **9,** 235-247.

Drew, K. L., Rice, M. E., Kuhn, T. B. and Smith, M. A. (2001) Neuroprotective adaptations in hibernation: Therapeutic implications for ischemia-reperfusion, traumatic brain injury and neurodegenerative diseases. *Free Radical Biology and Medicine,* **31,** 563-573.

El Kossi, M. M. and Zakhary, M. M. (2000) Oxidative stress in the context of acute cerebrovascular stroke. *Stroke; a journal of cerebral circulation,* **31,** 1889-1892.

Elsner, R., Shurley, J. T., Hammond, D. D. and Brooks, R. E. (1970) Cerebral tolerance to hypoxemia in asphyxiated Weddell seals. *Respir Physiol,* **9,** 287-297.

Erecinska, M. and Silver, I. A. (2001) Tissue oxygen tension and brain sensitivity to hypoxia. *Respir Physiol,* **128,** 263-276.

Featherstone, D. E. (2010) Intercellular glutamate signaling in the nervous system and beyond. *ACS Chem Neurosci,* **1,** 4-12.

Fernandes, J. A., Lutz, P. L., Tannenbaum, A., Todorov, A. T., Liebovitch, L. and Vertes, R. (1997) Electroencephalogram activity in the anoxic turtle brain. *The American journal of physiology,* **273,** R911-919.

Folkow, L. P., Ramirez, J. M., Ludvigsen, S., Ramirez, N. and Blix, A. S. (2008) Remarkable neuronal hypoxia tolerance in the deep-diving adult hooded seal (Cystophora cristata). *Neuroscience letters,* **446,** 147-150.

Frerichs, K. U. and Hallenbeck, J. M. (1998) Hibernation in ground squirrels induces state and species-specific tolerance to hypoxia and aglycemia: an in vitro study in hippocampal slices. *Journal of cerebral blood flow and metabolism : official journal of the International Society of Cerebral Blood Flow and Metabolism,* **18,** 168-175.

Frerichs, K. U., Kennedy, C., Sokoloff, L. and Hallenbeck, J. M. (1994) Local cerebral blood flow during hibernation, a model of natural tolerance to "cerebral ischemia". *Journal of cerebral blood flow and metabolism : official journal of the International Society of Cerebral Blood Flow and Metabolism,* **14,** 193-205.

Fukuda, A., Czurko, A., Hida, H., Muramatsu, K., Lenard, L. and Nishino, H. (1995) Appearance of deteriorated neurons on regionally different time tables in rat brain thin slices maintained in physiological condition. *Neuroscience letters,* **184,** 13-16.

Gill, D. L., Ghosh, T. K. and Mullaney, J. M. (1989) Calcium signalling mechanisms in endoplasmic reticulum activated by inositol 1,4,5-trisphosphate and GTP. *Cell Calcium,* **10,** 363-374.

Go, A. S., Mozaffarian, D., Roger, V. L. et al. (2014) Heart disease and stroke statistics--2014 update: a report from the American Heart Association. *Circulation,* **129,** e28-e292.

Guix, F. X., Uribesalgo, I., Coma, M. and Munoz, F. J. (2005) The physiology and pathophysiology of nitric oxide in the brain. *Prog Neurobiol,* **76,** 126-152.

Gunter, T. E. and Pfeiffer, D. R. (1990) Mechanisms by which mitochondria transport calcium. *The American journal of physiology,* **258,** C755-786.

Hindell, M. A., Slip, D. J. and Burton, H. R. (1991) The diving behaviour of adult male and female southern elephant seals, Mirounga leonina (Pinnipedia: Phocidae). *Aust. J. Zool,* **39,** 595-619.

Hochachka, P. W. and Lutz, P. L. (2001) Mechanism, origin, and evolution of anoxia tolerance in animals. *Comparative biochemistry and physiology. Part B, Biochemistry & molecular biology,* **130,** 435-459.

Hotchkiss, R. S., Strasser, A., McDunn, J. E. and Swanson, P. E. (2009) Cell death. *N Engl J Med,* **361,** 1570-1583.

Huie, R. E. and Padmaja, S. (1993) The reaction of no with superoxide. *Free Radic Res Commun,* **18,** 195-199.

Hylland, P., Nilsson, G. E. and Lutz, P. L. (1994) Time course of anoxia-induced increase in cerebral blood flow rate in turtles: evidence for a role of adenosine. *Journal of cerebral blood flow and metabolism : official journal of the International Society of Cerebral Blood Flow and Metabolism,* **14,** 877-881.

Ikonomidou, C. and Turski, L. (2002) Why did NMDA receptor antagonists fail clinical trials for stroke and traumatic brain injury? *Lancet Neurol,* **1,** 383-386.

Jackson, D. C. and Ultsch, G. R. (2010) Physiology of hibernation under the ice by turtles and frogs. *J Exp Zool A Ecol Genet Physiol,* **313,** 311-327.

Johansen, K., Lykkeboe, G., Weber, R. E. and Maloiy, G. M. (1976) Blood respiratory properties in the naked mole rat Heterocephalus glaber, a mammal of low body temperature. *Respir Physiol,* **28,** 303-314.

Kader, A., Frazzini, V. I., Solomon, R. A. and Trifiletti, R. R. (1993) Nitric oxide production during focal cerebral ischemia in rats. *Stroke; a journal of cerebral circulation,* **24,** 1709-1716.

Kalimo, H., Rehncrona, S. and Soderfeldt, B. (1981) The role of lactic acidosis in the ischemic nerve cell injury. *Acta neuropathologica. Supplementum,* **7,** 20-22.

Kalogeris, T., Baines, C. P., Krenz, M. and Korthuis, R. J. (2012) Cell biology of ischemia/reperfusion injury. *Int Rev Cell Mol Biol,* **298,** 229-317.

Kerem, D. and Elsner, R. (1973) Cerebral tolerance to asphyxial hypoxia in the harbor seal. *Respir Physiol,* **19,** 188-200.

Kesaraju, S., Schmidt-Kastner, R., Prentice, H. M. and Milton, S. L. (2009) Modulation of stress proteins and apoptotic regulators in the anoxia tolerant turtle brain. *Journal of neurochemistry,* **109,** 1413-1426.

Kirschner, D. L., Wilson, A. L., Drew, K. L. and Green, T. K. (2009) Simultaneous efflux of endogenous D-ser and L-glu from single acute hippocampus slices during oxygen glucose deprivation. *Journal of neuroscience research,* **87,** 2812-2820.

Krivoruchko, A. and Storey, K. B. (2010) Regulation of the heat shock response under anoxia in the turtle, Trachemys scripta elegans. *Journal of comparative physiology. B, Biochemical, systemic, and environmental physiology,* **180,** 403-414.

Kurtz, C. C., Lindell, S. L., Mangino, M. J. and Carey, H. V. (2006) Hibernation confers resistance to intestinal ischemia-reperfusion injury. *American journal of physiology. Gastrointestinal and liver physiology,* **291,** G895-901.

Kweon, H. J. and Suh, B. C. (2013) Acid-sensing ion channels (ASICs): therapeutic targets for neurological diseases and their regulation. *BMB Rep,* **46,** 295-304.

Larson, J. and Park, T. J. (2009) Extreme hypoxia tolerance of naked mole-rat brain. *Neuroreport,* **20,** 1634-1637.

Lee, J. M., Grabb, M. C., Zipfel, G. J. and Choi, D. W. (2000) Brain tissue responses to ischemia. *J Clin Invest,* **106,** 723-731.

Lenfant, C., Johansen, K. and Torrance, J. D. (1970) Gas transport and oxygen storage capacity in some pinnipeds and the sea otter. *Respir Physiol,* **9,** 277-286.

Lindell, S. L., Klahn, S. L., Piazza, T. M., Mangino, M. J., Torrealba, J. R., Southard, J. H. and Carey, H. V. (2005) Natural resistance to liver cold ischemia-reperfusion injury associated with the hibernation phenotype. *American journal of physiology. Gastrointestinal and liver physiology,* **288,** G473-480.

Ma, Y. L., Zhu, X., Rivera, P. M., Toien, O., Barnes, B. M., LaManna, J. C., Smith, M. A. and Drew, K. L. (2005) Absence of cellular stress in brain after hypoxia induced by arousal from hibernation in Arctic ground squirrels. *American journal of physiology. Regulatory, integrative and comparative physiology,* **289,** R1297-1306.

Milton, S. L., Dirk, L. J., Kara, L. F. and Prentice, H. M. (2008) Adenosine modulates ERK1/2, PI3K/Akt, and p38MAPK activation in the brain of the anoxia-tolerant turtle Trachemys scripta. *Journal of cerebral blood flow and metabolism : official journal of the International Society of Cerebral Blood Flow and Metabolism,* **28,** 1469-1477.

Milton, S. L. and Lutz, P. L. (1998) Low extracellular dopamine levels are maintained in the anoxic turtle (Trachemys scripta) striatum. *Journal of cerebral blood flow and metabolism : official journal of the International Society of Cerebral Blood Flow and Metabolism,* **18,** 803-807.

Milton, S. L. and Lutz, P. L. (2005) Adenosine and ATP-sensitive potassium channels modulate dopamine release in the anoxic turtle (Trachemys scripta) striatum. *American journal of physiology. Regulatory, integrative and comparative physiology,* **289,** R77-83.

Milton, S. L., Thompson, J. W. and Lutz, P. L. (2002) Mechanisms for maintaining extracellular glutamate levels in the anoxic turtle striatum. *American journal of physiology. Regulatory, integrative and comparative physiology,* **282,** R1317-1323.

Mitani, A., Andou, Y., Matsuda, S., Arai, T., Sakanaka, M. and Kataoka, K. (1994) Origin of ischemia-induced glutamate efflux in the CA1 field of the gerbil hippocampus: an in vivo brain microdialysis study. *Journal of neurochemistry,* **63,** 2152-2164.

Mitz, S. A., Reuss, S., Folkow, L. P., Blix, A. S., Ramirez, J. M., Hankeln, T. and Burmester, T. (2009) When the brain goes diving: glial oxidative metabolism may confer hypoxia tolerance to the seal brain. *Neuroscience,* **163,** 552-560.

Moquin, D. and Chan, F. K. (2010) The molecular regulation of programmed necrotic cell injury. *Trends Biochem Sci,* **35,** 434-441.

Murphy, M. P. (1999) Nitric oxide and cell death. *Biochimica et biophysica acta,* **1411,** 401-414.

Nayak, G. H., Prentice, H. M. and Milton, S. L. (2011) Neuroprotective signaling pathways are modulated by adenosine in the anoxia tolerant turtle. *Journal of cerebral blood flow and metabolism : official journal of the International Society of Cerebral Blood Flow and Metabolism,* **31,** 467-475.

Nilsson, G. E. and Lutz, P. L. (1991) Release of inhibitory neurotransmitters in response to anoxia in turtle brain. *The American journal of physiology,* **261,** R32-37.

Orrenius, S., Zhivotovsky, B. and Nicotera, P. (2003) Regulation of cell death: the calcium-apoptosis link. *Nat Rev Mol Cell Biol,* **4,** 552-565.

Pamenter, M. E. and Buck, L. T. (2008) delta-Opioid receptor antagonism induces NMDA receptor-dependent excitotoxicity in anoxic turtle cortex. *The Journal of experimental biology,* **211,** 3512-3517.

Pamenter, M. E., Hogg, D. W., Gu, X. Q., Buck, L. T. and Haddad, G. G. (2012) Painted turtle cortex is resistant to an in vitro mimic of the ischemic mammalian penumbra. *Journal of cerebral blood flow and metabolism : official journal of the International Society of Cerebral Blood Flow and Metabolism,* **32,** 2033-2043.

Park, T. J., Reznick, J., Peterson, B. L. et al. (2017) Fructose-driven glycolysis supports anoxia resistance in the naked mole-rat. *Science,* **356,** 307-311.

Pek, M. and Lutz, P. L. (1997) Role for adenosine in channel arrest in the anoxic turtle brain. *The Journal of experimental biology,* **200,** 1913-1917.

Perez-Pinzon, M. A., Lutz, P. L., Sick, T. J. and Rosenthal, M. (1993) Adenosine, a "retaliatory" metabolite, promotes anoxia tolerance in turtle brain. *Journal of cerebral blood flow and metabolism : official journal of the International Society of Cerebral Blood Flow and Metabolism,* **13,** 728-732.

Peterson, B. L., Park, T. J. and Larson, J. (2012) Adult naked mole-rat brain retains the NMDA receptor subunit GluN2D associated with hypoxia tolerance in neonatal mammals. *Neuroscience letters,* **506,** 342-345.

Pignataro, G., Simon, R. P. and Xiong, Z. G. (2007) Prolonged activation of ASIC1a and the time window for neuroprotection in cerebral ischaemia. *Brain : a journal of neurology,* **130,** 151-158.

Prentice, H. M., Milton, S. L., Scheurle, D. and Lutz, P. L. (2004) The upregulation of cognate and inducible heat shock proteins in the anoxic turtle brain. *Journal of cerebral blood flow and metabolism : official journal of the International Society of Cerebral Blood Flow and Metabolism,* **24,** 826-828.

Rehncrona, S., Rosen, I. and Siesjo, B. K. (1981) Brain lactic acidosis and ischemic cell damage: 1. Biochemistry and neurophysiology. *Journal of cerebral blood flow and metabolism : official journal of the International Society of Cerebral Blood Flow and Metabolism,* **1,** 297-311.

Reiter, C. D., Teng, R. J. and Beckman, J. S. (2000) Superoxide reacts with nitric oxide to nitrate tyrosine at physiological pH via peroxynitrite. *The Journal of biological chemistry,* **275,** 32460-32466.

Rider, M. H., Hussain, N., Dilworth, S. M. and Storey, K. B. (2009) Phosphorylation of translation factors in response to anoxia in turtles, Trachemys scripta elegans: role of the AMP-activated protein kinase and target of rapamycin signalling pathways. *Molecular and cellular biochemistry,* **332,** 207-213.

Ross, A. P., Christian, S. L., Zhao, H. W. and Drew, K. L. (2006) Persistent tolerance to oxygen and nutrient deprivation and N-methyl-D-aspartate in cultured hippocampal slices from hibernating Arctic ground squirrel. *Journal of cerebral blood flow and metabolism : official journal of the International Society of Cerebral Blood Flow and Metabolism,* **26,** 1148-1156.

Saeidnia, S., Manayi, A. and Abdollahi, M. (2015) From in vitro Experiments to in vivo and Clinical Studies; Pros and Cons. *Current drug discovery technologies,* **12,** 218-224.

Santos, M. S., Moreno, A. J. and Carvalho, A. P. (1996) Relationships between ATP depletion, membrane potential, and the release of neurotransmitters in rat nerve terminals. An in vitro study under conditions that mimic anoxia, hypoglycemia, and ischemia. *Stroke; a journal of cerebral circulation,* **27,** 941-950.

Schmidt-Kastner, R. and Freund, T. F. (1991) Selective vulnerability of the hippocampus in brain ischemia. *Neuroscience,* **40,** 599-636.

Schneuer, M., Flachsbarth, S., Czech-Damal, N. U., Folkow, L. P., Siebert, U. and Burmester, T. (2012) Neuroglobin of seals and whales: evidence for a divergent role in the diving brain. *Neuroscience,* **223,** 35-44.

Siesjo, B. K. (1988) Acidosis and ischemic brain damage. *Neurochemical pathology,* **9,** 31-88.

Simon, R. P., Griffiths, T., Evans, M. C., Swan, J. H. and Meldrum, B. S. (1984) Calcium overload in selectively vulnerable neurons of the hippocampus during and after ischemia: an electron microscopy study in the rat. *Journal of cerebral blood flow and metabolism : official journal of the International Society of Cerebral Blood Flow and Metabolism,* **4,** 350-361.

Skou, J. C. (1988) The Na,K-pump. *Methods in enzymology,* **156,** 1-25.

Soler, E. P. and Ruiz, V. C. (2010) Epidemiology and risk factors of cerebral ischemia and ischemic heart diseases: similarities and differences. *Current cardiology reviews,* **6,** 138-149.

Stecyk, J. A., Couturier, C. S., Fagernes, C. E., Ellefsen, S. and Nilsson, G. E. (2012) Quantification of heat shock protein mRNA expression in warm and cold anoxic turtles (Trachemys scripta) using an external RNA control for normalization. *Comp Biochem Physiol Part D Genomics Proteomics,* **7,** 59-72.

Suh, S. W., Shin, B. S., Ma, H., Van Hoecke, M., Brennan, A. M., Yenari, M. A. and Swanson, R. A. (2008) Glucose and NADPH oxidase drive neuronal superoxide formation in stroke. *Ann Neurol,* **64,** 654-663.

Tang, X. N., Cairns, B., Kim, J. Y. and Yenari, M. A. (2012) NADPH oxidase in stroke and cerebrovascular disease. *Neurol Res,* **34,** 338-345.

Thompson, J. W., Prentice, H. M. and Lutz, P. L. (2007) Regulation of extracellular glutamate levels in the long-term anoxic turtle striatum: coordinated activity of glutamate transporters, adenosine, K (ATP) (+) channels and GABA. *Journal of biomedical science,* **14,** 809-817.

Toda, N., Ayajiki, K. and Okamura, T. (2009) Cerebral blood flow regulation by nitric oxide: recent advances. *Pharmacol Rev,* **61,** 62-97.

Waldmann, R., Champigny, G., Bassilana, F., Heurteaux, C. and Lazdunski, M. (1997) A proton-gated cation channel involved in acid-sensing. *Nature,* **386,** 173-177.

Wang, L. C., Belke, D., Jourdan, M. L., Lee, T. F., Westly, J. and Nurnberger, F. (1988) The "hibernation induction trigger": specificity and validity of bioassay using the 13-lined ground squirrel. *Cryobiology,* **25,** 355-362.

Watkins, W. A., Moore, K. E. and Tyack, P. (1985) Investigations of sperm whale acoustic behaviours in the southeast Caribbean. *Cetology,* 1-15.

White, B. C., Wiegenstein, J. G. and Winegar, C. D. (1984) Brain ischemic anoxia. Mechanisms of injury. *JAMA,* **251,** 1586-1590.

Xia, Y. and Haddad, G. G. (2001) Major difference in the expression of delta- and mu-opioid receptors between turtle and rat brain. *J Comp Neurol,* **436,** 202-210.

Xiong, Z. G., Pignataro, G., Li, M., Chang, S. Y. and Simon, R. P. (2008) Acid-sensing ion channels (ASICs) as pharmacological targets for neurodegenerative diseases. *Curr Opin Pharmacol,* **8,** 25-32.

Xiong, Z. G., Zhu, X. M., Chu, X. P. et al. (2004) Neuroprotection in ischemia: blocking calcium-permeable acid-sensing ion channels. *Cell,* **118,** 687-698.

Yermolaieva, O., Leonard, A. S., Schnizler, M. K., Abboud, F. M. and Welsh, M. J. (2004) Extracellular acidosis increases neuronal cell calcium by activating acid-sensing ion channel 1a. *Proceedings of the National Academy of Sciences of the United States of America,* **101,** 6752-6757.

Zenteno-Savin, T., Clayton-Hernandez, E. and Elsner, R. (2002) Diving seals: are they a model for coping with oxidative stress? *Comparative biochemistry and physiology. Toxicology & pharmacology : CBP,* **133,** 527-536.

Zhou, F., Zhu, X., Castellani, R. J., Stimmelmayr, R., Perry, G., Smith, M. A. and Drew, K. L. (2001) Hibernation, a model of neuroprotection. *The American journal of pathology,* **158,** 2145-2151.

Zielonka, J., Sikora, A., Joseph, J. and Kalyanaraman, B. (2010) Peroxynitrite is the major species formed from different flux ratios of co-generated nitric oxide and superoxide: direct reaction with boronate-based fluorescent probe. *The Journal of biological chemistry,* **285,** 14210-14216.

CHAPTER 2: Acidotoxicity via acid sensing ion channel 1a (Asic1a) mediates cell death during oxygen glucose deprivation and abolishes excitotoxicity[1]

2.1 Abstract

Ischemia-reperfusion (I/R) injury is associated with a complex and multifactorial cascade of events involving excitotoxicity, acidotoxicity, and ionic imbalance. While it is known that acidosis occurs concomitantly with glutamate-mediated excitotoxicity during brain ischemia, it remains elusive, how acidosis-mediated acidotoxicity interacts with glutamate-mediated excitotoxicity. Here, we investigated the effect of acidosis on glutamate-mediated excitotoxicity in acute hippocampal slices. We tested the hypothesis that mild acidosis protects against I/R injury via modulation of NMDAR, but produces injury via activation of acid sensing ion channels (ASIC1a). Using a novel microperfusion approach, we monitored time course of injury in acutely prepared, adult hippocampal slices. We varied the duration of insult to delay the return to pre-insult conditions to determine if injury was caused by the primary insult or by the modeled reperfusion phase. We also manipulated pH in presence and absence of oxygen glucose deprivation (OGD). The role of ASIC1a and NMDAR was deciphered by treating the slices with and without an ASIC or NMDAR antagonist. Our results show that injury due to OGD or low pH occurs during the insult rather than the modeled reperfusion phase. Injury mediated by low pH or low pH OGD requires ASIC1a and is ischemic cell death caused by stroke and cardiac arrest.

---

[1] Published as Bhowmick S, Moore JT, Kirschner DL, Curry MC, Westbrook EG, Rasley BT, Drew KL. "Acidotoxicity via ASIC1a Mediates Cell Death during Oxygen-Glucose Deprivation and Abolishes Excitotoxicity." ACS Chem Neurosci. 2017 Mar 1. doi: 10.1021/acschemneuro.6b00355. [Epub ahead of print]. PubMed PMID: 28117962

2.2 Introduction

Ischemic reperfusion (I/R) injury associated with stroke and cardiac arrest can lead to severe morbidity and has a mortality rate between 30-100% (Go et al. 2014). Several clinical trials aimed at NMDA (N-methyl-d-aspartic acid) mediated excitotoxicity have failed.(Lipton 2004, Hoyte et *al.* 2004). Acidosis exacerbates ischemic brain injury due to a drop in tissue pH to 6.5 – 6.0 (Rehncrona et al. 1981, Nedergaard *et al.* 1991). However, an intriguing debate has emerged regarding the influence of mild acidosis on cell damage/ protection during cerebral I/R injury. One line of evidence suggests that mild acidosis is neuroprotective (Tombaugh & Sapolsky 1990, Kaku et *al.* 1993) and the neuroprotection is due to modulation of the NMDA receptor mediated ischemic cascade (Giffard et *al.* 1990, Tang et *al.* 1990, Traynelis & Cull-Candy 1990). On the contrary, several other works suggest that acidosis activates acid sensing ion channels (ASICs) which results in intracellular Ca^{2+} overload causing acidotoxicity independent of NMDA mediated excitotoxicity (Xiong et al. 2004, Yermolaieva et al. 2004).

Although previous *in vitro* and *in vivo* studies show that brain ischemia triggers excessive glutamate release (Benveniste et al. 1984, Mitani et al. 1994), activation of NMDA receptors (Choi 1992) and concomitant tissue acidosis (Siemkowicz & Hansen 1981), it remains elusive how the acidotic component interacts with glutamate-mediated excitotoxicity. Challenges in deciphering the interaction between these two mechanisms are overcome in the current study by use of a novel *in vitro* microperfusion technique in which pH is manipulated independently from oxygen glucose deprivation (OGD).

The present study tested the hypothesis that low pH during OGD blocks NMDA mediated excitotoxicity but produces acidotoxicity via ASIC1a. We utilized acute rat

hippocampal slices to ascertain the time course of injury from OGD with and without acidosis as well as acidosis alone. Cell death subsequent to these manipulations was assessed by lactate dehydrogenase (LDH) release (Koh & Choi 1987).

2.3 Methods

2.3.1 Animals

Adult Male Sprague Dawley rats (Simonsen labs, Gilroy, CA; age 3-4 months, 250-400 g) were used for all experiments. The animals used in this study were housed in University of Alaska Fairbanks Animal Resource Center (ARC), fed ad libitum, and kept under a 12:12 light: dark cycle with lights on at 0700 and off at 1900. During housing, animals were monitored once daily for health status. No adverse events were observed during housing. All experimental procedures were approved by the University of Alaska Fairbanks Institutional Animal Care and use Committee (IACUC), performed in accordance with the strict guidelines of the 8th edition of the Guide for the Care and Use of Laboratory Animals published by the US National Institutes of Health. Research were conducted in accordance with ARRIVE guidelines for reporting animal research (Kilkenny et *al.* 2010).

2.3.2 Acute hippocampus slice preparation

Slices were prepared between 0800 and 1030. Animals were anesthetized using 5% (v/v) isoflurane with medical graded O_2 at a constant flow rate of 1.5 L/min. Once unresponsive, the animals were euthanized via rapid decapitation and their brains quickly removed. The whole brain was then placed in ice chilled, oxygenated HEPES buffered artificial cerebral spinal fluid (HEPES-aCSF) containing 120 mM NaCl, 20 mM $NaHCO_3$,

6.68 mM HEPES acid, 3.3 mM HEPES sodium salt, 5.0 mM KCl, 2.0 mM $MgSO_4$ (pH 7.3 - 7.4) to attenuate edema during the course of slicing and incubation. Rapidly dissected hippocampi were embedded in 2.5 % agar and transverse hippocampal slices. Approximately 10 mm were discarded from both ends and 400 µm thick slices from each hippocampus were cut at approximately 2°C in oxygenated HEPES-aCSF using a Vibratome® 1000plus sectioning system (The Vibratome Company, St. Louis, MO). The slices were then transferred to a brain slice keeper (Scientific Systems Design Inc., Mississauga, Ontario, CA) and allowed to recover for 1-1.5 h at room temperature in HEPES-aCSF bubbled continuously with 95% O_2/ 5% CO_2 before transferring to experimental conditions as indicated.

2.3.3 Microperfusion chamber

To address the time course of injury, treatment was applied using an *in vitro* microperfusion technique described previously (Kirschner et al. 2009). Briefly, after 1-1.5 h recovery as described above, individual slices were transferred gently to microperfusion chambers and lids sealed. The 4-8 parallel chambers were perfused with artificial cerebrospinal fluid (aCSF), pH 7.3 containing 120 mM NaCl, 45 mM $NaHCO_3$, 10 mM glucose, 3.3 mM KCl, 1.2 mM NaH_2PO_4, 2.4 mM $MgSO_4$, 1.8 mM $CaCl_2$ bubbled with 95% O_2/5% CO_2 and submerged in aCSF bath at 36°C (±0.2°C) at a flow rate of 7 µL/min. Sampling began 75 min after submerging the sealed chambers to allow adequate time for stabilization of neurochemical efflux. At 15 min interval, perfusates (7 µL /min X 15 min =105 µL) was collected and analyzed as indicated. The volume of each chamber was estimated at 35µL based on dimensions of 9×5×0.7 mm (L×W×H) with 0.3-mm deep microchannels. Approximately half of this volume was displaced by the 400µm thick slice.

2.3.4 Treatment / injury conditions

To model ischemia-induced alterations in the ionic microenvironment in the hippocampus, acute hippocampal slices were exposed to 30 min of one of the four treatments: (1) aCSF, pH 7.3, (2) OGD, pH 7.3 (glucose-oxygen free aCSF), (3) aCSF, pH 6.4 (120 mM NaCl, 7.03 mM $NaHCO_3$, 10 mM glucose, 3.3 mM KCl, 1.2 mM NaH_2PO_4, 2.4 mM $MgSO_4$ 1.8 mM $CaCl_2$, (4) OGD, pH 6.4 (glucose-oxygen free low pH aCSF). Acidosis was induced with a pH of 6.4 based on previous studies that suggest hippocampal homomeric ASIC1a peak current showed a high sensitivity to pH 6.4 (pH0.5 = 6.4 and nH = 1.65 for ASIC1a) (Baron et *al.* 2001). Ischemia-induced alteration was made by switching the solution (from aCSF pH 7.3 to OGD pH 7.3, aCSF, pH 6.4 and OGD, pH 6.4) 8 min prior to the start of insult, the time it takes to completely replace the solution in the chamber with a flow rate of 7 µL/min. All aCSF solutions were equilibrated with 95% O_2 and 5% CO_2 whereas the OGD solutions were equilibrated with 5% CO_2 and 95% N_2, for a minimum of 1 h until pH stabilized in the desired range. The osmolarity of these solutions was between 290 and 300 mOsm. The PO_2 in OGD solution varied from 0-2.9 mmHg with an average for 6 determinations of 1.1 mm-Hg as measured using a miniature Clark-style electrode (Instech Laboratories, Plymouth Meeting, PA). Collected fractions were analyzed for cell death (LDH release) on the day of collection. Remaining volume was kept at -80°C for subsequent analysis. For evaluating the effect of NMDAR and ASIC1a on OGD or acidosis mediated cellular injury in acute hippocampal slices, the respective inhibitors were added throughout the experiment (during pretreatment, the insult phase and reperfusion). MK-801 (noncompetitive NMDAR antagonist, 100 µM, Sigma-Aldrich, St Louis, MO), Amiloride (non-specific ASIC inhibitor,

100 µM, Cayman chemical, Ann Arbor, MI), Psalmotoxin (PcTX1 - specific ASIC1a inhibitor, 50 nM, Abcam, Cambridge, MA) were used for NMDAR and ASIC manipulations.

2.3.5 Assessment of cellular injury- LDH measurement

Cell injury was assessed by the measurement of LDH release (Koh & Choi 1987). Following collection of perfusates every 15 min during the course of the experiment, 50 µl of perfusate was transferred to 384-well plates and mixed with 50 µl reaction solution provided by the LDH assay kit (Cayman chemical, Ann Arbor, MI). Optical density was measured at 490 nm 60 min later, using a microplate reader (Epoch Microplate Spectrophotometer, BioTek, Winooski, VT). Background absorbance at 620nm was subtracted. The LDH release was quantified as an arbitrary unit per mg of protein (Bio-Rad protein assay kit, Hercules, CA) and represented as a fraction of baseline LDH release. The maximal releasable LDH was also obtained by treating the slices with 1% NP-40 lysis buffer (50 mM Tris-HCl, 0.5% sodium deoxycholate, 0.1% SDS, 1% Igepal, 150 mM NaCl, 0.05% Triton X-100) at the end of each experiment.

2.3.6 Assessment of metabolic efflux

Glutamate and aspartate were analyzed by capillary electrophoresis. Perfusates were derivatized as described previously (Kirschner et *al.* 2007, Kirschner et al. 2009) to form highly fluorescent cyanobenz[f]isoindole amino acids (CBI-amino acids). Briefly, 2 µL thawed perfusate was reacted with 2 µL 2 mM naphthalene-2,3-dicarboxaldehyde (NDA) in methanol and 2 µL NaCN (5.5 mM) in 60 mM sodium tetraborate. Cyanide solution contained 3µM D-amino adipic acid as internal standard. Samples were reacted at room temperature for approximately 20 min prior to analysis. CE-LIF was performed

on a custom in-house-built instrument using a 420-nm diode laser, 490-nm bandpass filter, and PMT for LIF detection. Samples were injected onto a bare fused silica capillary of dimensions 25 cm x 25 μm (22.5 cm to detection window) for 1-3 sec at 380-mbar vacuum and separated by using positive polarity (20 kV). Separation buffer optimized for analysis of L-glutamate and L-aspartate is a 50mM sodium tetraborate background electrolyte (BGE) adjusted to pH 9.3. BGE additionally contained 1.0 mM β-cyclodextrin to decrease sample run time for glutamate and aspartate analysis. The addition of β-cyclodextrin allowed for baseline resolution of glutamate, aspartate, and the internal standard in less than 2 min. PeakFit software (SeaSolve Software Inc., Framingham, MA) was used to process raw data and quantify peak areas in all experiments based on a Gaussian peak shape for each analyte. Linear calibration curves were constructed for glutamate and aspartate as a function of concentration verses the peak area ratio (analytes area/internal standard area). Efflux of analytes was quantified as a concentration of glutamate or aspartate normalized to total protein for the slice used in the efflux experiment and represented as a fraction of baseline glutamate or aspartate release.

2.3.7 Determination of ATP and adenosine

ATP was determined after bath application of OGD or normoxic conditions as described previously.(Christian et al. 2008) In brief, slices were incubated in either aCSF or OGD solution and collected at the time point indicated. From each treatment conditions, 3 hippocampal slices were transferred to a flat-bottomed microfuge tube containing 200 μL of ice-cold 5% trichloroacetic acid, sonicated (8 pulses), centrifuged at 16,000 g for 1 min at 4°C. Supernatant was then collected and assayed for ATP using

ENLITEN ATP assay (Promega, Madison, WI). The pellets were further reconstituted with 200 µL 1M NaOH and protein concentration was analyzed (Bio-Rad protein assay kit, Hercules, CA). ATP level was represented as a concentration of ATP normalized to total protein for the slices.

Adenosine level was determined using HPLC as previously reported with slight modifications. In brief, 2mM acetic acid (pH 4.0) in 7% acetonitrile constitute the mobile phase having a flow rate of 20 µL/min produced by a PrimeLine pump (ASI, Analytical Scientific Instruments, El Sobrante, CA). The process of separation was achieved by a BAS microbore column (MF-8949; 1x 100 mm and 1x14mm guard column, with C18 packing of 3-µm particle size, BASi, West Lafayette, IN), which was attached directly to the injector (Rheodyne 9125, Rohnert Park, CA) and to the UV detector (Waters 2487 UV detector, outfitted with a Waters microbore cell kit, Waters Corporation, Milford, MA). Adenosine was detected at a wavelength of 258 nm. Chromatographic data were recorded with a Peak Simple Chromatography data system (SRI, model 203, SRI Instruments, Torrance, CA) and the peak areas of microperfusion samples were compared to the peak areas of adenosine standards (10µL of 50nM) for quantification. The detection limit of the assay was 33 fmol (based on a signal-to-noise ratio of 3:1). Concentration is expressed as nM and retention time for adenosine was between 11.0 and 11.3min.

2.3.8 Statistical analysis

A priori power analysis (using G*Power software) was performed to estimate sample size needed to yield 80% power for detecting a therapeutically significant effect of treatment. No animal was excluded from the study. Slices from animals were randomly

assigned to treatment and control groups without prior knowledge to the treatment conditions. Data processing and statistical analyses were performed using Microsoft Office Excel 2010 and Graph PadPrism6. Data were analyzed with one-way or two-way ANOVA with repeated measures. Significant main effects or interactions were followed by t-tests with Bonferroni's correction. Data are expressed as mean ± SEM, and $P < 0.05$ was considered as statistically significant.

2.4 Results and discussion

2.4.1 OGD injury via microperfusion approach resembles similar disruption in energy homeostasis and excitatory neurotransmitter efflux that mimics *in vivo* I/R injury.

During cerebral ischemia *in vivo*, acidotoxicity and excitotoxicity occur concomitantly and it is unclear how these two mechanisms interact. Moreover, it is not possible to manipulate acidosis to decipher how it interacts with excitotoxicity. Traditional *in vitro* slice preparations do not produce the same changes in the extracellular milieu as what occurs *in vivo* because of rapid washing with a highly diluted bath solution (Yao *et al.* 2007). The finding of this study involves using a novel microperfusion technique that allows for time resolved study of cell death and manipulation of pH with and without OGD thus allowing for study of the interaction between acidosis and OGD-induced injury. The advantages of this model include the opportunity for temporal resolution of injury as well as overflow of metabolites and neurotransmitters and to manipulate each of the components of the ischemic cascade to better understand interactions. With the microperfusion approach we measured only LDH release as a marker of cell death. Cytosolic lactate dehydrogenase release following injury is due to membrane disruption that correlates with cell death. In the present study, for the first time we have monitored

continuous LDH release in an acute slice preparation where it allows for observation of the time course of membrane disruption. Here, we investigated the effect of *in vitro* ischemia like condition (OGD) exposure on energy homeostasis (Dale & Frenguelli 2009) and excitotoxic neurotransmitter efflux (Benveniste et al. 1984), a hallmark of ischemic injury in acute hippocampal slices from rat. Results show that exposure of acute hippocampal slices to 30 min OGD insult resulted in a significant depletion in ATP levels. Slices treated with OGD showed a significant drop in ATP when compared to control slices. Slices with OGD showed no signs of ATP restoration even after 3 hours of reperfusion (Figure 2.1 A). This indicates that energy homeostasis is highly dysregulated due to OGD exposure. To further validate the disruption of energy homeostasis in correlation to adenosine, we investigated the level of adenosine efflux upon OGD exposure. Slices exposed to 30 min of OGD showed significant efflux in extracellular adenosine when compared to the control slices. The adenosine level returned to baseline within 15 min of the onset of reperfusion (Figure 2.1 B). From our results, we conclude that when acute hippocampal slices are subjected to 30 min of OGD insult, they release extracellular adenosine produced from rapid degradation of ATP due to ischemic-like conditions.

We next investigated the effect of OGD exposure on excitotoxic neurotransmitter efflux such as glutamate and aspartate. Consistent with previous *in vivo* studies (Mitani et al. 1994, Cui et *al.* 1999), perfused slices exposed to OGD injury for 30 min released glutamate (62-fold increase over basal level) (Figure 2.2 A). Similarly, aspartate efflux also increased during OGD (11.4-fold increase over basal level) (Figure 2.2 B). After the onset of reperfusion, the glutamate levels returned to baseline levels within 60 min,

aspartate returned to baseline levels within 45 min.

The observations reported herein validate the microperfusion approach. Dysregulation in energy homeostasis and excessive release of excitatory neurotransmitters are decisive for the development of excitotoxicity during cerebral ischemia. With our approach, when hippocampal slices are subjected to OGD, tissue ATP declines and adenosine, glutamate, and aspartate are released into the extracellular space. These observations are in accord with previous *in vitro* and *in vivo* studies that supports similar energy dysregulation (Latini & Pedata 2001, Dunwiddie et *al.* 1997), and excitatory neurotransmitter release during cerebral ischemia *in vivo* and OGD *in vitro* (Benveniste et al. 1984, Mitani et al. 1994, Hagberg et *al.* 1985, Butcher et *al.* 1990, Shimizu et *al.* 1993).

2.4.2 OGD or acidosis causes injury during insult rather than during reperfusion

How much injury occurs during the ischemic and reperfusion phases continues to be controversial in both experimental animal and clinical studies (Kloner 1993). Intrinsic to ischemia reperfusion injury is the concept that harmful events are occurring during both ischemia and reperfusion (Jaeschke 1999, Kalogeris et al. 2012). With the microperfusion approach, we monitored the timing of injury to decipher whether cell death was due to "insult" (OGD or low pH) or to "reperfusion". In these experiments, reperfusion was modeled by returning oxygen and glucose or by returning pH to 7.3. We varied the duration of insult between 15, 30, and 45 min with the expectation that delayed return of oxygen and glucose or delayed return to pH 7.3 would delay LDH release if injury was caused by the modeled reperfusion phase. Delaying onset of modeled reperfusion (for 15 min, 30 min, or 45 min) or the return to pH 7.4 from pH 6.4 (for 15 min, 30 min, or 45 min)

did not delay the peak time of LDH release. However, the magnitude of injury was increased (Figure 2.3 A-B). This indicates that injury was caused by the primary OGD or low pH insult and not by modeled reperfusion.

One study suggests that low pH causes detrimental effect during reperfusion (Gu et *al.* 2010). However, extracellular pH decreases immediately (Simon et *al.* 1985) after the onset of ischemia and is restored to the normal physiological range upon reoxygenation (Regli et *al.* 1995). Given this time course of acidosis, a sustained severe acidosis during the reperfusion phase is unlikely. When acidosis was prolonged during the low pH insult phase, injury increased in magnitude but was not offset by the time of reperfusion. A similar observation was made with OGD insult. Thus, with regards to timing of acidosis, our experimental set-up mimicked the *in vivo* scenario and shows that injury associated with OGD or low pH occurs during insult rather than during reperfusion.

2.4.3 Low pH delays OGD injury and shows injury independent of OGD insult

Buffering of the OGD solution during *in vitro* experiments eliminates the acidotic component that occurs during cerebral ischemia *in vivo*. To study the interaction between acidosis and OGD on cellular injury, the pH of the OGD solution was adjusted from 7.3 to 6.4. OGD at pH 6.4 decreased and delayed LDH release as compared to OGD at physiological pH 7.3. Results show that OGD with low pH shows similar time course of injury as observed with low pH alone. With similar time course of injury, no significant statistical differences were observed at any given time point between OGD with low pH and low pH alone (Figure 2.4 A). This suggests that when low pH is introduced along with OGD, low pH overrides OGD mediated injury. When the total injury represented by the area under the curve was considered, LDH released by pH 6.4 was not different from

LDH released by OGD, pH 7.3 or by OGD pH 6.4 (Figure 2.4 B). This indicates that low pH delays OGD injury, but on its own, causes injury that is as deleterious as OGD.

2.4.4 Injury caused by OGD insult is due to NMDAR activation whereas low pH injury is ASIC1a mediated

We next ask whether the delay in injury caused by acidosis is due to modulation of NMDAR. While application of NMDAR antagonist (MK-801) decreased LDH release in groups subjected to OGD, pH 7.3 (Figure 2.5 A), no significant effect on LDH release was observed in slices subjected to acidosis, pH 6.4 (Figure 2.5 B) or OGD with acidosis, pH 6.4 (Figure 2.5 C). This suggests that OGD injury at physiological pH involves NMDAR activation whereas injury associated with acidosis alone or acidosis in combination with OGD is independent of NMDAR mediated excitotoxicity.

Because acidosis contributes to cell death independent of OGD (Figure 2.4 A-B), we next explored the role of ASICs. We expected that targeting the ASIC1a with specific and non-specific blocker would attenuate pH 6.4-mediated cell death. As illustrated in Figure 2.6 A-B, continuous perfusion of 100 μM amiloride (nonspecific ASIC blocker which acts by blocking the channel pore) during acidosis, pH 6.4 and OGD pH 6.4 tended to decrease LDH release; however, failed to produce a statistically significant effect. Next, we tested the effect of Psalmotoxin (PcTx), a specific blocker of Ca^{2+}-permeable homomeric ASIC1a. Application of PcTx (50 nM) blocked aCSF pH 6.4 and OGD pH 6.4–induced LDH release (Figure 2.6 C-D). This result supports the involvement of ASIC1a in low pH mediated injury.

Results reported herein demonstrate that delayed injury was solely due to ASIC1a activation since NMDAR blockade had no effect on OGD-induced cell death in the

presence of proton load. No decrease in LDH release with NMDAR blockade in presence of proton load could also be due to high concentration of MK-801(100 μM). The higher concentration might have compromised the specificity of MK-801 on the NMDAR receptor favoring non-specific binding that masked the neuroprotective effect of NMDAR blockade. Since, with the same concentration of MK-801, we observed decreased LDH release in groups subjected to OGD at pH 7.3, we believe that the non-specificity associated with high concentration of MK-801 did not confound the results of our study. Blocking the NMDAR with MK-801 will block the NR2B-NMDARs/CaMKII cascade described previously to enhance ASIC1a-mediated current (Gao et *al.* 2005). The present work cannot rule out a NR2B-specific pathway, however, injury caused by low pH alone or with OGD did not depend on a NR2B/CaMKII pathway since MK-801 blocks all NMDARs including those that contain NR2B.

Preclinical *in vivo* studies and clinical trials have also failed to show neuroprotective effects of MK-801 (Ellison 1995, LeBlanc et *al.* 1991, Horvath et *al.* 1997). The interpretation that low pH abolishes NMDAR mediated excitotoxicity contrasts with other studies where authors have suggested that OGD-induced cell death is due to NMDAR, but delayed by pH dependent inhibition of NMDA (Kaku et al. 1993, Giffard et al. 1990, Sapolsky et *al.* 1996). Here we show that delayed injury is solely due to ASIC1a, that is unmasked by complete attenuation of excitotoxicity.

This interpretation is consistent with prior work showing that mild acidosis during brain ischemia protects against excitotoxic injury by modulating glutamate-mediated excitotoxicity (Tombaugh & Sapolsky 1990, Kaku et al. 1993). These results also support prior work showing that increased load of proton due to acidosis (Rehncrona et al. 1981,

Kalimo et al. 1981) activates a distinct family of ligand-gated channels, the acid-sensing ion channels, ASICs (ENaC/Deg superfamily) (Waldmann et al. 1997, Baron et al. 2002, Alvarez de la Rosa et al. 2003) and mediates injury unrelated to NMDAR. The role of ASIC1a activation during acidotoxicity has been previously confirmed in *in vivo* studies. Furthermore, ASIC1a knock-out or pharmacological blockade of ASIC1a attenuates injury associated with brain ischemia. Our present results with selective antagonism of ASIC1a with PcTX1 are consistent with the role of ASIC1a in ischemic damage as previously reported. The less robust ability of amiloride to attenuate the effect of low pH could be due to dose. The IC50 of amiloride to inhibit ASICs is between 5 and 100 μM (Baron & Lingueglia 2015). In this dose range, amiloride is not specific for ASIC1a. For example, at 100 μmol/L, the concentration used in this study, amiloride enhances the sustained current evoked in cells transfected with ASIC3 (Yagi et *al.* 2006, Li et *al.* 2011). At slightly higher concentrations amiloride affects other targets including other ion channels (e.g., epithelial Na^+ channel and calcium channels) and exchangers (e.g., Na^+/H^+ and Na^+/Ca^{2+}) (Frelin et *al.* 1988, Kleyman & Cragoe 1988). Thus, it was not feasible to test a higher dose of amiloride without confounding results by nonspecific effects. For this reason, we tested the specific ASIC1a blocker PcTX1. This specific blocker of ASIC1a completely abolished LDH release caused by both low pH alone and low pH with OGD.

Both activation of NMDAR and ASIC1a causes high influx of intercellular Ca^{2+} that causes cell damage. Previous studies provide strong evidence that ASIC1-a mediated increase in Ca^{2+} influx could contribute to Ca^{2+} overload, an important mechanism of cell damage and death in ischemia (Yermolaieva et al. 2004, Xiong et al. 2004). Others have shown that Ca^{2+} is not required for ASIC1a - mediated cell death (Wang et *al.* 2015). Our

study of the interaction of OGD and pH was enabled through the use of a novel microperfusion technique. This *in vitro* preparation allowed for independent manipulation of OGD and pH and for time resolved assessment of cell death. The approach was validated by demonstrating that it mimics an *in vivo* cerebral ischemia scenario in terms of dysregulation in energy homeostasis and excessive release of excitatory neurotransmitters, hallmarks of ischemic injury. With the microperfusion approach, we measured only LDH release as a marker of cell death throughout the slice and cannot distinguish between sub regions of the hippocampus or between cell type. LDH release is a standard approach to monitor cell death (Chan et *al.* 2013) which is released from the cytosol due to membrane disruption and not due to metabolic changes related to OGD. In the present study, for the first time we have monitored continuous LDH release in an acute slice preparation where it allows for observation of the time course of membrane disruption from the entire slice. We interpret membrane disruption as an early indicator of cell death. Other markers of cell death such as propidium iodide (PI) staining produce high background due damage of the cells at the surface during acute slice preparation. Results here, based on time resolved release of LDH are consistent with prior work from this laboratory, based on PI staining in acutely prepared or short-term cultured slices (Christian et al. 2008, Ross et al. 2006). Although slices are incubated until high baseline levels of LDH reach a stable minimum, there is a possibility that acutely injured cells on the surface of the slice are affected more than cells at the center of the slice. Thus, the novel microperfusion method developed in our laboratory (Kirschner et al. 2009) for study of cell death in acute, adult slices overcomes the limitations of methods used in prior studies where high baseline cell death may compromise interpretation.(Ross

et al. 2006, Christian et al. 2008) The microperfusion approach minimizes background cell death caused by trauma at the surface of the slice by capturing LDH release from the entire slice. The microperfusion approach also monitors the time course of injury as well as the overflow of metabolites and neurotransmitters. Despite these advantages over other *in vitro* approaches to monitor cell death, we acknowledge that the slice preparation differs from the *in vivo* scenario (Cho et al. 2007, Saeidnia et al. 2015). However, the microperfusion approach gives superior control over the extracellular environment that could not be achieved *in vivo*. Here we show that LDH release during OGD or low pH insult reaches a maximum peak and then subsides. We suggest that the decay in the LDH signal peak is not a consequence of dilution because flow rate and sampling rate are constant throughout the experiment. Furthermore, the waning in LDH release is not due to depletion of LDH since no difference in total LDH content was observed in slices subjected to aCSF, OGD or low pH treatment (Data not shown). Further study will be required to understand why LDH release subsides over time.

Previous *in vitro* studies performed in cell culture or in cultured post-natal brain tissue (Giffard et al. 1990, Gu et al. 2010, Tang et al. 1990, Lushnikova et *al.* 2004) suggest that cell death typically occurs 4 hours after OGD treatment. By contrast, our study shows that 30 minutes of insult is sufficient to cause immediate membrane disruption marked by LDH release. It is to be noted that there is a difference in how each model responds to a commonly studied ischemic-like paradigm, oxygen-glucose deprivation. Previous studies show that acute slice viability is affected by OGD lasting as little as 10 min (Small et *al.* 1995, Taylor et *al.* 1999) whereas, organotypic hippocampal slice cultures tolerate a much longer duration of challenge (Lushnikova et al. 2004,

Sullivan et *al.* 2002, McManus et *al.* 2004). We chose to use acute slices, because it allows for study of cell death in adult tissue not possible with organotypic hippocampal slice culture. Organotypic cultures differ from adult brain slices in several ways such as influence of age (adult vs. neonatal) which may influence the mechanisms of resistance to injury, the proportion of neurons to glia, synaptic connections between neurons, neural circuitry that influences metabolic demand of the tissue and maturity of the neurons studied (Lein et *al.* 2011, De Simoni et *al.* 2003, Lossi et *al.* 2009). Thus, study in cultured cells or post-natal tissue may not reflect mechanisms operative in adult brain tissue.

2.5 Conclusion

This paper reports several important findings using a novel microperfusion technique that for the first time provides time-resolved observations of excitotoxicity and acidotoxicity in an *in vitro* model of cerebral ischemia/reperfusion in adult hippocampus. Firstly, our results demonstrate that injury associated with acidosis (pH 6.4) or OGD (pH 7.3) occurs during insult rather than during the reperfusion phase. Secondly, we show that acidosis combined with OGD delays OGD injury. Finally, we show that when OGD is combined with acidosis as occurs *in vivo*, acidotoxicity mediated via ASIC1a occurs but low pH abolishes NMDAR mediated excitotoxicity.

In conclusion, we show that acidosis eliminates the NMDAR contribution to OGD-induced cell death but causes injury through an ASIC1a mediated mechanism. Although this study resolves controversy surrounding the interplay between NMDA and ASIC1a, the translational potential of ASIC1a may be limited. Acidosis may have longer-term effects not addressed here. Pignataro et al., 2007 observed protective effects when an ASIC1a antagonist was applied as late as 5 h after occlusion *in vivo* (Pignataro et al.

2007). Other mechanisms such as uncoupling of NADPH oxidase from NMDAR activation by intracellular acidosis (Lam et *al.* 2013) or acidosis mediated reorganization of mitochondrial efficiency (Khacho et *al.* 2014) could also contribute to longer-lasting intercellular acidosis mediated protective effects. Identification and understanding of the interaction between acidotoxicity and NMDAR mediated excitotoxicity point towards a better mechanistic approach in design of an effective therapeutic strategy for brain ischemia caused by stroke and cardiac arrest.

2.6 Acknowledgements

Research reported in this publication was supported by the US Army Medical research and Material Command, No 0517800; the National Institute of Neurological Disorder and Stroke, Nos. NS041069-06 and R15NS070779; Institutional Development Award (IDeA) from the National Institute of General Medical Sciences of the National Institutes of Health under grant number P20GM103395. The funders had no role in study design, data collection and analysis, decision to publish, or preparation of the manuscript. The authors thank Dr. Tom Kuhn for helpful discussions and Ian Herriott, technician, UAF DNA core facility for assisting with the microplate reader.

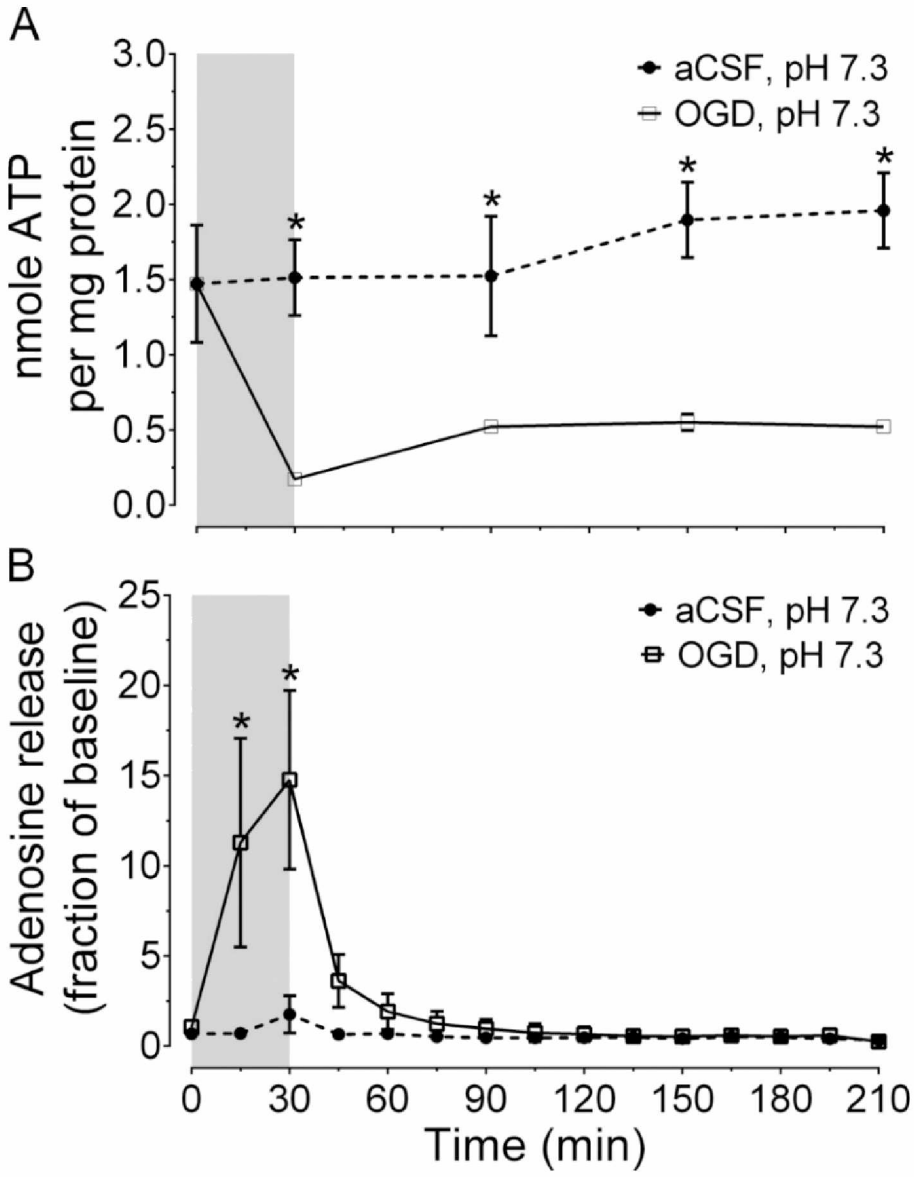

Figure 2.1: Integrity of acute slices is validated from observation that OGD injury causes disruption in energy homeostasis.

(A) Levels of whole tissue ATP were determined over a course of time using bath application in normoxic slices or slices treated with OGD. Grey bar indicates 30 min insult period. *p< 0.05 OGD, n= 4 versus aCSF, n= 4. Triplicate slices were pooled per treatment per time point, n= 4 animals. (B) Level of adenosine efflux monitored in slices subjected to 30 min aCSF or OGD using the microperfusion approach. Grey bar indicates 30 min insult period. *p< 0.05 represents adenosine efflux normalized to baseline (n= 7 control slices, 4 animals; n= 7 OGD slices, 4 animals).

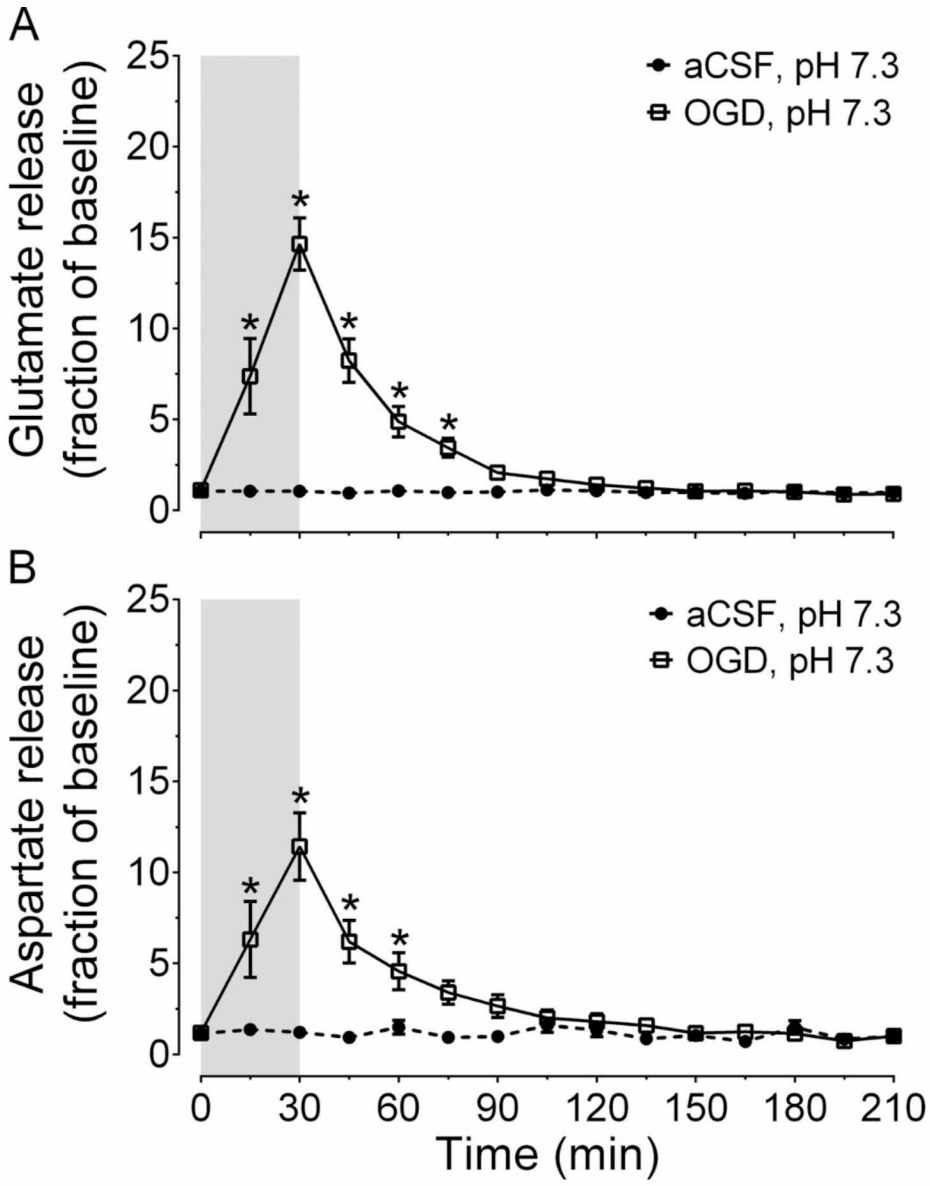

Figure 2.2. Oxygen glucose deprivation triggers efflux of excitatory amino acids similar to *in vivo* brain ischemia.

Time-dependent efflux in rat hippocampal slices induced by 30 min OGD insult. (A, B) Glutamate and aspartate efflux in hippocampal slices during OGD insult (n = 17 slices from 6 animals) and during aCSF (aCSF, pH = 7.3–7.4, n = 16 slices from 6 animals). Gray bar indicates insult period. Data shown are normalized to baseline (glutamate (μM/mg protein): aCSF = 3.7; OGD= 4.7; aspartate: aCSF = 1.2; OGD = 1.9); *$p < 0.05$ for OGD versus aCSF.

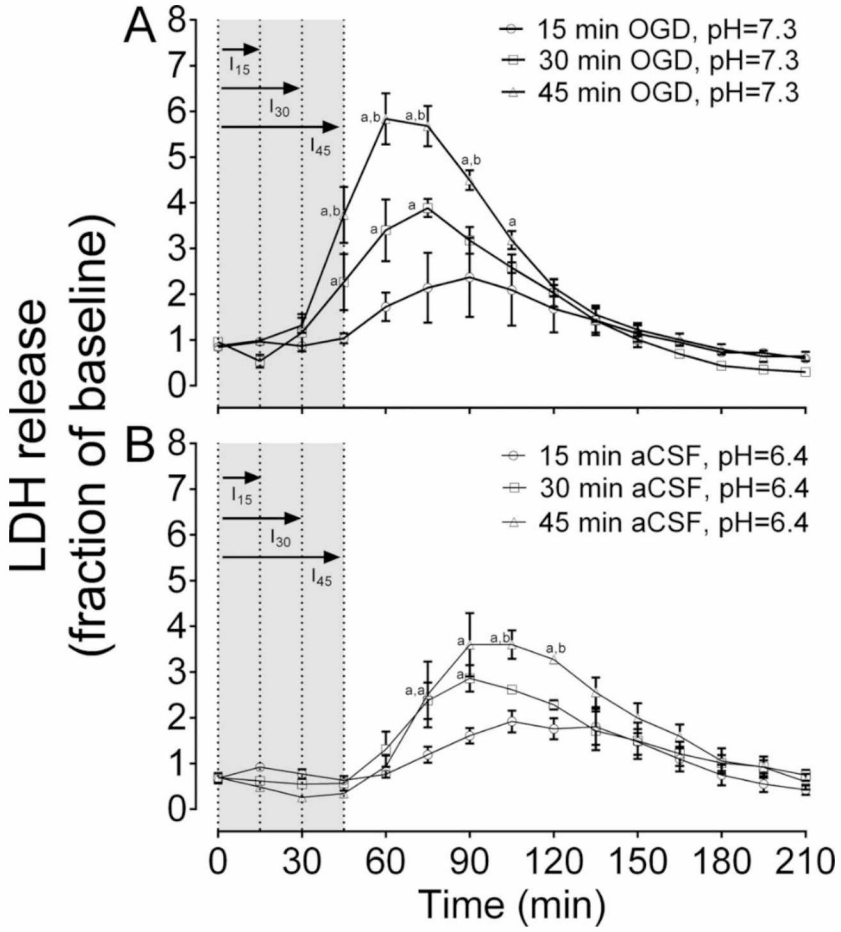

Figure 2.3. OGD or low pH acidosis causes injury during insult rather than during reperfusion.

Time course of LDH release induced by (A) OGD, pH 7.3 insult for 15 min (n = 4 slices), 30 min (n = 5 slices), or 45 min (n = 5 slices) followed by reperfusion (aCSF, pH = 7.3–7.4); Significant differences are represented as $^{a}p < 0.05$ versus OGD, pH 7.3 for 15 min, $^{b}p < 0.05$ versus OGD, pH 7.3 for 30 min. (B) aCSF, pH 6.4 insult for 15 min (n = 3 slices), 30 min (n = 3 slices) or 45 min (n = 3 slices) followed by reperfusion (aCSF, pH = 7.3). Significant differences are represented as $^{a}p < 0.05$ versus aCSF, pH 6.4 for 15 min, $^{b}p < 0.05$ versus aCSF, pH 6.4 for 30 min. Gray bar indicates insult period. "I" indicates insult phase (I_{15} = 15 min, I_{30} = 30 min, I_{45} = 45 min). All data were normalized to baseline measured as LDH release per mg of protein (15 min OGD, pH 7.3 = 0.315, 30 min OGD, pH 7.3 = 0.250, 45 min OGD, pH 7.3 = 0.359; 15 min aCSF, pH 6.4 = 0.163, 30 min aCSF, pH 6.4 = 0.169, 45 min aCSF, pH 6.4 = 0.162).

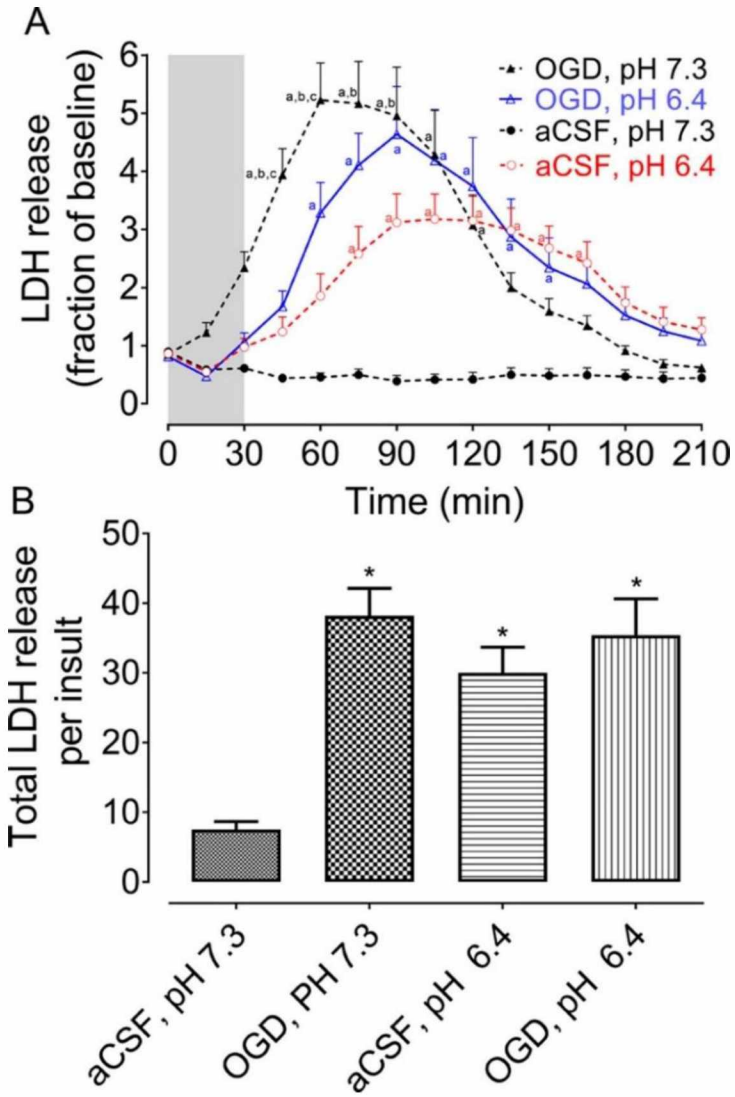

Figure 2.4. Acidosis (pH 6.4) delays OGD induced injury but produces injury independent of OGD.

(A) Shows time course of LDH release as a marker of cell death in acute hippocampal slices exposed to OGD, pH 7.3 (n= 23 slices from 23 animals); OGD, pH 6.4 (n=17 slices from 9 animals) or aCSF, pH 6.4 (n=28 slices from 14 animals). Grey bar indicates insult period. Data were normalized to baseline measured as LDH release per mg of protein (aCSF, pH 7.3 = 0.276; OGD, pH 7.3 = 0.324; aCSF, pH 6.4 = 0.174; OGD, pH= 0.244). Note that acidosis (pH 6.4) during OGD delays OGD induced cell death. $^{a}p< 0.05$ versus aCSF (pH 7.3), $^{b}p< 0.05$ versus aCSF (pH 6.4), $^{c}p< 0.05$ versus OGD (pH 6.4). Two-way ANOVA repeated measure with Bonferroni correction; means ± SEM. (B) Total LDH release represented by area under the curve. Note that the overall injury caused by pH 6.4 is as large as OGD or OGD with pH 6.4. *p<0.05 versus aCSF, pH 7.3 (n= 19).

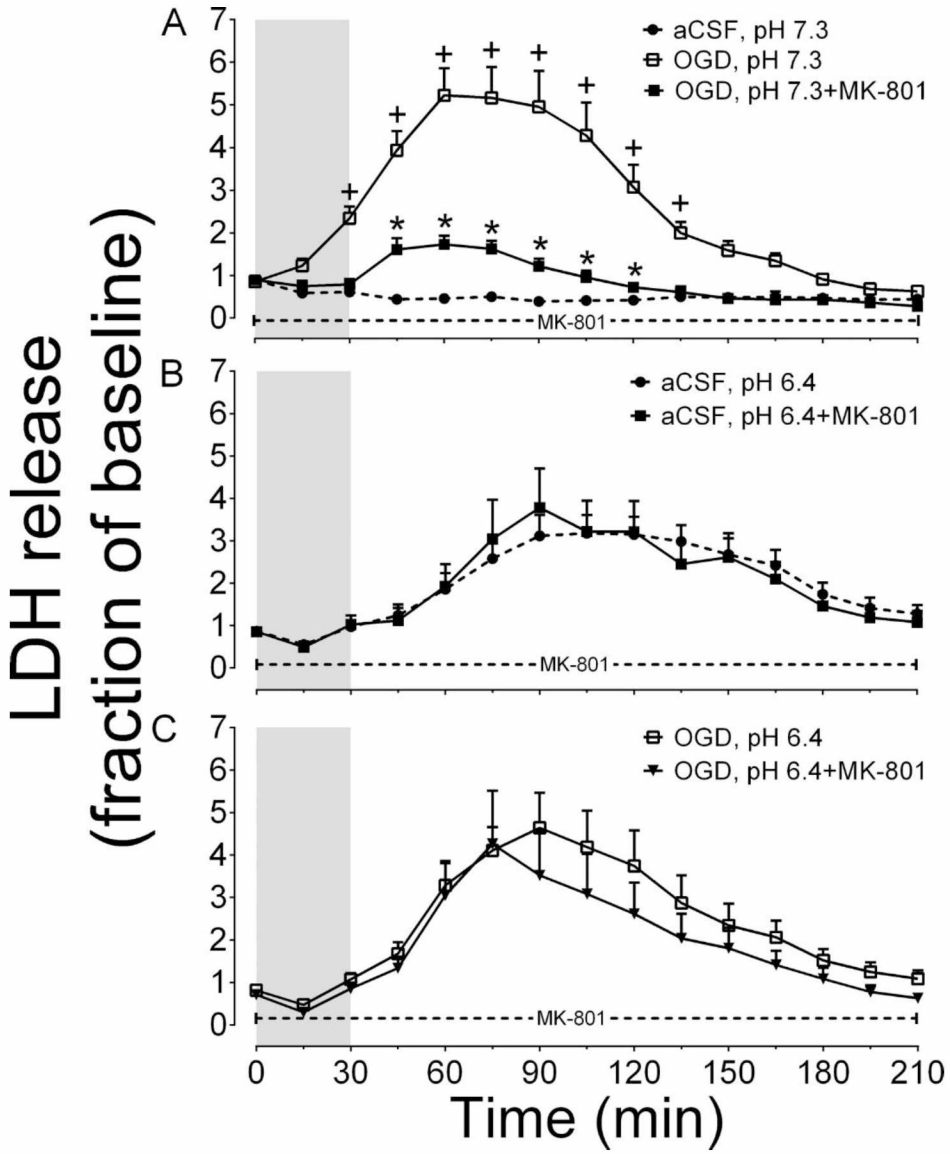

Figure 2.5. OGD insult is largely due to NMDAR activation whereas low pH injury is independent of NMDAR-mediated cytotoxic cascade.

(A) Slices incubated with 100 µM MK-801 followed by 30 min OGD, pH 7.3 (n= 6 slices, 3 animals) insult and LDH release was compared to OGD, pH 7.3 (n=23 slices, 23 animals). **(B-C)** Slices pre-incubated with 100 µM MK-801, exposed to either aCSF pH 6.4 (n=12 slices, 3 animals) or OGD pH 6.4 (n=12 slices, 4 animals) and LDH release was compared to aCSF pH 6.4 (n=28 slices, 14 animals) or OGD pH 6.4 (n=17 slices, 9 animals). Grey bar indicates insult period and dotted line indicates presence of MK-801. Data normalized to baseline measured as LDH release per mg of protein (aCSF, pH 7.3 = 0.276; OGD, pH 7.3 = 0.324; OGD + MK-801 = 0.677). *$p < 0.05$ versus OGD, pH 7.3; $^{+}p < 0.05$ versus aCSF, pH 7.3.

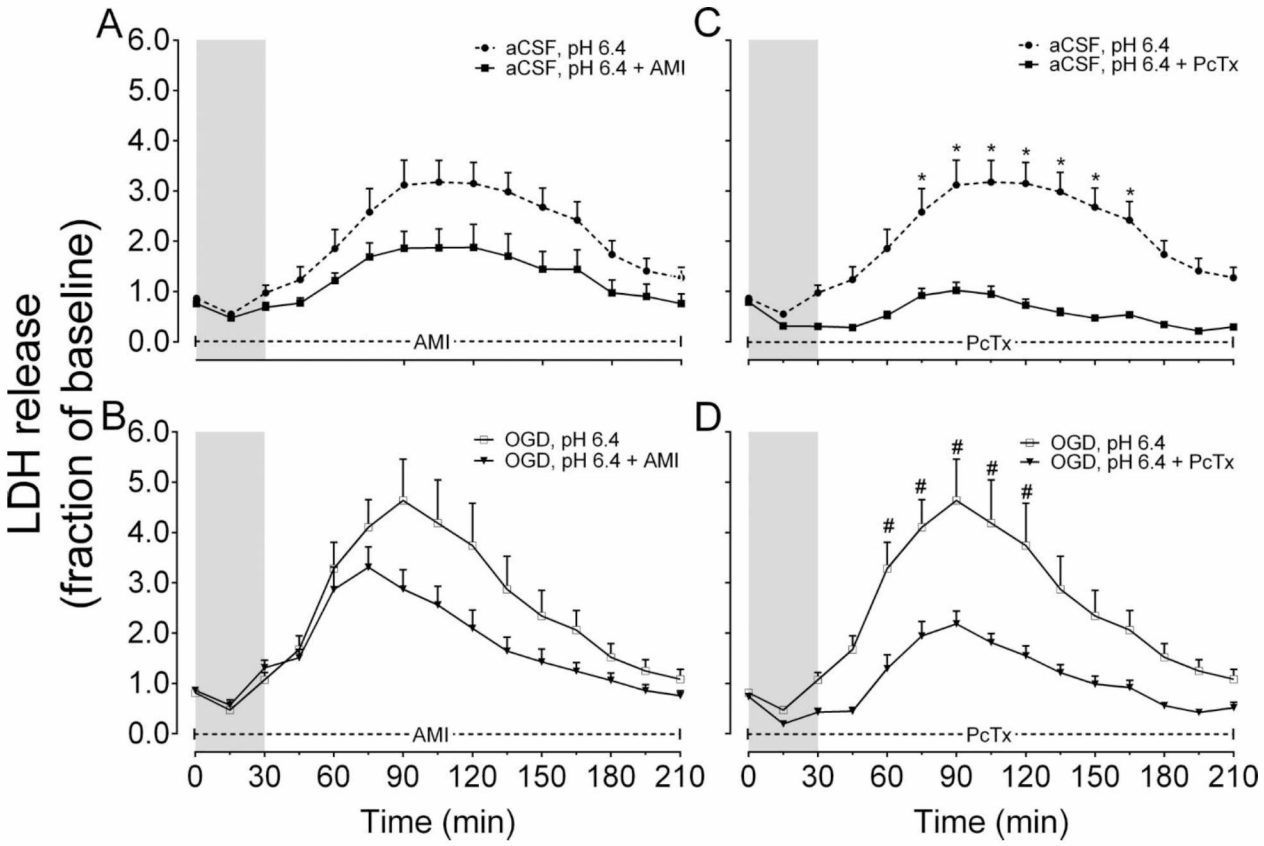

Figure 2.6. ASIC1a is partly responsible for mediating low pH mediated injury.

LDH measurement in response to aCSF pH 6.4 (n= 28) and during OGD pH 6.4 (n= 17) in presence of (A) aCSF pH 6.4 + 100μM AMI (n=20 slices, 7 animals), (B) OGD pH 6.4 + 100μM AMI (n= 9 slices, 5 animals), (C) aCSF pH 6.4 + 50 nM PcTx (n= 12 slices, 3 animals), (D) OGD pH 6.4 + 50 nM PcTx (n= 12 slices, 3 animals). Grey bar indicates insult period and dotted line indicates presence of AMI or PcTx. Note that blocking ASIC1a channels with PcTx1 significantly attenuates LDH release in both aCSF pH 6.4 and OGD pH 6.4 groups. Data were normalized to baseline measured as LDH release per mg of protein (aCSF pH 6.4 = 0.174; OGD pH 6.4= 0.244; aCSF pH 6.4 + AMI = 0.361, aCSF pH 6.4 + PcTx = 0.482, OGD pH 6.4 + AMI = 0.398, OGD pH 6.4 + PcTx = 0.299). Significant differences indicated as *$p< 0.05$ versus aCSF pH 6.4; #$p< 0.05$ versus OGD, pH 6.4.

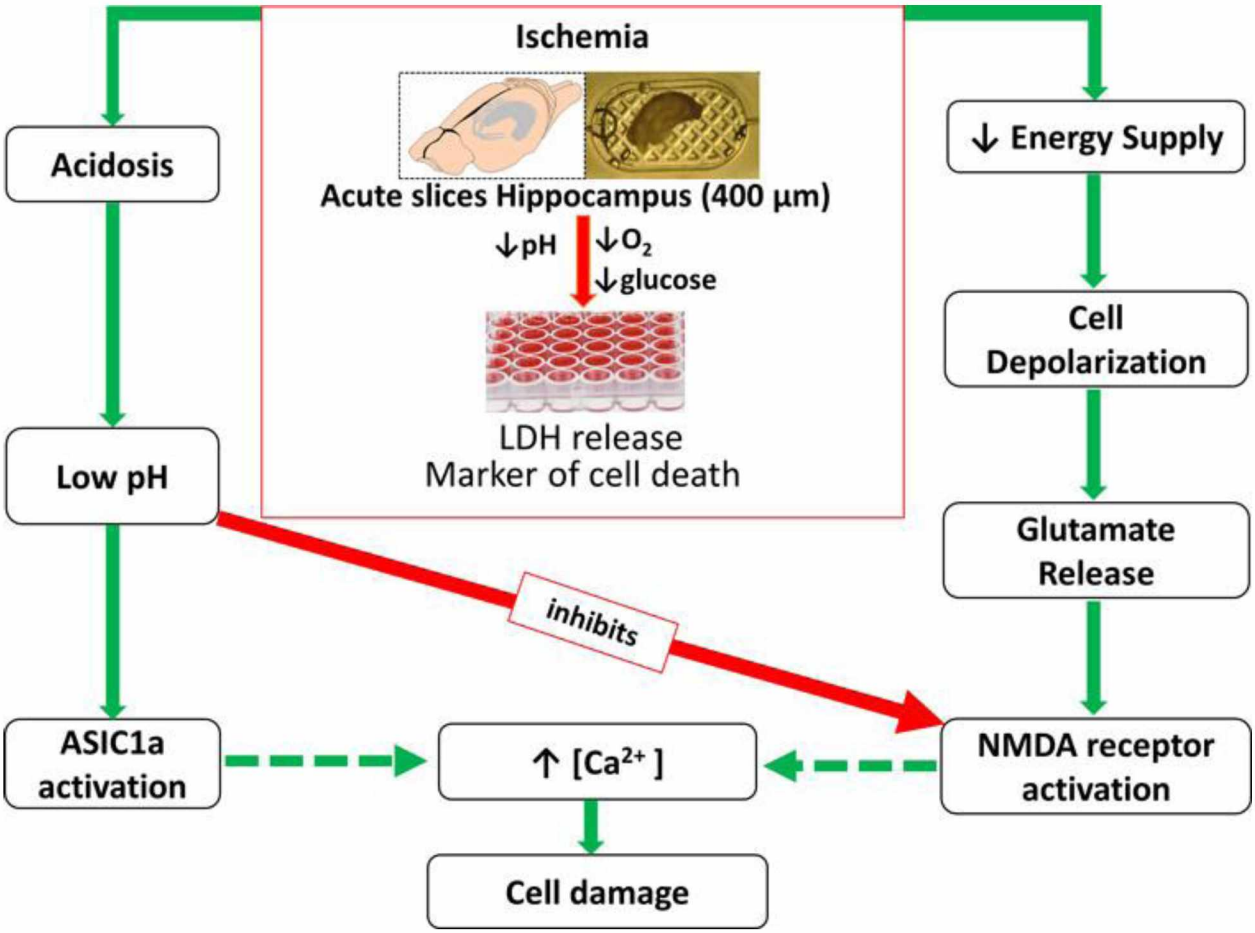

Figure 2.7 Graphical abstract. Acidosis overrides NMDA mediated excitotoxicity.

Schematic diagram illustrates that invitro ischemic like state (OGD) initiates a cascade of events leading to cell death wherein low pH abolishes OGD injury induced by NMDAR activation but causes cell death (LDH release) via ASIC1a activation. Green solid line represents ischemic cascade induced by OGD, green dotted line not addressed in this study but supported by others, red arrow represents low pH mediated elimination of NMDAR contribution to OGD-induced cell death.

2.7 References

Alvarez de la Rosa, D., Krueger, S. R., Kolar, A., Shao, D., Fitzsimonds, R. M. and Canessa, C. M. (2003) Distribution, subcellular localization and ontogeny of ASIC1 in the mammalian central nervous system. *The Journal of physiology,* **546,** 77-87.

Baron, A. and Lingueglia, E. (2015) Pharmacology of acid-sensing ion channels - Physiological and therapeutical perspectives. *Neuropharmacology,* **94,** 19-35.

Baron, A., Schaefer, L., Lingueglia, E., Champigny, G. and Lazdunski, M. (2001) Zn2+ and H+ are coactivators of acid-sensing ion channels. *The Journal of biological chemistry,* **276,** 35361-35367.

Baron, A., Waldmann, R. and Lazdunski, M. (2002) ASIC-like, proton-activated currents in rat hippocampal neurons. *The Journal of physiology,* **539,** 485-494.

Benveniste, H., Drejer, J., Schousboe, A. and Diemer, N. H. (1984) Elevation of the extracellular concentrations of glutamate and aspartate in rat hippocampus during transient cerebral ischemia monitored by intracerebral microdialysis. *Journal of neurochemistry,* **43,** 1369-1374.

Butcher, S. P., Bullock, R., Graham, D. I. and McCulloch, J. (1990) Correlation between amino acid release and neuropathologic outcome in rat brain following middle cerebral artery occlusion. *Stroke; a journal of cerebral circulation,* **21,** 1727-1733.

Chan, F. K., Moriwaki, K. and De Rosa, M. J. (2013) Detection of necrosis by release of lactate dehydrogenase activity. *Methods Mol Biol,* **979,** 65-70.

Cho, S., Wood, A. and Bowlby, M. R. (2007) Brain slices as models for neurodegenerative disease and screening platforms to identify novel therapeutics. *Current neuropharmacology,* **5,** 19-33.

Choi, D. W. (1992) Excitotoxic cell death. *Journal of neurobiology,* **23,** 1261-1276.

Christian, S. L., Ross, A. P., Zhao, H. W., Kristenson, H. J., Zhan, X., Rasley, B. T., Bickler, P. E. and Drew, K. L. (2008) Arctic ground squirrel (Spermophilus parryii) hippocampal neurons tolerate prolonged oxygen-glucose deprivation and maintain baseline ERK1/2 and JNK activation despite drastic ATP loss. *Journal of cerebral blood flow and metabolism : official journal of the International Society of Cerebral Blood Flow and Metabolism,* **28,** 1307-1319.

Cui, Y., Zhang, L., Utsunomiya, K., Yanase, H., Mitani, A. and Kataoka, K. (1999) Ischemia-induced glutamate release in the dentate gyrus. A microdialysis study in the gerbil. *Neuroscience letters,* **271,** 191-194.

Dale, N. and Frenguelli, B. G. (2009) Release of adenosine and ATP during ischemia and epilepsy. *Current neuropharmacology,* **7,** 160-179.

De Simoni, A., Griesinger, C. B. and Edwards, F. A. (2003) Development of rat CA1 neurones in acute versus organotypic slices: role of experience in synaptic morphology and activity. *The Journal of physiology,* **550,** 135-147.

Dunwiddie, T. V., Diao, L. and Proctor, W. R. (1997) Adenine nucleotides undergo rapid, quantitative conversion to adenosine in the extracellular space in rat hippocampus. *The Journal of neuroscience : the official journal of the Society for Neuroscience,* **17,** 7673-7682.

Ellison, G. (1995) The N-methyl-D-aspartate antagonists phencyclidine, ketamine and dizocilpine as both behavioral and anatomical models of the dementias. *Brain Res Brain Res Rev,* **20,** 250-267.

Frelin, C., Barbry, P., Vigne, P., Chassande, O., Cragoe, E. J., Jr. and Lazdunski, M. (1988) Amiloride and its analogs as tools to inhibit Na+ transport via the Na+ channel, the Na+/H+ antiport and the Na+/Ca2+ exchanger. *Biochimie,* **70,** 1285-1290.

Gao, J., Duan, B., Wang, D. G., Deng, X. H., Zhang, G. Y., Xu, L. and Xu, T. L. (2005) Coupling between NMDA receptor and acid-sensing ion channel contributes to ischemic neuronal death. *Neuron,* **48,** 635-646.

Giffard, R. G., Monyer, H., Christine, C. W. and Choi, D. W. (1990) Acidosis reduces NMDA receptor activation, glutamate neurotoxicity, and oxygen-glucose deprivation neuronal injury in cortical cultures. *Brain research,* **506,** 339-342.

Go, A. S., Mozaffarian, D., Roger, V. L. et al. (2014) Heart disease and stroke statistics--2014 update: a report from the American Heart Association. *Circulation,* **129,** e28-e292.

Gu, L., Liu, X., Yang, Y., Luo, D. and Zheng, X. (2010) ASICs aggravate acidosis-induced injuries during ischemic reperfusion. *Neuroscience letters,* **479,** 63-68.

Hagberg, H., Lehmann, A., Sandberg, M., Nystrom, B., Jacobson, I. and Hamberger, A. (1985) Ischemia-induced shift of inhibitory and excitatory amino acids from intra- to extracellular compartments. *Journal of cerebral blood flow and metabolism : official journal of the International Society of Cerebral Blood Flow and Metabolism,* **5,** 413-419.

Horvath, Z. C., Czopf, J. and Buzsaki, G. (1997) MK-801-induced neuronal damage in rats. *Brain research,* **753,** 181-195.

Hoyte, L., Barber, P. A., Buchan, A. M. and Hill, M. D. (2004) The rise and fall of NMDA antagonists for ischemic stroke. *Current molecular medicine,* **4,** 131-136.

Jaeschke, H. (1999) Kupffer cell-induced oxidant stress during hepatic ischemia-reperfusion: does the controversy continue? *Hepatology,* **30,** 1527-1528.

Kaku, D. A., Giffard, R. G. and Choi, D. W. (1993) Neuroprotective effects of glutamate antagonists and extracellular acidity. *Science,* **260,** 1516-1518.

Kalimo, H., Rehncrona, S. and Soderfeldt, B. (1981) The role of lactic acidosis in the ischemic nerve cell injury. *Acta neuropathologica. Supplementum,* **7,** 20-22.

Kalogeris, T., Baines, C. P., Krenz, M. and Korthuis, R. J. (2012) Cell biology of ischemia/reperfusion injury. *Int Rev Cell Mol Biol,* **298,** 229-317.

Khacho, M., Tarabay, M., Patten, D. et al. (2014) Acidosis overrides oxygen deprivation to maintain mitochondrial function and cell survival. *Nat Commun,* **5,** 3550.

Kilkenny, C., Browne, W. J., Cuthill, I. C., Emerson, M. and Altman, D. G. (2010) Improving bioscience research reporting: the ARRIVE guidelines for reporting animal research. *PLoS biology,* **8,** e1000412.

Kirschner, D. L., Jaramillo, M. and Green, T. K. (2007) Enantioseparation and stacking of Cyanobenz[f]isoindole-amino acids by reverse polarity capillary electrophoresis and sulfated beta-cyclodextrin. *Analytical chemistry,* **79,** 736-743.

Kirschner, D. L., Wilson, A. L., Drew, K. L. and Green, T. K. (2009) Simultaneous efflux of endogenous D-ser and L-glu from single acute hippocampus slices during oxygen glucose deprivation. *Journal of neuroscience research,* **87,** 2812-2820.

Kleyman, T. R. and Cragoe, E. J., Jr. (1988) Amiloride and its analogs as tools in the study of ion transport. *J Membr Biol,* **105,** 1-21.

Kloner, R. A. (1993) Does reperfusion injury exist in humans? *J Am Coll Cardiol,* **21,** 537-545.

Koh, J. Y. and Choi, D. W. (1987) Quantitative determination of glutamate mediated cortical neuronal injury in cell culture by lactate dehydrogenase efflux assay. *Journal of neuroscience methods,* **20,** 83-90.

Lam, T. I., Brennan-Minnella, A. M., Won, S. J., Shen, Y., Hefner, C., Shi, Y., Sun, D. and Swanson, R. A. (2013) Intracellular pH reduction prevents excitotoxic and ischemic neuronal death by inhibiting NADPH oxidase. *Proceedings of the National Academy of Sciences of the United States of America,* **110,** E4362-4368.

Latini, S. and Pedata, F. (2001) Adenosine in the central nervous system: release mechanisms and extracellular concentrations. *Journal of neurochemistry,* **79,** 463-484.

LeBlanc, M. H., Vig, V., Smith, B., Parker, C. C., Evans, O. B. and Smith, E. E. (1991) MK-801 does not protect against hypoxic-ischemic brain injury in piglets. *Stroke; a journal of cerebral circulation,* **22,** 1270-1275.

Lein, P. J., Barnhart, C. D. and Pessah, I. N. (2011) Acute hippocampal slice preparation and hippocampal slice cultures. *Methods Mol Biol,* **758,** 115-134.

Li, W. G., Yu, Y., Huang, C., Cao, H. and Xu, T. L. (2011) Nonproton ligand sensing domain is required for paradoxical stimulation of acid-sensing ion channel 3 (ASIC3) channels by amiloride. *The Journal of biological chemistry,* **286,** 42635-42646.

Lipton, S. A. (2004) Failures and successes of NMDA receptor antagonists: molecular basis for the use of open-channel blockers like memantine in the treatment of acute and chronic neurologic insults. *NeuroRx : the journal of the American Society for Experimental NeuroTherapeutics,* **1,** 101-110.

Lossi, L., Alasia, S., Salio, C. and Merighi, A. (2009) Cell death and proliferation in acute slices and organotypic cultures of mammalian CNS. *Prog Neurobiol,* **88,** 221-245.

Lushnikova, I. V., Voronin, K. Y., Malyarevskyy, P. Y. and Skibo, G. G. (2004) Morphological and functional changes in rat hippocampal slice cultures after short-term oxygen-glucose deprivation. *J Cell Mol Med,* **8,** 241-248.

McManus, T., Sadgrove, M., Pringle, A. K., Chad, J. E. and Sundstrom, L. E. (2004) Intraischaemic hypothermia reduces free radical production and protects against ischaemic insults in cultured hippocampal slices. *Journal of neurochemistry,* **91,** 327-336.

Mitani, A., Andou, Y., Matsuda, S., Arai, T., Sakanaka, M. and Kataoka, K. (1994) Origin of ischemia-induced glutamate efflux in the CA1 field of the gerbil hippocampus: an in vivo brain microdialysis study. *Journal of neurochemistry,* **63,** 2152-2164.

Nedergaard, M., Goldman, S. A., Desai, S. and Pulsinelli, W. A. (1991) Acid-induced death in neurons and glia. *The Journal of neuroscience : the official journal of the Society for Neuroscience,* **11,** 2489-2497.

Pignataro, G., Simon, R. P. and Xiong, Z. G. (2007) Prolonged activation of ASIC1a and the time window for neuroprotection in cerebral ischaemia. *Brain : a journal of neurology,* **130,** 151-158.

Regli, L., Anderson, R. E. and Meyer, F. B. (1995) Effects of intermittent reperfusion on brain pHi, rCBF, and NADH during rabbit focal cerebral ischemia. *Stroke; a journal of cerebral circulation,* **26,** 1444-1451; discussion 1451-1442.

Rehncrona, S., Rosen, I. and Siesjo, B. K. (1981) Brain lactic acidosis and ischemic cell damage: 1. Biochemistry and neurophysiology. *Journal of cerebral blood flow and metabolism : official journal of the International Society of Cerebral Blood Flow and Metabolism,* **1,** 297-311.

Ross, A. P., Christian, S. L., Zhao, H. W. and Drew, K. L. (2006) Persistent tolerance to oxygen and nutrient deprivation and N-methyl-D-aspartate in cultured hippocampal slices from hibernating Arctic ground squirrel. *Journal of cerebral blood flow and metabolism : official journal of the International Society of Cerebral Blood Flow and Metabolism,* **26,** 1148-1156.

Saeidnia, S., Manayi, A. and Abdollahi, M. (2015) From in vitro Experiments to in vivo and Clinical Studies; Pros and Cons. *Current drug discovery technologies,* **12,** 218-224.

Sapolsky, R. M., Trafton, J. and Tombaugh, G. C. (1996) Excitotoxic neuron death, acidotic endangerment, and the paradox of acidotic protection. *Advances in neurology,* **71,** 237-244; discussion 244-235.

Shimizu, H., Graham, S. H., Chang, L. H., Mintorovitch, J., James, T. L., Faden, A. I. and Weinstein, P. R. (1993) Relationship between extracellular neurotransmitter amino acids and energy metabolism during cerebral ischemia in rats monitored by microdialysis and in vivo magnetic resonance spectroscopy. *Brain research,* **605,** 33-42.

Siemkowicz, E. and Hansen, A. J. (1981) Brain extracellular ion composition and EEG activity following 10 minutes ischemia in normo- and hyperglycemic rats. *Stroke; a journal of cerebral circulation,* **12,** 236-240.

Simon, R. P., Benowitz, N., Hedlund, R. and Copeland, J. (1985) Influence of the blood-brain pH gradient on brain phenobarbital uptake during status epilepticus. *The Journal of pharmacology and experimental therapeutics,* **234,** 830-835.

Small, D. L., Monette, R., Mealing, G., Buchan, A. M. and Morley, P. (1995) Neuroprotective effects of omega-Aga-IVA against in vitro ischaemia in the rat hippocampal slice. *Neuroreport,* **6,** 1617-1620.

Sullivan, B. L., Leu, D., Taylor, D. M., Fahlman, C. S. and Bickler, P. E. (2002) Isoflurane prevents delayed cell death in an organotypic slice culture model of cerebral ischemia. *Anesthesiology,* **96,** 189-195.

Tang, C. M., Dichter, M. and Morad, M. (1990) Modulation of the N-methyl-D-aspartate channel by extracellular H+. *Proceedings of the National Academy of Sciences of the United States of America,* **87,** 6445-6449.

Taylor, C. P., Weber, M. L., Gaughan, C. L., Lehning, E. J. and LoPachin, R. M. (1999) Oxygen/glucose deprivation in hippocampal slices: altered intraneuronal elemental composition predicts structural and functional damage. *The Journal of neuroscience : the official journal of the Society for Neuroscience,* **19,** 619-629.

Tombaugh, G. C. and Sapolsky, R. M. (1990) Mild acidosis protects hippocampal neurons from injury induced by oxygen and glucose deprivation. *Brain research,* **506,** 343-345.

Traynelis, S. F. and Cull-Candy, S. G. (1990) Proton inhibition of N-methyl-D-aspartate receptors in cerebellar neurons. *Nature,* **345,** 347-350.

Waldmann, R., Champigny, G., Bassilana, F., Heurteaux, C. and Lazdunski, M. (1997) A proton-gated cation channel involved in acid-sensing. *Nature,* **386,** 173-177.

Wang, Y. Z., Wang, J. J., Huang, Y., Liu, F., Zeng, W. Z., Li, Y., Xiong, Z. G., Zhu, M. X. and Xu, T. L. (2015) Tissue acidosis induces neuronal necroptosis via ASIC1a channel independent of its ionic conduction. *Elife,* **4**.

Xiong, Z. G., Zhu, X. M., Chu, X. P. et al. (2004) Neuroprotection in ischemia: blocking calcium-permeable acid-sensing ion channels. *Cell,* **118,** 687-698.

Yagi, J., Wenk, H. N., Naves, L. A. and McCleskey, E. W. (2006) Sustained currents through ASIC3 ion channels at the modest pH changes that occur during myocardial ischemia. *Circulation research,* **99,** 501-509.

Yao, H., Sun, X., Gu, X., Wang, J. and Haddad, G. G. (2007) Cell death in an ischemic infarct rim model. *Journal of neurochemistry,* **103,** 1644-1653.

Yermolaieva, O., Leonard, A. S., Schnizler, M. K., Abboud, F. M. and Welsh, M. J. (2004) Extracellular acidosis increases neuronal cell calcium by activating acid-sensing ion channel 1a. *Proceedings of the National Academy of Sciences of the United States of America,* **101,** 6752-6757.

Chapter 3: Arctic ground squirrel hippocampus tolerates oxygen glucose deprivation independent of hibernation season even when not hibernating and after ATP depletion, acidosis, and glutamate efflux[2]

3.1 Abstract

Cerebral ischemia/reperfusion (I/R) triggers a cascade of uncontrolled cellular processes that perturb cell homeostasis. The arctic ground squirrel (AGS), a seasonal hibernator resists brain damage following cerebral I/R caused by cardiac arrest and resuscitation. However, it remains unclear if tolerance to I/R injury in AGS depends on the hibernation season. Moreover, it is also not clear if events such as depletion of ATP, acidosis, and glutamate efflux that are associated with anoxic depolarization are attenuated in AGS. Here, we employ a novel microperfusion technique to test the hypothesis that tolerance to I/R injury modeled in an acute hippocampal slice preparation in AGS is independent of the hibernation season and persists even after glutamate efflux. Acute hippocampal slices were harvested from summer euthermic AGS, hibernating AGS, and interbout euthermic AGS. Slices were subjected to oxygen glucose deprivation (OGD), an *in vitro* model of I/R injury to determine cell death marked by lactate dehydrogenase (LDH) release. ATP was assayed using ENLITEN ATP assay. Glutamate and aspartate efflux was measured using capillary electrophoresis. For acidosis, slices

---

[2] Published as Bhowmick S, Moore JT, Kirschner DL, Drew KL. "Arctic ground squirrel hippocampus tolerates oxygen glucose deprivation independent of hibernation season even when not hibernating and after ATP depl*et*ion, acidosis and glutamate efflux." J Neurochem. 2017 Feb 21. doi: 10.1111/jnc.13996. [Epub ahead of print]. PubMed PMID: 28222226

were subjected to pH 6.4 or ischemic shift solution (ISS). Acute hippocampal slices from rats were used as a positive control, susceptible to I/R injury. Our results indicate that when tissue temperature is maintained at 36°C, hibernation season has no influence on OGD-induced cell death in AGS hippocampal slices. Our data also show that tolerance to OGD in AGS hippocampal slices occurs despite loss of ATP and glutamate release, and persists during conditions that mimic acidosis and ionic shifts, characteristic of cerebral I/R.

3.2 Introduction

Brain tissue is highly vulnerable to ischemic injury in almost all species wherein occlusion of cerebral arteries causes either a transient or a permanent decrease in blood flow to the brain. This, in part, leads to tissue hypoxia (reduced O_2) wherein the tissue is unable to extract adequate O_2, the partial pressure of O_2within the tissue falls leading to a reduction in mitochondrial respiration and oxidative metabolism. In addition to hypoxia, decreased blood flow limits delivery of nutrients such as glucose and removal of metabolic waste such as lactate. This cascade of events results in irreversible neurological damage and leads to high rates of disability and death; nearly half of the survivors never regain functional independence (Go et al. 2014).

Arctic ground squirrels (AGS), *Urocitellus parryii*, resist cerebral ischemia injury. AGS is an obligate hibernating species that expends up to several weeks at a time in a highly regulated and reversible state of prolonged torpor. During torpor, metabolic rate, core body temperature (Tb), heart rate, and blood flow fall to ischemic-like levels without any evidence of ischemic injury (Frerichs et al. 1994, Ma et al. 2005, Weltzin *et al.* 2006). Previous work provides strong evidence that following cerebral I/R caused by cardiac

arrest or mimicked by *in vitro* preparations, AGS have the innate ability to tolerate cerebral ischemia/reperfusion (Christian et al. 2008, Ross et al. 2006, Dave et al. 2009). Ion homeostasis assessed by anoxic depolarization is delayed in AGS brain by 1.23 min compared to rat brain (Dave et al. 2009). Nonetheless, AGS hippocampus resists up to 2 h of oxygen glucose deprivation (OGD) (Christian et al. 2008), despite anoxic depolarization that occurs within ~ 6.6 min after onset of OGD (Dave et al. 2009).

Cerebral I/R initiates a cascade of events that causes excitatory release of glutamate leading to detrimental effects (Benveniste et al. 1984). However, it remains unclear, if glutamate is released in AGS after anoxic depolarization. Moreover, the contribution of hibernating season or state to ischemia tolerance in mammalian hibernators remains a matter of debate. Some studies suggest that the hibernation state increases tolerance to injury (Frerichs & Hallenbeck 1998, Zhou et al. 2001), and others show that tolerance is lost or decreased in animals during the summer season (Kurtz et al. 2006, Lindell et al. 2005). In contrast, other studies suggest that tolerance to modeled ischemia persists outside of the hibernation season (Dave et al. 2006, Ross et al. 2006, Christian et al. 2008).

In view of these observations, one goal of this study was to assess the influence of hibernating state (i.e., hibernating or not hibernating) and hibernation season (i.e., winter vs. summer) on resistance to OGD in AGS brain tissue. A second goal was to identify if events such as depletion of ATP, acidosis, and glutamate efflux that are associated with anoxic depolarization are attenuated in AGS. Here, we tested the hypothesis that tolerance to I/R injury modeled in an acute hippocampal slice preparation in AGS is independent of the hibernation season and persists even after glutamate efflux.

In this study, we specifically focused on acute hippocampal slices because prior results show that hippocampus plays an important role in both memory and learning and is more vulnerable to ischemic insults than other regions of the brain (Ouyang et *al.* 2007, Erfani et *al.* 2015).

Our results show that at the tissue level when tissue temperature is maintained at 36°C, hibernation season or state has no influence on OGD-induced cell death in AGS. Moreover, AGS tolerate OGD better than ischemic-susceptible Sprague-Dawley rats despite loss of ATP, excitatory amino acid release, and acidosis. In addition, tolerance persists under conditions that mimic acidosis and ischemic shifts characteristic of cerebral I/R *in vivo*.

3.3 Methods

3.3.1 Animal groups and determination of hibernation status

Arctic ground squirrel (AGS, *Urocitellus parryii*) and Sprague-Dawley rats were used for these experiments. All procedures were performed in accordance with University of Alaska Fairbanks Institutional Animal Care and use Committee (IACUC) and performed in accordance with the guidelines of the eighth edition of the Guide for the Care and Use of Laboratory Animals published by the US National Institutes of Health. Research was conducted in accordance with ARRIVE guidelines for reporting animal research (Kilkenny et al. 2010). AGS resist brain damage caused by global cerebral ischemia *in vivo* (Dave et al. 2009, Dave et al. 2006). The degree of ischemia resistance demonstrated by AGS is greater than other models of tolerance such as ischemia pre-conditioning. Moreover, unlike short-lived ischemia pre-conditioning that can be demonstrated in most species, ischemia resistance in AGS is chronic. Thus, AGS offer a unique and robust model of

resistance to ischemia that is unparalleled by any other species and cannot be mimicked by other known manipulations. AGS of both sexes were trapped during mid-July in the northern foothills of the Brooks Range, Alaska, 40 miles south of the Toolik Field Station of the University of Alaska Fairbanks (68°38 N, 149°38 W; elevation 809 m) and were transported to Fairbanks, AK under permit obtained from The Alaska Department of Fish and Game. AGS were housed individually in facilities with an ambient temperature (Ta) of 16–18°C and a 12:12-h light–dark cycle and fed rodent chow, sunflower seeds, and fresh carrots and apples *ad libitum* until mid-September, when they were moved to a cold chamber set to a Ta of 2°C and a 4: 20-h light–dark cycle. Male Sprague-Dawley rats (3–4 months of age at the time of the experiment) were purchased from Simonsen Laboratories (Gilroy, CA, USA) and were transported by air to the University of Alaska Fairbanks. Rats were housed in groups of two to four at 20–21°C, with a 12:12-h light–dark cycle, and were fed rodent chow *ad libitum*.

The arctic ground squirrels hibernate only in the winter season; so, hibernating and interbout arousal groups are from the winter season. Tissue from summer AGS was collected during the summer season. Differences between summer AGS and all other AGS were assessed to determine if season influenced tolerance to cerebral I/R injury. AGS late in a torpor bout were collected after 80–90% of the duration of the previous torpor bout (8–12 days) and were defined as hibernating AGS (*hAGS*); AGS early after inducing arousal from torpor (4 and 20 h) were used as interbout euthermy AGS (*ibe*AGS). Post-reproductive summer euthermic animals sampled in July and August 2–3 months after ending hibernation were used as summer euthermic AGS (*se*AGS). Subjects were matched as best as possible given the animals that were available for

study. Detailed characteristics are provided in Table S3.1. T_{rectal} and $T_{temporalis}$ were recorded at time of tissue collection. Arousal was induced by handling hibernating AGS. During interbout euthermy, tissue was collected 4 h after inducing arousal (4 h *ibe*AGS) or 20 h after inducing arousal (20 h *ibe*AGS). Ambient temperature and light–dark cycle remained the same for all groups.

3.3.2 Acute hippocampal slice preparation and *in vitro* modeled ischemia / reperfusion

Animals were anesthetized using 5% (v/v) isoflurane with medical grade O_2 at a constant flow rate of 1.5 L/min. Once unresponsive, the animals were killed via rapid decapitation and brains were removed within 2 min. The whole brain was then placed in ice chilled, oxygenated HEPES-buffered artificial cerebral spinal fluid (HEPES-aCSF) containing 120 mM NaCl, 20 mM $NaHCO_3$, 6.68 mM HEPES acid, 3.3 mM HEPES sodium salt, 5.0 mM KCl, and 2.0 mM $MgSO_4$ (pH 7.3–7.4) to attenuate edema during the course of slicing and incubation. Rapidly dissected hippocampi were embedded in 2.5% agar and transverse hippocampal slices. Approximately, 10 mm were discarded from both ends and 400 µm thick slices from each hippocampus (~50–60 slices) were cut at approximately 2°C in oxygenated HEPES-aCSF using a Vibratome®1000 plus sectioning system (The Vibratome Company, St. Louis, MO, USA). The slices were then transferred to a brain slice keeper (Scientific Systems Design Inc., Mississauga, Ontario, CA, USA) and allowed to recover for 1–1.5 h at room temperature 20–21°C in HEPES-aCSF bubbled continuously with 95% O_2/5% CO_2 before transferring to microperfusion chambers.

To address the time course of injury, treatment was applied using an *in vitro* microperfusion technique described previously. Briefly, after 1–1.5 h recovery

as described above, individual slices were transferred gently to microperfusion chambers and lids sealed. The 4–8 parallel chambers were perfused with artificial cerebrospinal fluid (aCSF), pH 7.3 containing 120 mM NaCl, 45 mM $NaHCO_3$, 10 mM glucose, 3.3 mM KCl, 1.2 mM NaH_2PO_4, 2.4 mM $MgSO_4$, and 1.8 mM $CaCl_2$ equilibrated with 95% O_2/5% CO_2 and submerged in aCSF bath at 36°C (± 0.2°C) at a flow rate of 7 µL/min. The osmolarity of these solutions was between 290 and 300 mOsm. Sampling began no sooner than 75 min after submerging the sealed chambers to allow adequate time for stabilization of neurochemical efflux. Perfusates was collected at 15 min intervals and analyzed as indicated.

3.3.3 Treatment and injury conditions

To model *in vivo* ischemia/reperfusion (I/R)-induced alterations in the ionic microenvironment, hippocampus slices were perfused with one of the following: (i) aCSF, pH 7.3 as a control solution, (ii) OGD, pH 7.3 (glucose-oxygen-free aCSF), (iii) aCSF, pH 6.4, (iv) ionic shift solution (ISS), pH 6.5. aCSF, pH 6.4 containing 120 mM NaCl, 7.03 mM $NaHCO_3$, 10 mM glucose, 3.3 mM KCl, 1.2 mM NaH_2PO_4, 2.4 mM $MgSO_4$, and 1.8 mM $CaCl_2$. Ionic shift solution (ISS), pH 6.5 contained 36.5 mM NaCl, 11 mM Na-gluconate, 65 mM K-gluconate, 38 mM NMDG-Cl, 1 mM NaH_2PO_4, 0.13 mM $CaCl_2$, 2.4 mM $MgCl_2$, and 1 mM $NaHCO_3$ as described previously (Ming et *al.* 2006). All aCSF solutions (pH 7.3 and 6.4) were equilibrated with 95% O_2 and 5% CO_2, whereas the OGD and ISS solutions were equilibrated with 5% CO_2 and 95% N_2, for a minimum of 1 h until pH stabilized in the desired range. The PO_2 in OGD and ISS solution varied from 0 to 2.9 mmHg with an average of six determinations of 1.1 mmHg as measured using a miniature Clark-style electrode (Instech Laboratories, Plymouth Meeting, PA, USA). Fractions were analyzed

for cellular injury (LDH release) on the day of collection. Remaining volume was kept at −80°C for subsequent analysis.

3.3.4 Quantification of cell death

Lactate dehydrogenase (LDH) concentration in the perfusates was used as a marker of necrotic tissue damage. Perfusates, 50 µL was transferred to 384-well plates and mixed with 50 µL reaction solution provided in the LDH assay kit (Cayman Chemical, Ann Arbor, MI, USA). Optical density was measured at 490 nm 60 min later, using a microplate reader (BioTek Epoch, Winooski, VT, USA). Background absorbance at 620 nm was subtracted. The LDH release was expressed in arbitrary units per mg of protein (Biorad protein assay kit, Hercules, CA, USA). The maximal releasable LDH was also obtained by treating the slices with 1% NP-40 lysis buffer (50 mM Tris-HCl, 0.5% sodium deoxycholate, 0.1% sodium dodecyl sulfate, 1% Igepal, 150 mM NaCl, 0.05% Triton X-100) at the end of each experiment.

3.3.5 Determination of ATP

ATP was determined after bath application of OGD or aCSF as described previously (Christian et al. 2008). In brief, slices were incubated in either aCSF or OGD solution and collected at the time point indicated. From each treatment condition, three hippocampal slices were transferred to a flat-bottomed microfuge tube containing 200 µL of ice-cold 5% trichloroacetic acid, and were sonicated (8 pulses), centrifuged at 16 000 g for 1 min at 4°C. Supernatant was then collected and assayed for ATP using ENLITEN ATP assay (Promega, Madison, WI, USA). The pellets were further reconstituted with 200 µL 1 M NaOH and protein concentration was analyzed (Bio-Rad protein assay kit,

Hercules, CA, USA). ATP activity was represented as a concentration of ATP normalized to total protein.

3.3.6 Capillary electrophoresis determination of glutamate and aspartate efflux

Glutamate and aspartate were analyzed by capillary electrophoresis. Perfusates were derivatized as described previously (Kirschner et al. 2009, Kirschner et al. 2007) to form highly fluorescent cyanobenz[f]isoindole amino acids (CBI-amino acids). Briefly, 2 µL of thawed perfusates was reacted with 2 µL of 2 mM naphthalene-2,3-dicarboxaldehyde in methanol and 2 µL NaCN (5.5 mM) in 60 mM sodium tetraborate. Cyanide solution contained 3 µM D-amino adipic acid as internal standard. Samples were reacted at 20–21°C for approximately 20 min prior to analysis. CE-LIF was performed on a custom in-house-built instrument using a 420-nm diode laser, 490-nm bandpass filter, and photomultiplier tube (PMT) for LIF detection. Samples were injected onto a bare fused silica capillary of dimensions 25 cm × 25 µm (22.5 cm to detection window) for 1–3 s at 380-mbar vacuum and separated using positive polarity (20 kV). Separation buffer optimized for analysis of L-glutamate and L-aspartate is a 50-mM sodium tetraborate background electrolyte adjusted to pH 9.3. Background electrolyte additionally contained 1.0 mM β-cyclodextrin to decrease sample run time for glutamate and aspartate analysis. The addition of β-cyclodextrin allowed for baseline resolution of glutamate, aspartate, and the internal standard in < 2 min. PeakFit software (SeaSolve Software Inc., Framingham, MA, USA) was used to process raw data and quantify peak areas in all experiments based on a Gaussian peak shape for each analyte. Linear calibration curves were constructed for glutamate and aspartate as a function of concentration versus the peak area ratio (analyte area/internal standard area). Efflux of analytes was quantified as a concentration

of glutamate or aspartate normalized to total protein for the slice used in the efflux experiment and represented as a fraction of baseline glutamate or aspartate release.

3.3.7 Statistical analysis

A priori power analysis (G*Power software, (Faul et *al.* 2007)) was performed to estimate sample size needed to yield 80% power for detecting a significant ($p < 0.05$) effect of treatment. An expected difference in means of 17.81 and standard deviations of 10.93 and 2.24, taken from rat OGD and seAGS OGD indicates that a sample size of five slices will have 80% power for detecting a difference. For experimental group with smaller sample size, no non-significant effect was under powered. No animal was excluded from the study. Slices from animals were randomly assigned to treatment and control groups without prior knowledge to the treatment conditions. The statistical analysis was performed on the data that were normalized to baseline and expressed as fraction of baseline to avoid any variation in the baseline values among the treatment groups. Baseline was calculated as the mean of the two samples preceding onset of treatment (Table S3.2). Data processing and statistical analyses were performed using Microsoft Office Excel 2010 and Prism6 (GraphPad, San Diego CA, USA). Data were analyzed with one-way or two-way ANOVA with repeated measures. Significant main effects or interactions were followed by *t*-tests with Bonferroni's correction. Data are expressed as mean ± SEM, and $p < 0.05$ was considered statistically significant. Treatment with aCSF and OGD were run in every experiment and combined for the final analysis; as a result, sample size was larger in aCSF and OGD groups than in many of the experimental manipulations.

3.4 Results

3.4.1 Tolerance to OGD injury in AGS hippocampus is not dependent on hibernation season

To investigate whether at the tissue level when tissue temperature is normalized to 36°C, AGS are more tolerant to OGD injury than ischemic-susceptible rats; hippocampal slices from a cohort of each species were examined. Following 30 min of OGD, slices harvested from rats displayed a significant increase in LDH release relative to control slices (aCSF, $n = 25$ slices; OGD, $n = 30$ slices, 15 animals, $p < 0.0001$, two-way ANOVA, treatment × time). *se*AGS showed a significant increase in LDH release relative to aCSF treated control slices (aCSF, $n = 28$ slices; OGD, $n = 30$ slices, 14 animals, $p = 0.0001$, two-way ANOVA, treatment × time). When OGD treated slices from rats and *se*AGS were compared, rat slices displayed a significantly greater degree of LDH efflux than AGS slices (rat, OGD, $n = 30$ from 15 animals; AGS, OGD, $n = 30$ from 14 animals, $p < 0.0001$, two-way ANOVA, species × time) (Figure. 3.1a).

Next, to confirm our ability to detect an increase in LDH release in AGS hippocampus, we applied TritonX-100, a non-ionic detergent to directly disrupt cell membrane as a positive control. Treatment of slices with 0.1% TritonX-100 produced a significant increase in LDH release (aCSF, $n = 4$ slices; 0.1% TritonX-100, $n = 4$ slices, two animals, $p < 0.0001$, two-way ANOVA, treatment × time) (Figure. 3.1b). We further analyzed the total LDH content per slice to investigate if the amount of LDH release following OGD is limited by total LDH content. No difference in total LDH content was observed in slices from rats or AGS that were subjected to either aCSF or OGD treatment (Figure S3.1). These results suggested that the difference in LDH release between rats

and AGS is not because of a difference in total LDH content but is because of a difference in the injury associated with OGD exposure.

Next, to address if tolerance to OGD injury depends on the hibernation season, groups of AGS – *se*AGS, *h*AGS, and *ibe*AGS, 4 or 20 h after inducing arousal, were matched as best as possible for season, frequency, age, sex, and body weight prior to tissue collection. Body weight of *se*AGS was greater than *h*AGS and *ibe*AGS because of the seasonal fattening of this species (Sheriff et *al.* 2013). Because date of birth is not known for AGS, age is only reported as adult which means > 1 year old. T_{rectal} and $T_{temporalis}$ did not differ between *se*AGS and *ibe*AGS, 4 h or 20 h after inducing arousal, but were as expected warmer than T_{rectal} and $T_{temporalis}$ in *h*AGS at time of tissue collection (Table S3.1). All tissues were normalized to 36°C prior to experimental manipulations. Results show that OGD induced a significant increase in total LDH release in the 20 h *ibe*AGS group compared to *se*AGS ($p = 0.01$, one-way ANOVA, $n = 30–33$ slices, (Figure 3.1c). Relative to aCSF (Figure 3.1c and d), OGD induced a onefold increase in total LDH release in *se*AGS, 4 h *ibe*AGS, and *h*AGS slices. In contrast, OGD induced a threefold increase in LDH release in 20 h *ibe*AGS. The same pattern was seen when the effect of OGD on LDH was assessed over time. A significant LDH response was observed in slices from 20 h *ibe*AGS during OGD compared to *seAGS*, 4 h *ibe*AGS, and *h*AGS slices ($p < 0.0001$, two-way ANOVA season x time). However, the statistically significant injury observed in slices taken from 20 h *ibe*AGS OGD, was less than the injury observed in slices from rat OGD ($p < 0.0001$, two-way ANOVA species (rat and 20 h *ibe*AGS) × time) (Figure 3.1a and c). These results suggest that 20 h into interbout euthermy, AGS hippocampus is the most vulnerable to OGD relative to other times in the hibernation

season. However, even at this most vulnerable time point, AGS are still less vulnerable to OGD-induced cell death than rats.

3.4.2 Tolerance to injury in AGS hippocampus is not reversed by ionic shift solution (ISS) or low pH

Ionic homeostasis has been tightly linked to cell injury/death (Bortner & Cidlowski 2004). To simulate the ionic microenvironment in our *in vitro* slice preparation to mimic the changes in the extracellular milieu that occurs *in vivo* during cerebral I/R, slices from rats and AGS were subjected to 30 min of an ionic shift solution insult (K^+ = 65 mM; Na^+ = 55 mM; HCO_3^- = 2.5 mM, Cl^- = 77.0 mM, pH 6.5) and LDH release was measured. Results show that slices from rats show significant release of LDH as compared to control slices (aCSF, $n = 3$; ISS, $n = 3$ slices from four animals, $p < 0.0001$, two-way ANOVA, treatment x time). In contrast, ISS had no influence on slices from *seAGS* (aCSF, $n = 3$; ISS, $n = 3$ from three animals, $p = 0.10$, two-way ANOVA, treatment × time). ISS-treated slices from rats also displayed significant increase in LDH release compared to *se*AGS slices. ($p < 0.0001$, two-way ANOVA, species × time) (Figure 3.2a). Next, we addressed the role of pH alone in acute hippocampal slices. Rat slices subjected to 30 min low pH 6.3 causes significant LDH release (aCSF, pH 7.4 = 7 slices, six animals; aCSF, pH 6.3 = 7 slices, five animals, $p = 0.001$, two-way ANOVA, treatment × time). In contrast, AGS slices displayed no significant release of LDH with low pH compared to control slices (aCSF, pH 7.4 = 7 slices, five animals; aCSF, pH 6.3 = 7 slices, four animals). When low pH-treated slices from rats and *se*AGS were compared, rat slices displayed significantly greater LDH efflux than AGS slices (rat aCSF pH 6.3, $n = 7$ slices, five animals; AGS

aCSF pH 6.3, $n = 7$ slices, four animals, $p < 0.0001$, two-way ANOVA, species × time) (Figure 3.2b).

We also explored pH-dependent injury over a wider range of pH (pH 7.4, 7.0, 6.6, 6.3) in *se*AGS. We found that pH did not influence LDH release in *se*AGS (aCSF pH 7.4, $n = 7$; aCSF pH 7.0, $n = 4$; aCSF pH 6.6, $n = 5$; aCSF pH 6.3, $n = 7$; 15 animals; $p = 0.33$, one-way ANOVA) (Figure S3.2). This suggests that AGS hippocampus is less vulnerable to the damaging effects of ISS or low pH than rats.

3.4.3 AGS hippocampus resists OGD injury not because of enhanced energy conservation

In the context of bioenergetics, the brain consumes large amounts of oxygen to maintain ionic gradients across neuronal plasma membranes. However, ischemic injury causes bioenergetic failure leading to depletion in cellular ATP and prevents neurons from maintaining membrane potential, resulting in neuronal depolarization. Here, we investigated whether resistance to ischemic injury in AGS is as a result of preservation of energy homeostasis. We tested this by exposing acute hippocampal slices from *se*AGS and rats to 30 min of OGD and monitoring ATP levels. Results show that exposure of rat hippocampal slices to 30 min OGD produced a significant depletion in ATP when compared to control slices. Slices with OGD showed no significant signs of ATP restoration even after 3 h of reperfusion (aCSF, $n = 4$ slices; OGD, $n = 4$, four animals, $p = 0.0037$, two-way ANOVA, treatment x time; Figure 3.3a. Hippocampal slices from *se*AGS displayed similar depletion in ATP following OGD when compared to slices exposed to aCSF (aCSF, $n = 3$ slices, OGD, $n = 3$ slices, three animals, $p = 0.0097$, two-way ANOVA, treatment × time). Tendency to restore ATP following reperfusion was similar

in rat and AGS slices Figure 3.3b. These results indicate that energy homeostasis is disrupted in AGS in a fashion similar to rats and that tolerance to OGD cannot be explained by enhanced energy homeostasis.

3.4.4 Tolerance to OGD in AGS hippocampus is not because of inhibition of excitatory neurotransmitter efflux

We next investigated if tolerance to ischemia in AGS is associated with dampening of excitatory neurotransmitter release, which occurs following ischemia-induced depletion of cellular ATP. This was tested by exposing acute hippocampal slices from *se*AGS and rats to 30 min of OGD and monitoring efflux of glutamate and aspartate using capillary electrophoresis. Results show that rat slices exposed to OGD displayed a 2.3-fold increase in glutamate efflux over basal efflux (n = 16 control slices, 12 animals; n = 17 OGD slices; 12 animals, $p < 0.0001$, two-way ANOVA, treatment × time) Figure 3.4a; aspartate efflux also increased during OGD in rats (1.7-fold increase over basal efflux, n = 16 control slices, 12 animals; n = 17 OGD slices; 12 animals, $p < 0.0001$, two-way ANOVA, treatment × time) Figure 3.4c. After the onset of reperfusion, the glutamate levels returned to baseline levels within 60 min, aspartate returned to baseline levels within 45 min. *se*AGS slices exposed to 30 min OGD displayed both glutamate (threefold increase over basal level, $p < 0.0001$, two-way ANOVA, treatment x time) and aspartate efflux (1.3-fold increase over basal level, $p < 0.0001$, two-way ANOVA, treatment × time; n = 14 slices from five *se*AGS) (Figure 3.4b and d). The magnitude and time course of excitatory amino acid efflux in AGS approximates efflux seen in rat hippocampal slices. Despite excitatory neurotransmitter efflux, AGS resist OGD-induced

injury suggesting that cerebral I/R injury is modulated in AGS downstream to, or independent of glutamate or aspartate release.

3.5 Discussion

Using an *in vitro* microperfusion approach to avoid the influence of cold tissue temperature that is unavoidable in whole animal studies, we have identified that the hibernating state or the hibernation season is not necessary for AGS tolerance to cerebral I/R modeled in acute hippocampal slices. The time that AGS are most vulnerable to OGD is 20 h into an interbout arousal although even at this most vulnerable period, resistance to OGD in AGS is substantially better than resistance to OGD in rat hippocampal slices. Secondly, our data unequivocally show that tolerance to OGD in AGS hippocampal slices occurs despite loss of ATP, and excitatory amino acid release and persists during conditions that mimic acidosis (Siesjo 1988) and ionic shifts characteristic of cerebral I/R (Hansen & Zeuthen 1981, Yanagihara & McCall 1982).

3.5.1 The hibernating state or the hibernation season is not necessary for AGS tolerance

This work showing that in AGS, the hibernation season or state does not define tolerance to OGD is significant because it is the first set of studies to systematically test the response to OGD in hippocampal tissue throughout the season and hibernation state in AGS. Dave et *al*., concluded that in AGS, hibernation season was not required for resistance to brain injury following cardiac arrest (Dave et al. 2006), however, studies were only performed during the summer season. (Christian et al. 2008) concluded that hippocampal slices from AGS were least vulnerable to OGD during the summer season. However, the propidium iodide staining used by (Christian et al. 2008) to measure cell death produced high background levels. Background levels of cell death were highest in

the summer season and could have masked effects of OGD. (Ross et al. 2006) also showed that the hibernation state did not influence tolerance to OGD in the first 24 h of culture. However, as with (Christian et al. 2008) , high background cell death measured in cultured slices using propidium iodide may have compromised sensitivity to detect cell death. These results confirm that when tissue temperature is normalized to 36°C both summer and hibernating AGS resist OGD. While vulnerability to OGD is always less in AGS than in rats, vulnerability in AGS does increase slightly toward the end of arousal. Arousal from prolonged torpor is the most stressful aspect of hibernation indicated by increased levels of Hypoxia-inducible factor 1-α (HIF-1α) and inducible nitric oxide synthase (Ma et al. 2005). It is likely that the physiological challenge of rewarming, reanimating, and reperfusing the brain contributes to vulnerability to OGD.

Tolerance, independent of season or state may be unique to the AGS. Others (Frerichs & Hallenbeck 1998) showed that hibernation state increases tolerance to OGD in 13-lined ground squirrel hippocampus. (Kurtz et al. 2006) demonstrated that hibernation season increases tolerance to I/R in 13-lined ground squirrel in liver and gut. In contrast, the hibernation season is not required for tolerance to I/R in other organs in AGS (Bogren et al. 2014a, Bogren et al. 2014b). A recent study in AGS, however, did reveal cardioprotective benefit of the hibernation season during cardiopulmonary bypass *in vivo* with a core body temperature of 18°C (Quinones et *al.* 2016). Heart may differ from brain and a longer duration (45 min) of ischemia studied in the cardiopulmonary bypass procedure may have revealed a seasonal difference not evident in studies of cerebral I/R tolerance in AGS.

Cold tissue temperature is protective (Busto et *al.* 1987) and confounds whole animal comparisons between hibernating and euthermic ground squirrels. With the acute slice model, it is possible to avoid the influence of cold tissue temperature which is not possible in whole animal models because hibernating animals have a core and brain temperature near 0°C and euthermic animals have a core and brain temperature near 37°C. Seasonal comparisons between summer and winter euthermic animals can be made in whole animals without confounding influence of temperature since both groups have body temperatures near 37°C. Our results are consistent with whole animal studies that show that tolerance to I/R or hypoxia does not require the hibernation season (D'Alecy et al. 1990, Dave et al. 2009, Dave et al. 2006, Bogren et al. 2014a, Bogren et al. 2014b). The present results confirm that AGS do not need to be cold to tolerate cerebral I/R better than rats although cold tissue temperature would likely enhance tolerance as noted by (Frerichs & Hallenbeck 1998).

Our results suggest that the contribution of A1 receptors to seasonal hibernation does not impact cerebral I/R tolerance since season did not play a significant role in tolerance. A1 receptor activation is necessary and sufficient to drive onset of hibernation, however, only in the winter season (Jinka et *al.* 2011). Sensitivity to A1 adenosine receptor agonists increase in the hibernation season (Olson et *al.* 2013) and A1 adenosine receptor agonists are neuroprotective (Cunha 2005). However, differences in A1 sensitivity between summer and winter is not relevant to cerebral I/R tolerance since we and others have not found a significant influence of season on tolerance. Indeed, tolerance in AGS does not depend on the hibernation state or season.

The novel microperfusion method developed in our laboratory (Kirschner et al. 2009) for study of cell death in acute, adult slices overcomes the limitations of methods used in prior studies where high baseline cell death may have compromised interpretation. The microperfusion approach minimizes background cell death by capturing LDH release from the entire slice. This approach is an improvement over other methods where stains such as propidium iodide show cell death only on the surface of the freshly cut slice (Ross et al. 2006, Christian et al. 2008). Moreover, the microperfusion approach allows us to study cell death in adult AGS tissue. The ability to study adult tissue is an advantage since access to perinatal tissue is restricted by the seasonal breeding cycle of AGS. In addition, interpretation of organotypic cultures is limited by developmental age of the tissue (Fukuda et al. 1995). The *in vitro* microperfusion approach in our study might not apply to the *in vivo* scenario wherein whole animal mechanisms such as pH buffering capacity and limited inflammatory response contribute to tolerance to ischemia reperfusion injury (Bogren et al. 2014a, Bogren et al. 2014b). Nonetheless, the microperfusion approach isolates processes occurring at the tissue level so that interpretation is not confounded by whole animal physiology. Moreover, the microperfusion approach allows for the concentration of each component in the perfusion fluid to be defined and manipulated and cell death quantified in a time-dependent manner. In this way, pH can be decreased without hypoxia and cell death monitored with temporal resolution relevant to onset and recovery from low pH. Such discrete manipulation of individual components of the extracellular milieu is not possible *in vivo* where, for example, pH decreases following anoxia. Thus, the microperfusion approach gives superior control over the extracellular environment that could not be achieved *in vivo*. We

acknowledge that the slice preparation differs from the *in vivo* scenario (Cho et al. 2007, Saeidnia et al. 2015) and in this way serves our objective to study processes at the tissue level that do not depend on cold tissue temperatures and confer tolerance to AGS.

LDH release was used to interpret cell death in our study. LDH release is a standard approach to monitor cell death (Chan et al. 2013) which is released from the cytosol because of membrane disruption and not because of metabolic changes related to OGD. This approach of monitoring cell death overcomes the limitations of methods used in prior studies where high baseline cell death because of acute damage at the slice surface challenged interpretation (Ross et al. 2006, Christian et al. 2008). The microperfusion approach minimizes background cell death by capturing LDH release from the entire slice. This approach overcomes problems with propidium iodide staining. Like LDH release, propidium iodide staining depicts increased membrane permeability; however, propidium iodide shows cell death only on the surface of the freshly cut slice.

3.5.2 AGS hippocampus resists OGD as well as ischemic shift solution better than rat

Traditionally, OGD is used to model *in vivo* ischemic insult, however, due to dilution OGD excludes other deleterious aspects of the ischemic milieu (Yao et *al.* 2007a, Lo 2008). This artifact of the *in vitro* preparation could not explain tolerance to OGD because resistance to modeled ischemia was observed in AGS even when the perfusion fluid was modified to mimic loss of ion homeostasis and subsequent changes in the extracellular fluid that occurs *in vivo*. AGS were not vulnerable to ischemic shift solution (ISS) or to acidic media (~pH 6.4). ISS includes ionic alterations sufficient to induce spreading depression in cortex (Zhou et al. 2001). ISS also mimics tissue acidosis sufficient to activate acid sensing ion channels which increase calcium permeability and

leads to cell death during cerebral I/R (Xiong (Xiong et al. 2004). Previous studies have shown that painted turtle neurons also tolerate prolonged ischemic solution treatment (Pamenter et al. 2012).

3.5.3 AGS hippocampus tolerates OGD despite ATP depletion

Resistance to OGD is evident in AGS although there is a depletion in ATP, a hallmark of ischemic injury (Sato et *al.* 1984). In contrast, a balance between ATP demand and ATP supply prevails in other anoxia-tolerant species such as the painted turtle via a coordinated reduction in ATP demand in the absence of oxygen (Bickler & Buck 2007). In AGS, tolerance to OGD resides despite ATP depletion and is not a result of restoration of ATP. This finding distinguishes AGS from anoxia-tolerant turtle where ATP recovers slowly over time (Pamenter et al. 2012). Depletion of ATP is also seen during OGD in hippocampal slices taken from hibernating AGS although the initial loss of ATP is delayed relative to AGS during interbout arousal (Christian et al. 2008). Here, we focused exclusively on seAGS since we found no difference in tolerance to OGD between winter hibernating and summer active AGS. Anoxia depletes ATP similarly in hippocampal slices from naked mole rats and mice (Larson et *al*. 2012).

3.5.4 AGS hippocampus tolerates OGD injury even after ischemic depolarization-associated excitatory glutamate efflux

This study also revealed that resistance to OGD in AGS hippocampus is not because of attenuation in excitatory amino acid efflux such as glutamate and aspartate. Ischemia-induced depolarization is delayed in AGS relative to rats *in vitro* and *in vivo*. Nonetheless, depolarization is observed within 7 min in acute slices and 3 min during cardiac arrest *in vivo (Dave* et *al. 2009)*. The 30 min of OGD applied in this study should

have been sufficient to depolarize hippocampal neurons and indeed led to an increase in glutamate and aspartate efflux that was similar to rats and occurred with a time course consistent with *in vivo* studies (Benveniste et al. 1984, Hagberg et al. 1985, Mitani et al. 1994). While delayed depolarization may contribute to tolerance, additional protective mechanisms are most likely unrelated to glutamate release. Our result is in contrast to anoxia-tolerant species such as fresh-water turtle and crucian carp that show a decrease in tissue level of excitatory neurotransmitter glutamate and aspartate (Nilsson 1990); Down-regulation of glutamate release is suggested to be modulated by synergistic activity of K (ATP) (+) channels, adenosine and GABA(A) receptors (Milton et al. 2002, Thompson et al. 2007). Our result suggests that tolerance to OGD in AGS is not because of inhibition of excitatory neurotransmitter release.

3.6 Conclusion

In agreement with previous results (Dave et al. 2006, Ross et al. 2006, Christian et al. 2008), this study shows that hippocampal slices from AGS are unique in lack of seasonal dependence associated with tolerance to OGD *in vitro* and cardiac arrest *in vivo*. Here, we show that although AGS, 20 h into an interbout arousal are vulnerable to OGD, the level of susceptibility is negligible when compared to rats. We also conclude that at the tissue level when tissue temperature is normalized to 36°C despite ATP depletion, ionic derangement, tissue acidosis, and excitatory neurotransmitter efflux, AGS hippocampus resists OGD injury. Unlike hypoxia- and anoxia-tolerant species where tolerance is linked to ATP restoration and neurotransmitter release, AGS may have evolved unique adaptations to physiological extremes and subsequently cerebral I/R.

3.7 Acknowledgments

This work was supported by the US Army Medical research and Material Command, No 0517800; the National Institute of Neurological Disorder and Stroke, Nos. NS041069-06 and R15NS070779; Institutional Development Award (IDeA) from the National Institute of General Medical Sciences of the National Institutes of Health under grant number P20GM103395.

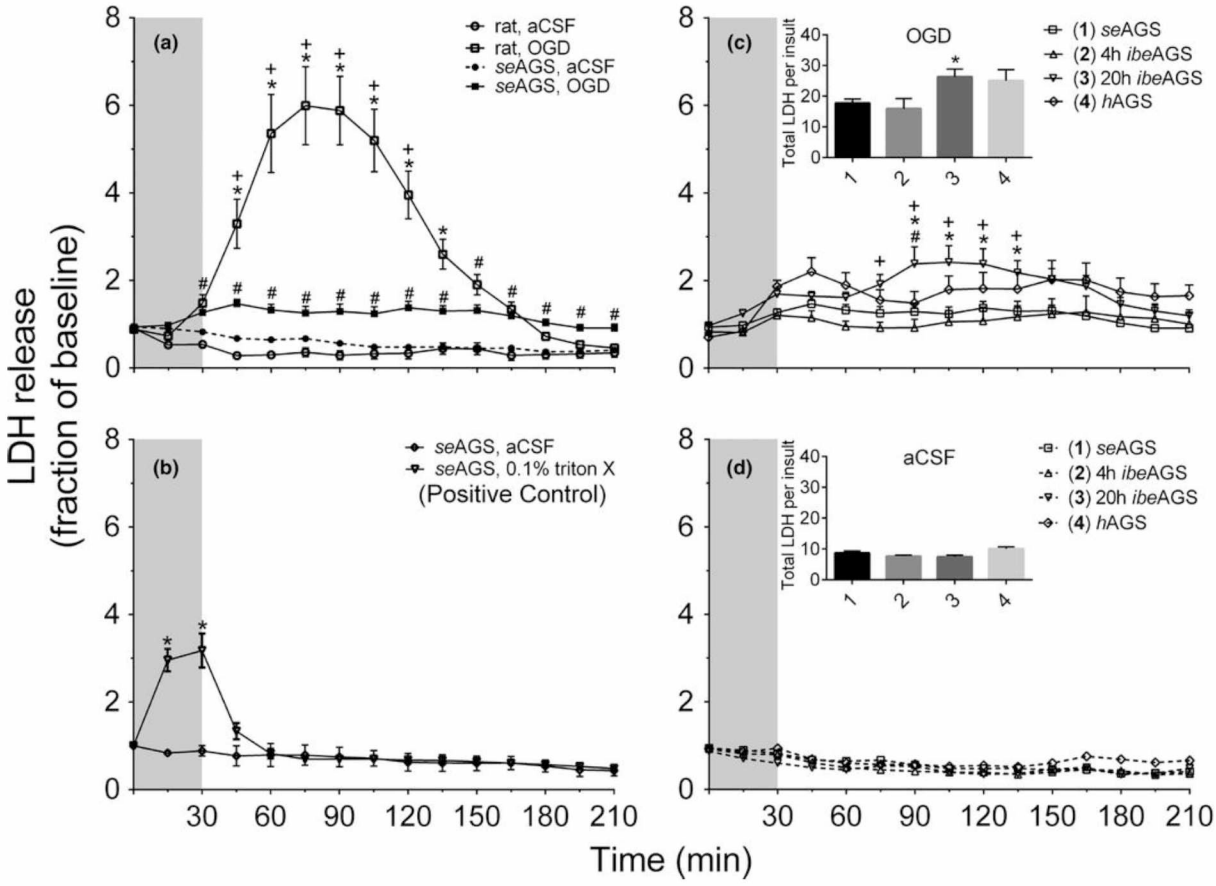

Figure 3.1: AGS brain tolerates OGD better than rat regardless of hibernation state or season.

(a) LDH in perfusates collected every 15min increases in rat hippocampal slices exposed to OGD (rat, OGD), but not in rat slices exposed to aCSF (rat, aCSF), nor in slices harvested from summer euthermic AGS and exposed to aCSF (seAGS, aCSF). A small amount of LDH is released from slices collected from seAGS and exposed to OGD (seAGS, OGD). $^{*}p < 0.05$ rat aCSF vs. rat OGD, $^{+}p < 0.05$ rat OGD vs. seAGS OGD, $^{\#}p < 0.05$ seAGS aCSF vs. seAGS OGD. (b) Exposing seAGS slices to TritonX increases LDH release ($^{*}p < 0.05$ 0.1% TritonX versus aCSF). (c) AGS hippocampal slices are most vulnerable to OGD when collected from AGS 20 h into an interbout arousal (20 h *ibe*AGS). Insert shows the sum of LDH in perfusates collected between 15 and 210 min from slices harvested from (1) seAGS, (2) AGS 4h into an interbout arousal (4h *ibe*AGS), (3) AGS 20h into an interbout arousal (20 h *ibe*AGS), or from (4) hibernating AGS (hAGS); $^{*}p < 0.05$ seAGS vs 20h *ibe*AGS, $^{+}p < 0.05$ 4h ibeAGS versus 20h *ibe*AGS, $^{\#}p < 0.05$ hAGS versus 20h *ibe*AGS. (d) Exposure of slices from the same groups of animals as in (c) to aCSF has no effect on LDH release. Gray bar indicates 30min treatment period. Data shown are means ± SEM.

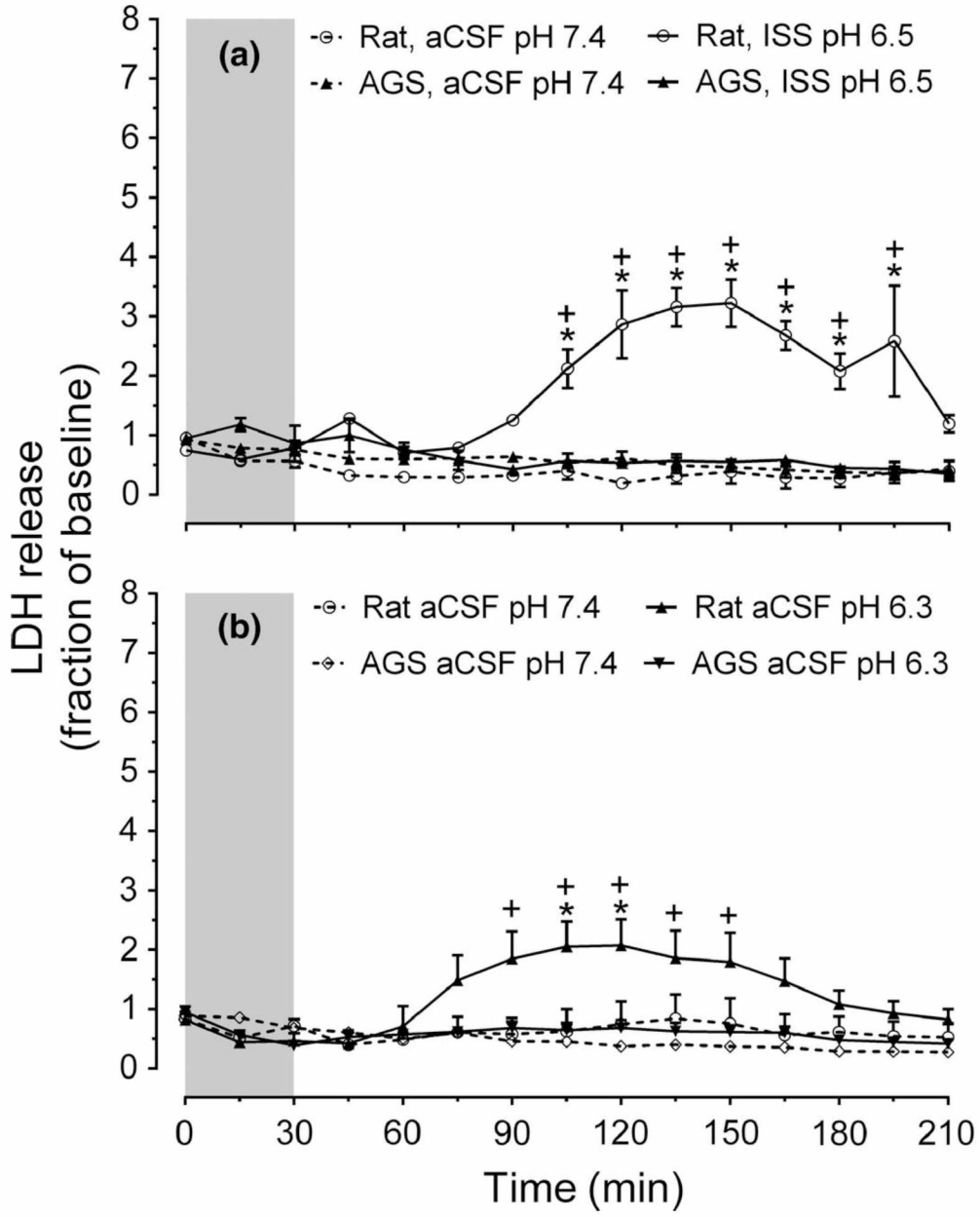

Figure 3.2: AGS brain is tolerant to ionic shift solution (ISS) or low pH injury.

(a) Shows time course of LDH release in acute hippocampal slices from rat and *se*AGS exposed to ISS, pH 6.3 or aCSF, pH 7.3. $^{*}p < 0.05$ rat aCSF versus rat ISS (pH 7.4), $^{+}p < 0.05$ rat ISS versus *se*AGS ISS (pH 6.3). (b) Shows time course of LDH release in acute hippocampal slices from rat and seAGS exposed to low pH 6.3 or aCSF, pH 7.3. $^{*}p < 0.05$ rat aCSF pH 7.4 versus rat aCSF pH 6.3, $^{+}p < 0.05$ rat aCSF pH 6.3 versus *se*AGS aCSF pH 6.3. Gray bar indicates treatment period. Means ± SEM.

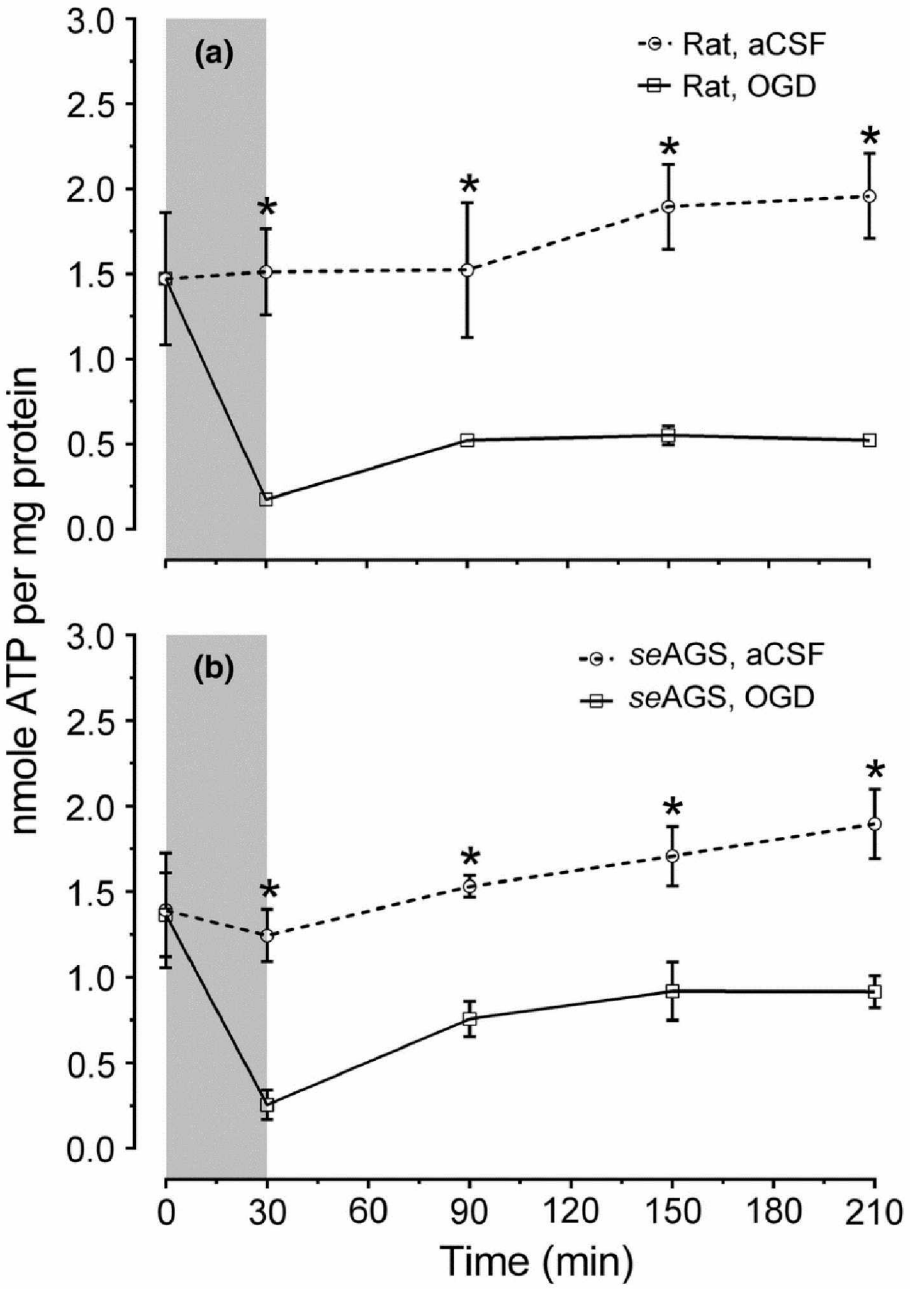

Figure 3.3: ATP declines in rat and ***se***AGS following OGD.

Levels of whole tissue ATP were determined over time following bath application of treatment in slices from (a) rat (aCSF versus OGD) and (b) *se*AGS (aCSF versus OGD) subjected to either 30 min of aCSF or OGD followed by 3 h reperfusion. Gray bar indicates insult period. Data shown are means ± SEM, $*p < 0.05$ versus aCSF.

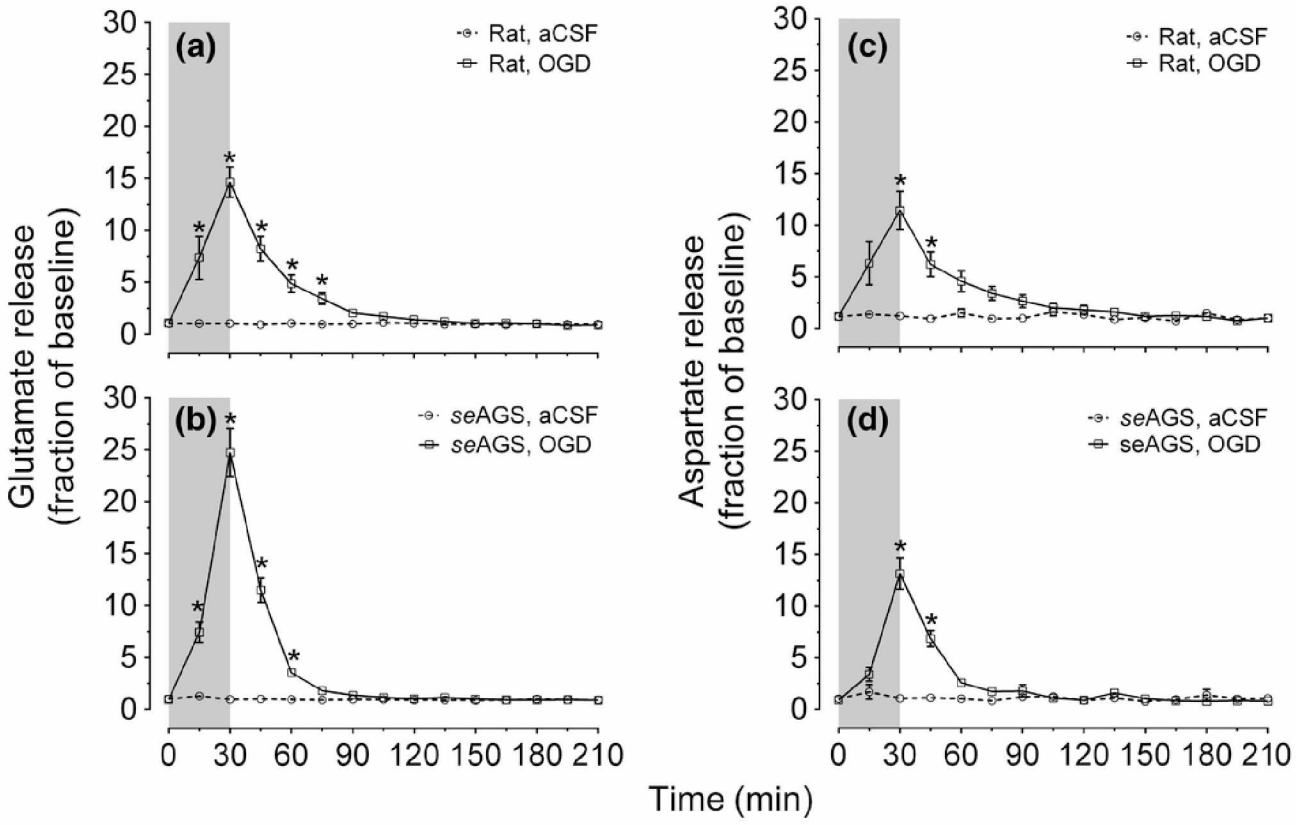

Figure 3.4: Oxygen glucose deprivation (OGD) induces efflux of glutamate and aspartate in both *se*AGS and rats.

Time-dependent excitatory neurotransmitter (glutamate and aspartate) efflux in rat and *se*AGS hippocampal slices induced by 30 min OGD insult. (a) and (b) illustrates glutamate efflux, (c) and (d) illustrate aspartate efflux in rat and *se*AGS hippocampal slices during OGD insult (n = 17 slices from six rats, n = 14 slices from five *se*AGS). Gray bar indicates insult period. *$p < 0.05$ for OGD versus artificial cerebral spinal fluid (aCSF) group. Data shown are means ± SEM.

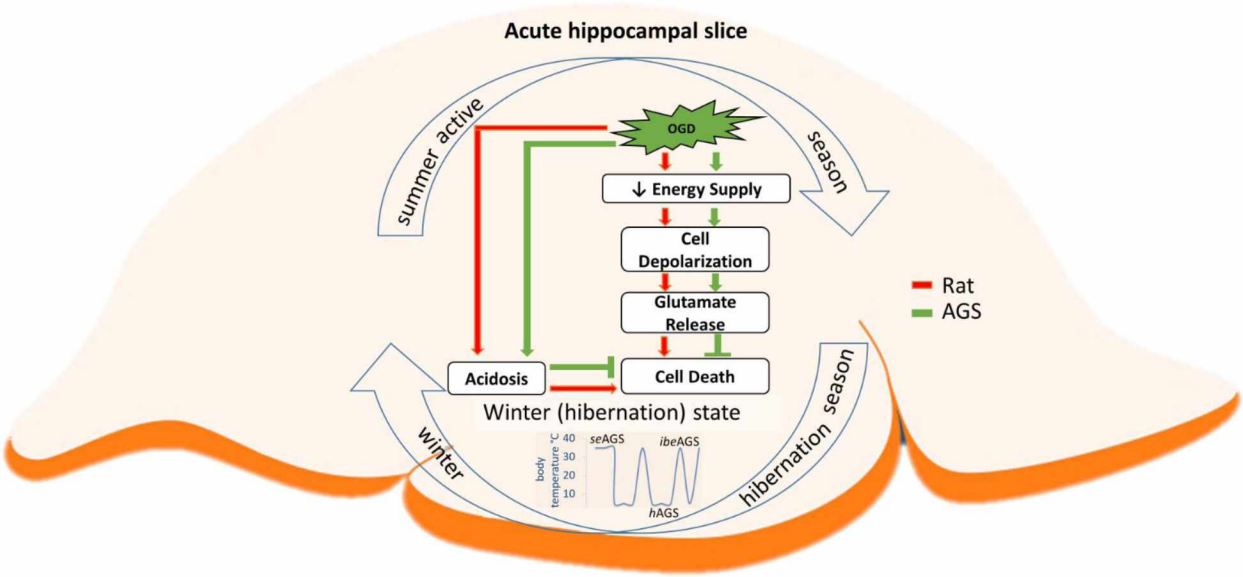

Figure 3.5. Graphical abstract. AGS tolerate OGD injury despite glutamate efflux and acidosis

AGS hippocampal slices tolerate OGD injury independent of hibernation season (summer versus winter) and state (hibernating versus interbout arousal). AGS tolerate OGD (green arrow) better than ischemic susceptible Sprague-Dawley rat (red arrow) despite loss of ATP, glutamate release, and acidosis. These findings point towards as yet undefined mechanisms of tolerance at the tissue level that are unique to AGS.

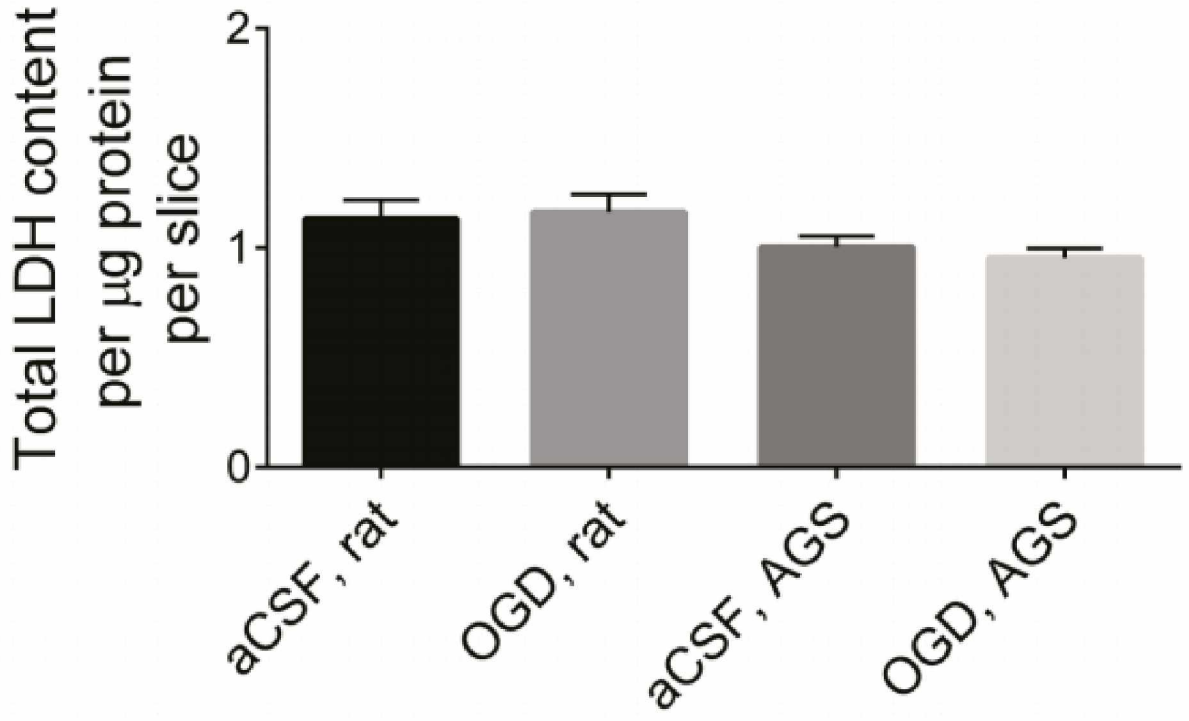

Supplementary Figure 3.1: Total LDH content from rat and AGS

Total LDH content per slice from rats (*n* = 15) and AGS (*n* = 34) subjected to 30 min of either aCSF or OGD treatment is not different. At the end of each experiment, slices were homogenized and total LDH content per slice was measured. Data shown are means ± SEM.

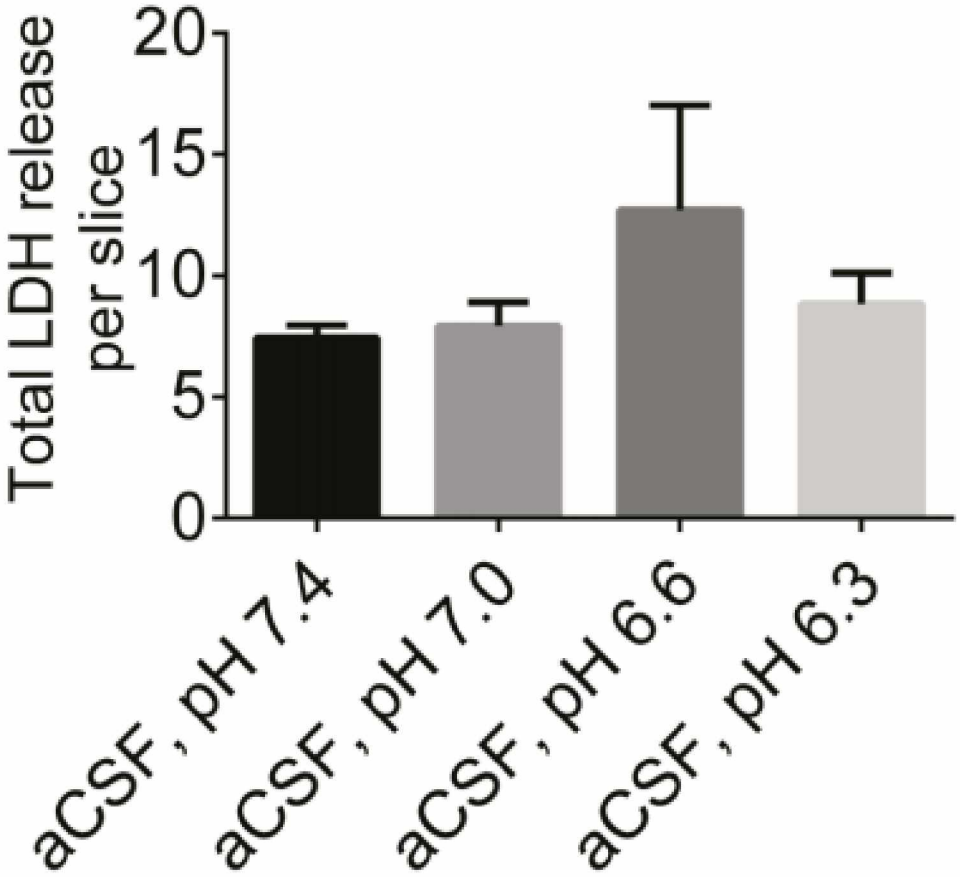

Supplementary Figure 3.2: Total LDH release in AGS subjected to different pH exposure

Total LDH release per slice from *se*AGS subjected to a range of low pH insult (aCSF pH 7.4, $n = 7$; aCSF pH 7.0, $n = 4$; aCSF pH 6.6, $n = 5$; aCSF pH 6.3, $n = 7$; 15 animals) for 30 min. Total LDH release per treatment was normalized to baseline LDH release per mg of protein (Baseline values for LDH in arbitrary units per mg protein: aCSF pH 7.4 = 0.218 ± 0.0668; aCSF pH 7.0 = 0.300 ± 0.0665; aCSF pH 6.6 = 0.240 ± 0.0686; aCSF pH 6.3 = 0.260 ± 0.0302). Data shown are means ± SEM.

Table1: Characteristics of study groups:					
Physiological Parameters	***se*AGS**	***ibe*AGS (20h)**	***ibe*AGS (4h)**	***h*AGS**	**Rat**
Age (days)	Adult	Adult	Adult	Adult	87.60±25.45
Sex	Male (n= 10) Female (n= 4)	Male (n= 8) Female (n= 5)	Male (n= 1) Female (n= 2)	Male (n= 4) Female (n= 0)	Male (n= 14) Female (n= 1)
Body Weight (g)	1037.6±247.3	616.9±160.3	585.4±224.3	619.5±132.7	354.3±50.5
T_{rectal} (°C)	36.7±1.4	36.1±0.8	36.6±0.6	4.5±1.2	36.6±0.9
$T_{temporalis}$ (°C)	35.9±1.1	35.6±0.8	35.8±0.6	5.7±1.5	35.7±0.4

Supplementary Table 3. 1: Characteristics of study groups

Treatment Group	Baseline values for LDH absorbance (Arbitrary unit)
Figure 1	
rat aCSF	0.139 ± 0.015
rat OGD	0.189 ± 0.020
*se*AGS aCSF	0.204 ± 0.025
*se*AGS OGD	0.189 ± 0.01
4h *ibe*AGS OGD	0.262 ± 0.036
*h*AGS OGD	0.124 ± 0.010
20h *ibe*AGS OGD	0.208 ± 0.021
Figure 2 (A)	
rat, aCSF pH 7.4	0.183 ± 0.017
rat ISS pH 6.5	0.099 ± 0.019
*se*AGS, aCSF pH 7.4	0.213 ± 0.056
*se*AGS ISS pH 6.5	0.126 ± 0.003
Figure 2 (B)	
rat, aCSF pH 7.4	0.109 ± 0.0164
rat aCSF pH 6.3	0.209 ± 0.0397
*se*AGS, aCSF pH 7.4	0.218 ± 0.0668
*se*AGS ISS pH 6.5	0.126 ± 0.003
*se*AGS aCSF pH 6.3	0.260 ± 0.0302

Supplementary Table 3. 2: LDH release (baseline values) in treatment groups

3.8 References

Benveniste, H., Drejer, J., Schousboe, A. and Diemer, N. H. (1984) Elevation of the extracellular concentrations of glutamate and aspartate in rat hippocampus during transient cerebral ischemia monitored by intracerebral microdialysis. *Journal of neurochemistry,* **43,** 1369-1374.

Bickler, P. E. and Buck, L. T. (2007) Hypoxia tolerance in reptiles, amphibians, and fishes: life with variable oxygen availability. *Annual review of physiology,* **69,** 145-170.

Bogren, L. K., Murphy, C. J., Johnston, E. L., Sinha, N., Serkova, N. J. and Drew, K. L. (2014a) 1H-NMR metabolomic biomarkers of poor outcome after hemorrhagic shock are absent in hibernators. *PloS one,* **9,** e107493.

Bogren, L. K., Olson, J. M., Carpluk, J., Moore, J. M. and Drew, K. L. (2014b) Resistance to systemic inflammation and multi organ damage after global ischemia/reperfusion in the arctic ground squirrel. *PloS one,* **9,** e94225.

Bortner, C. D. and Cidlowski, J. A. (2004) The role of apoptotic volume decrease and ionic homeostasis in the activation and repression of apoptosis. *Pflugers Archiv : European journal of physiology,* **448,** 313-318.

Busto, R., Dietrich, W. D., Globus, M. Y., Valdes, I., Scheinberg, P. and Ginsberg, M. D. (1987) Small differences in intraischemic brain temperature critically determine the extent of ischemic neuronal injury. *Journal of cerebral blood flow and metabolism : official journal of the International Society of Cerebral Blood Flow and Metabolism,* **7,** 729-738.

Chan, F. K., Moriwaki, K. and De Rosa, M. J. (2013) Detection of necrosis by release of lactate dehydrogenase activity. *Methods Mol Biol,* **979,** 65-70.

Cho, S., Wood, A. and Bowlby, M. R. (2007) Brain slices as models for neurodegenerative disease and screening platforms to identify novel therapeutics. *Current neuropharmacology,* **5,** 19-33.

Christian, S. L., Ross, A. P., Zhao, H. W., Kristenson, H. J., Zhan, X., Rasley, B. T., Bickler, P. E. and Drew, K. L. (2008) Arctic ground squirrel (Spermophilus parryii) hippocampal neurons tolerate prolonged oxygen-glucose deprivation and maintain baseline ERK1/2 and JNK activation despite drastic ATP loss. *Journal of cerebral blood flow and metabolism : official journal of the International Society of Cerebral Blood Flow and Metabolism,* **28,** 1307-1319.

Cunha, R. A. (2005) Neuroprotection by adenosine in the brain: From A(1) receptor activation to A (2A) receptor blockade. *Purinergic Signal,* **1,** 111-134.

D'Alecy, L. G., Lundy, E. F., Kluger, M. J., Harker, C. T., LeMay, D. R. and Shlafer, M. (1990) Beta-hydroxybutyrate and response to hypoxia in the ground squirrel, Spermophilus tridecimlineatus. *Comp Biochem Physiol B,* **96,** 189-193.

Dave, K. R., Anthony Defazio, R., Raval, A. P., Dashkin, O., Saul, I., Iceman, K. E., Perez-Pinzon, M. A. and Drew, K. L. (2009) Protein kinase C epsilon activation delays neuronal depolarization during cardiac arrest in the euthermic arctic ground squirrel. *Journal of neurochemistry,* **110,** 1170-1179.

Dave, K. R., Prado, R., Raval, A. P., Drew, K. L. and Perez-Pinzon, M. A. (2006) The arctic ground squirrel brain is resistant to injury from cardiac arrest during euthermia. *Stroke; a journal of cerebral circulation,* **37,** 1261-1265.

Erfani, S., Khaksari, M., Oryan, S., Shamsaei, N., Aboutaleb, N. and Nikbakht, F. (2015) Nampt/PBEF/visfatin exerts neuroprotective effects against ischemia/reperfusion injury via modulation of Bax/Bcl-2 ratio and prevention of caspase-3 activation. *J Mol Neurosci,* **56,** 237-243.

Faul, F., Erdfelder, E., Lang, A. G. and Buchner, A. (2007) G*Power 3: a flexible statistical power analysis program for the social, behavioral, and biomedical sciences. *Behavior research methods,* **39,** 175-191.

Frerichs, K. U. and Hallenbeck, J. M. (1998) Hibernation in ground squirrels induces state and species-specific tolerance to hypoxia and aglycemia: an in vitro study in hippocampal slices. *Journal of cerebral blood flow and metabolism : official journal of the International Society of Cerebral Blood Flow and Metabolism,* **18,** 168-175.

Frerichs, K. U., Kennedy, C., Sokoloff, L. and Hallenbeck, J. M. (1994) Local cerebral blood flow during hibernation, a model of natural tolerance to "cerebral ischemia". *Journal of cerebral blood flow and metabolism : official journal of the International Society of Cerebral Blood Flow and Metabolism,* **14,** 193-205.

Fukuda, A., Czurko, A., Hida, H., Muramatsu, K., Lenard, L. and Nishino, H. (1995) Appearance of deteriorated neurons on regionally different time tables in rat brain thin slices maintained in physiological condition. *Neuroscience letters,* **184,** 13-16.

Go, A. S., Mozaffarian, D., Roger, V. L. et al. (2014) Heart disease and stroke statistics--2014 update: a report from the American Heart Association. *Circulation,* **129,** e28-e292.

Hagberg, H., Lehmann, A., Sandberg, M., Nystrom, B., Jacobson, I. and Hamberger, A. (1985) Ischemia-induced shift of inhibitory and excitatory amino acids from intra- to extracellular compartments. *Journal of cerebral blood flow and metabolism : official journal of the International Society of Cerebral Blood Flow and Metabolism,* **5,** 413-419.

Hansen, A. J. and Zeuthen, T. (1981) Extracellular ion concentrations during spreading depression and ischemia in the rat brain cortex. *Acta physiologica Scandinavica,* **113,** 437-445.

Jinka, T. R., Toien, O. and Drew, K. L. (2011) Season primes the brain in an arctic hibernator to facilitate entrance into torpor mediated by adenosine A(1) receptors. *The Journal of neuroscience : the official journal of the Society for Neuroscience,* **31,** 10752-10758.

Kilkenny, C., Browne, W. J., Cuthill, I. C., Emerson, M. and Altman, D. G. (2010) Improving bioscience research reporting: the ARRIVE guidelines for reporting animal research. *PLoS biology,* **8,** e1000412.

Kirschner, D. L., Jaramillo, M. and Green, T. K. (2007) Enantioseparation and stacking of Cyanobenz[f]isoindole-amino acids by reverse polarity capillary electrophoresis and sulfated beta-cyclodextrin. *Analytical chemistry,* **79,** 736-743.

Kirschner, D. L., Wilson, A. L., Drew, K. L. and Green, T. K. (2009) Simultaneous efflux of endogenous D-ser and L-glu from single acute hippocampus slices during oxygen glucose deprivation. *Journal of neuroscience research,* **87,** 2812-2820.

Kurtz, C. C., Lindell, S. L., Mangino, M. J. and Carey, H. V. (2006) Hibernation confers resistance to intestinal ischemia-reperfusion injury. *American journal of physiology. Gastrointestinal and liver physiology,* **291,** G895-901.

Lindell, S. L., Klahn, S. L., Piazza, T. M., Mangino, M. J., Torrealba, J. R., Southard, J. H. and Carey, H. V. (2005) Natural resistance to liver cold ischemia-reperfusion injury associated with the hibernation phenotype. *American journal of physiology. Gastrointestinal and liver physiology,* **288,** G473-480.

Lo, E. H. (2008) A new penumbra: transitioning from injury into repair after stroke. *Nature medicine,* **14,** 497-500.

Ma, Y. L., Zhu, X., Rivera, P. M., Toien, O., Barnes, B. M., LaManna, J. C., Smith, M. A. and Drew, K. L. (2005) Absence of cellular stress in brain after hypoxia induced by arousal from hibernation in Arctic ground squirrels. *American journal of physiology. Regulatory, integrative and comparative physiology,* **289,** R1297-1306.

Milton, S. L., Thompson, J. W. and Lutz, P. L. (2002) Mechanisms for maintaining extracellular glutamate levels in the anoxic turtle striatum. *American journal of physiology. Regulatory, integrative and comparative physiology,* **282,** R1317-1323.

Ming, Y., Zhang, H., Long, L., Wang, F., Chen, J. and Zhen, X. (2006) Modulation of Ca2+ signals by phosphatidylinositol-linked novel D1 dopamine receptor in hippocampal neurons. *Journal of neurochemistry,* **98,** 1316-1323.

Mitani, A., Andou, Y., Matsuda, S., Arai, T., Sakanaka, M. and Kataoka, K. (1994) Origin of ischemia-induced glutamate efflux in the CA1 field of the gerbil hippocampus: an in vivo brain microdialysis study. *Journal of neurochemistry,* **63,** 2152-2164.

Nilsson, G. E. (1990) Long-term anoxia in crucian carp: changes in the levels of amino acid and monoamine neurotransmitters in the brain, catecholamines in chromaffin tissue, and liver glycogen. *The Journal of experimental biology,* **150,** 295-320.

Olson, J. M., Jinka, T. R., Larson, L. K., Danielson, J. J., Moore, J. T., Carpluck, J. and Drew, K. L. (2013) Circannual rhythm in body temperature, torpor, and sensitivity to A(1) adenosine receptor agonist in arctic ground squirrels. *Journal of biological rhythms,* **28,** 201-207.

Ouyang, Y. B., Voloboueva, L. A., Xu, L. J. and Giffard, R. G. (2007) Selective dysfunction of hippocampal CA1 astrocytes contributes to delayed neuronal damage after transient forebrain ischemia. *The Journal of neuroscience : the official journal of the Society for Neuroscience,* **27,** 4253-4260.

Pamenter, M. E., Hogg, D. W., Gu, X. Q., Buck, L. T. and Haddad, G. G. (2012) Painted turtle cortex is resistant to an in vitro mimic of the ischemic mammalian penumbra. *Journal of cerebral blood flow and metabolism : official journal of the International Society of Cerebral Blood Flow and Metabolism,* **32,** 2033-2043.

Quinones, Q. J., Zhang, Z., Ma, Q. et al. (2016) Proteomic Profiling Reveals Adaptive Responses to Surgical Myocardial Ischemia-Reperfusion in Hibernating Arctic Ground Squirrels Compared to Rats. *Anesthesiology,* **124,** 1296-1310.

Ross, A. P., Christian, S. L., Zhao, H. W. and Drew, K. L. (2006) Persistent tolerance to oxygen and nutrient deprivation and N-methyl-D-aspartate in cultured hippocampal slices from hibernating Arctic ground squirrel. *Journal of cerebral blood flow and metabolism : official journal of the International Society of Cerebral Blood Flow and Metabolism,* **26,** 1148-1156.

Saeidnia, S., Manayi, A. and Abdollahi, M. (2015) From in vitro Experiments to in vivo and Clinical Studies; Pros and Cons. *Current drug discovery technologies,* **12,** 218-224.

Sato, M., Paschen, W., Pawlik, G. and Heiss, W. D. (1984) Neurologic deficit and cerebral ATP depletion after temporary focal ischemia in cats. *Journal of cerebral blood flow and metabolism : official journal of the International Society of Cerebral Blood Flow and Metabolism,* **4,** 173-177.

Sheriff, M. J., Fridinger, R. W., Toien, O., Barnes, B. M. and Buck, C. L. (2013) Metabolic rate and prehibernation fattening in free-living arctic ground squirrels. *Physiological and biochemical zoology : PBZ,* **86,** 515-527.

Siesjo, B. K. (1988) Acidosis and ischemic brain damage. *Neurochemical pathology,* **9,** 31-88.

Thompson, J. W., Prentice, H. M. and Lutz, P. L. (2007) Regulation of extracellular glutamate levels in the long-term anoxic turtle striatum: coordinated activity of glutamate transporters, adenosine, K (ATP) (+) channels and GABA. *Journal of biomedical science,* **14,** 809-817.

Weltzin, M. M., Zhao, H. W., Drew, K. L. and Bucci, D. J. (2006) Arousal from hibernation alters contextual learning and memory. *Behavioural brain research,* **167,** 128-133.

Xiong, Z. G., Zhu, X. M., Chu, X. P. et al. (2004) Neuroprotection in ischemia: blocking calcium-permeable acid-sensing ion channels. *Cell,* **118,** 687-698.

Yanagihara, T. and McCall, J. T. (1982) Ionic shift in cerebral ischemia. *Life sciences,* **30,** 1921-1925.

Yao, H., Shu, Y., Wang, J., Brinkman, B. C. and Haddad, G. G. (2007) Factors influencing cell fate in the infarct rim. *Journal of neurochemistry,* **100,** 1224-1233.

Zhou, F., Zhu, X., Castellani, R. J., Stimmelmayr, R., Perry, G., Smith, M. A. and Drew, K. L. (2001) Hibernation, a model of neuroprotection. *The American journal of pathology,* **158,** 2145-2151.

Chapter 4: Arctic Ground Squirrel resist peroxynitrite-mediated cell death in response to oxygen glucose deprivation[3]

4.1 Abstract

Cerebral ischemia-reperfusion (I/R) injury initiates a complex cascade of events, which causes generation of nitric oxide (NO) and superoxide($O_2^{\bullet-}$). NO and $O_2^{\bullet-}$ rapidly combine to form peroxynitrite ($ONOO^-$), a potent oxidant. Arctic ground squirrel (AGS; *Urocitellus parryii*) is a natural model of high tolerance to I/R injury, however, the mechanisms that contribute to tolerate this pathological scenario remains elusive. Here, we hypothesize that tolerance to I/R injury modeled in an acute hippocampal slice preparation in AGS is modulated by reduced oxidative and nitrative stress associated with oxygen-glucose deprivation (OGD).

Hippocampal slices (400 microns) from rat and AGS were subjected to OGD to mimic I/R *in vivo* using a novel microperfusion technique. Brain slices were exposed to NO, $O_2^{\cdot-}$ donors with and without OGD; pretreatment of slices with inhibitors of NO, $O_2^{\cdot-}$ and $ONOO^-$ followed by OGD. In control slices, treatment was administered by switching to standard aCSF. Perfusates were collected every 15 min and analyzed for LDH release, an indicator of cell death. Oxidative and nitrative damage was monitored using the markers: 3-nitrotyrosine (3NT) and 4-hydroxynonenal (4HNE).

Results show that 1) NO donor alone is not sufficient to cause cell death, but with OGD enhances the cell death more in rat than AGS; an inhibitor of nNOS attenuates OGD

[3] Published as Bhowmick S, Drew KL. "Arctic ground squirrel resist peroxynitrite-mediated cell death in response to oxygen glucose deprivation." Free Radic Biol Med. 2017 Sep 28. doi: 10.1016/j.freeradbiomed.2017.09.024. [Epub ahead of print]. PubMed PMID: 28962873

induced injury in rat but has no effect in AGS. 2) $O_2^{\cdot-}$ donor alone causes injury in rat more than in AGS and the injury aggravates when combined with OGD; SOD mimetic attenuates OGD injury in rat, but no has effect in AGS. 3) $ONOO^-$ inhibitor attenuates OGD injury in rat but has no effect in AGS. Rat also shows a higher level of 3-nitrotyrosine (3NT) and 4-hydroxynonenal (4HNE) with OGD insult than AGS suggesting that greater level of injury is via formation of $ONOO^-$ during cerebral I/R injury.

4.2 Introduction

Cerebral ischemia-reperfusion (I/R) injury remains an important cause of mortality and chronic morbidity in patients suffering from stroke and cardiac arrest (Soler & Ruiz 2010). Ischemic condition initiates a cascade of molecular events wherein ATP levels rapidly decline, arresting metabolic activity (Erecinska & Silver 2001). Since the maintenance of the membrane potential relies on ATP-dependent ion pumps, the cell membrane depolarizes. This causes an excess influx of calcium through voltage-gated calcium channels. As the sodium gradient dissipates, sodium-glutamate cotransporters release glutamate into the extracellular space (Rossi et *al.* 2000), which activates postsynaptic glutamate receptors, particularly N-methyl-D-aspartate (NMDA) channels. The activated NMDA channels are responsible for a significant part of the calcium (Ca^{2+}) influx. Excessive intercellular Ca^{2+} overexcites cells and causes generation of harmful chemicals such as free radicals and reactive oxygen and nitrogen species (Uttara et *al.* 2009).

A major event during cerebral ischemia is the generation of nitrogen and oxygen free radicals. These reactive species include superoxide ($O_2^{\cdot-}$) and nitric oxide (NO) that has the great tendency to react with each other to form a potent oxidant peroxynitrite

($ONOO^-$). In the brain, NO is formed by the NO synthase (NOS) isoforms, a family of enzymes (Guix et al. 2005, Calabrese et al. 2007). Under physiological conditions, NO is responsible for maintenance of basal cerebral blood flow (CBF) (Toda et al. 2009). However, during ischemia, cerebral NO rapidly increases to 2–4 μM, producing damaging levels of NO (Murphy 1999, Kader et al. 1993). Concomitantly, a burst of free radicals such as $O_2^{\bullet-}$ (Cuzzocrea et al. 2001, El Kossi & Zakhary 2000, Tang et al. 2012, Suh et al. 2008) is produced after the ischemic event. This scenario is deleterious because $O_2^{\bullet-}$ anion has a high affinity for NO, higher than for the superoxide dismutase (Huie & Padmaja 1993, Cudd & Fridovich 1982). NO and $O_2^{\bullet-}$ react with each other in an equimolar stoichiometric ratio forming a potent oxidant, $ONOO^-$ further contributing to injury (Beckman et al. 1990, Reiter et al. 2000, Zielonka et al. 2010).

Studies have confirmed that some invertebrates and vertebrates exhibit tolerance to ischemic or hypoxic injury (Larson et al. 2012). Ischemia causes a decrease in cerebral blood flow which in part leads to tissue hypoxia (reduced O_2). Low O_2 causes a reduction in mitochondrial respiration and oxidative metabolism. In addition to hypoxia, decreased blood flow limits delivery of nutrients such as glucose and removal of metabolic waste such as lactate. Arctic ground squirrel (AGS), *Urocitellus parryii*, is an obligate hibernating species that tolerate cerebral I/R caused by cardiac arrest or mimicked by *in vitro* preparations (Dave et al. 2009, Ross et al. 2006, Christian et al. 2008). Resistance to brain injury does not depend on hibernation state and persists at warm tissue temperatures (Bhowmick et *al.* 2017b). Studies show that AGS hippocampus resists up to 2 hr of OGD (Christian et al. 2008), despite anoxic depolarization that occurs within ~ 6.6 min after onset of OGD (Dave et al. 2009). Subsequent studies ruled out preservation

of ATP levels, decreased excitatory amino acid release as mechanism of tolerance in AGS (Bhowmick et al. 2017b). Until now, it was unclear what mechanisms, downstream of depolarization and glutamate release, contribute to AGS resistance to cerebral I/R. Here, we tested the hypothesis that tolerance to I/R injury modeled in an acute hippocampal slice preparation in AGS is modulated by reduced oxidative and nitrative stress associated with OGD.

Our results confirm that at the tissue level, AGS tolerate OGD better than ischemic susceptible Sprague-Dawley rats. The tolerance to OGD in AGS is due to less oxidative and nitrative stress marked by reduced levels of 4-Hydroxynonenal (4-HNE) and nitrotyrosine (3-NT) generation. The findings suggest that tolerance to OGD in AGS is modulated in part by means to mitigate oxidative and nitrative stress.

4.3 Methods

4.3.1 Animal groups

Arctic ground squirrel (AGS, *Urocitellus parryii*) and Sprague-Dawley rats were used for these experiments. All procedures were performed in accordance with the University of Alaska Fairbanks Institutional Animal Care and use Committee (IACUC) and performed in accordance with the guidelines of the 8th edition of the Guide for the Care and Use of Laboratory Animals published by the US National Institutes of Health. Research was conducted in accordance with ARRIVE guidelines for reporting animal research (Kilkenny et al. 2010).

AGS of both sexes were trapped in the wild during mid-July in the northern foothills of the Brooks Range, Alaska, 40 miles south of the Toolik Field Station of the University of Alaska Fairbanks (68°38 N, 149°38 W; elevation 809 m). AGS were then transported

to Fairbanks, AK under permit obtained from The Alaska Department of Fish and Game. Once transported, AGS were quarantined for two weeks and housed individually in facilities with an ambient temperature (Ta) of 16–18°C and a 12:12-h light-dark cycle. Food (rodent chow) was available *ad libitum* at all times. Experiments in AGS were conducted between July and September when AGS were in the summer euthermic state. Both males and females AGS were included in the study. Female AGS are reproductive only once a year in the spring. Neither males nor females were used during the breeding season. Male Sprague-Dawley rats (3–4 months of age at the time of the experiment) were purchased from Simonsen Laboratories (Gilroy, CA) and were transported by air to the University of Alaska Fairbanks. Rats were housed in groups of two to four at 20–21°C, with a 12:12-h light-dark cycle. Only male rats were used to avoid the influence of estrous on the results. Ambient temperature and light-dark cycle remained the same for all groups. AGS and Sprague–Dawley rats weighing 389 – 1036g (701.54g ± 37.98) and 300– 392g (401.35g ± 5.30), respectively, were used for the study.

4.3.1 Acute hippocampal slice preparation and *in vitro* modeled ischemia / reperfusion

Animals were anesthetized using 5% (v/v) isoflurane with medical grade O_2 at a constant flow rate of 1.5 L/min. Once unresponsive, the animals were euthanized via rapid decapitation and brains were removed within 2 minutes. The whole brain was then placed in ice chilled, oxygenated HEPES buffered artificial cerebral spinal fluid (HEPES-aCSF) containing 120 mM NaCl, 20 mM $NaHCO_3$, 6.68 mM HEPES acid, 3.3 mM HEPES sodium salt, 5.0 mM KCl, 2.0 mM $MgSO_4$ (pH 7.3 - 7.4) to attenuate edema during slicing and incubation. Rapidly dissected hippocampi were embedded in 2.5 % agar and transverse hippocampal slices, 400 µm thick were cut at approximately 2°C in oxygenated

HEPES-aCSF using a Vibratome® 1000plus sectioning system (The Vibratome Company, St. Louis, MO). The slices were then transferred to a brain slice keeper (Scientific Systems Design Inc., Mississauga, Ontario, CA) and allowed to recover for 1-1.5 h at room temperature (20-21°C) in HEPES-aCSF bubbled continuously with 95% O_2/ 5% CO_2 before transferring to microperfusion chambers.

To address the time course of injury, treatment was applied using an *in vitro* microperfusion technique described previously (Kirschner et al. 2009) and validated for study of modeled I/R in rats (Bhowmick et *al.* 2017a). Briefly, after 1-1.5 h recovery as described above, individual slices were transferred gently to microperfusion chambers and lids sealed. The 4-8 parallel chambers (dimensions L×W×H~9×5×0.7 mm, 700 µm deep with an additional with 0.3-mm deep microchannel support each with an estimated volume of ~ 35 µL without tissue in place) were perfused with artificial cerebrospinal fluid (aCSF), pH 7.3 containing 120 mM NaCl, 45 mM $NaHCO_3$, 10 mM glucose, 3.3 mM KCl, 1.2 mM NaH_2PO_4, 2.4 mM $MgSO_4$, 1.8 mM $CaCl_2$ bubbled with 95% O_2 /5% CO_2 and submerged in aCSF bath at 36°C (±0.2°C) at a flow rate of 7 µL/min using Harvard Apparatus PHD 2000 syringe pump (Harvard Apparatus Holliston, MA). The osmolarity of these solutions was between 290 and 300 mOsm. Sampling began 75 min after submerging the sealed chambers to allow adequate time for stabilization of neurochemical efflux.

To model *in vivo* ischemia/reperfusion (I/R)-induced alterations in the ionic microenvironment, we perfused the hippocampus slices with one of the following, (1) aCSF, pH 7.3 as a control solution, (2) OGD, pH 7.3 (glucose-oxygen free aCSF). All aCSF solutions (pH 7.3) were equilibrated with 95% O_2 and 5% CO_2 whereas the OGD

solutions were equilibrated with 5% CO_2 and 95% N_2, for a minimum of 1 h until pH stabilized in the desired range. The PO_2 in OGD solution varied from 0-2.9 mmHg with an average of six determinations of 1.1 mmHg as measured using a miniature Clark-style electrode (Instech Laboratories, Plymouth Meeting, PA). The ischemia-induced alteration was made by switching the solution (from aCSF pH 7.3 to OGD pH 7.3) 8 min before the start of insult, the time it takes to completely replace the solution in the chamber with a flow rate of 7 µL/min. Perfusates were collected at 15 min intervals, and fractions were analyzed for cellular injury (LDH release) on the day of collection. Remaining volume was kept at -80°C for subsequent analysis.

Drug Treatment. To evaluate the role of NO, spermine NONOate (NO donor), or 3-bromo-7-Nitroindazole (NOS inhibitor) (Cayman Chemical) was included in the perfusion medium with and without OGD. To evaluate the role of $O_2^{\bullet-}$, hypoxanthine-xanthine oxidase (HX-XO) system was used to generate $O_2^{\bullet-}$: Bovine milk xanthine oxidase (≥0.4 units/mg protein) and hypoxanthine (≥99.0%) was obtained from Sigma. $O_2^{\bullet-}$ was decreased by the addition of the superoxide dismutase (SOD) mimetic 4-hydroxy-2,2,6,6-tetramethylpiperidine-N-oxyl (TEMPOL) obtained from Sigma-Aldrich Corp. FetMPyP (Cayman Chemical), a synthetic porphyrin complexed with iron is an $ONOO^-$ decomposition catalyst and was used to decrease peroxynitrite in the microchamber.

4.3.3 Quantification of cell death

Lactate dehydrogenase (LDH) concentration in the perfusates was used as a marker of necrotic tissue damage. Fifty µL of 105 µL perfusates collected at 15min intervals was transferred to 384-well plates and mixed with 50 µL reaction solution

provided in the LDH assay kit (Cayman Chemical). After 60min incubation, optical density was measured at 490 nm using a microplate reader (BioTek Epoch). Background absorbance at 620nm was subtracted. The LDH release was expressed in arbitrary units per mg of protein (Biorad protein assay kit). The maximal releasable LDH was also obtained by treating the slices with 1% NP-40 lysis buffer (50 mM Tris-HCl, 0.5% sodium deoxycholate, 0.1% SDS, 1% Igepal, 150 mM NaCl, 0.05% Triton X-100) at the end of each experiment.

4.3.4 Determination of 4-hydroxynonenal protein adducts as a marker of lipid peroxidation

Following perfusion, each slice was homogenized in a ground glass homogenizer with 1% NP-40 lysis buffer, and the insoluble proteins were removed by centrifugation at 4°C. Protein levels in an aliquot from each supernatant were measured according to the Bradford Assay. 4-Hydroxynonenal (4-HNE) levels were then determined by competitive ELISA from aliquots of the homogenate supernatants using a 96-well OxiSelect HNE Adduct Competitive ELISA Assay Kit (Cell Biolabs®, San Diego, CA, USA) according to the manufacturer's instructions.

4.3.5 Determination of 3-nitrotyrosine concentration as a marker of protein nitration

Acute hippocampal slices were homogenized on ice in 1% NP-40 lysis buffer. The slices were sonicated three times for 5 seconds each, centrifuged at 15,000g for 20 min at 4 °C. Finally, 3- nitrotyrosine (3-NT) concentrations were measured in supernatants using an OxiSelect™ Nitrotyrosine ELISA Kit (Cat. No. STA-305, Cell Biolabs, Inc., USA) according to the manufacturer's instructions. Briefly, 50 µL of sample was added per well of ELISA plate and shaken for 10 min on an orbital shaker. Fifty µL of anti-tyrosine antibody was then added and incubated for 1 h on an orbital shaker at room temperature.

Then, each well was washed thoroughly three times with 250 µL wash buffer. After removal of all wash buffer, 100 µL secondary antibody-enzyme conjugate was added to all wells and incubated for 1 h at room temperature on orbital shaker. Again, each well was washed thrice with 1× wash buffer. Substrate solution (100 µL) was added to each well and incubated for about 15 min and as color developed 100 µL of stop solution was added per well. Immediately the plate was read at 450 nm on a spectrophotometer using a microplate reader (Epoch Microplate Spectrophotometer, BioTek, Winooski, VT). Results were normalized per mg of protein.

4.3.3 Statistical analysis

A priori power analysis (G*Power software, (Faul et al. 2007)) was performed to estimate sample size needed to yield 80% power for detecting a significant ($p<0.05$) effect of treatment. An expected difference in means of 17.81 and standard deviations of 10.93 and 2.24, taken from rat OGD and AGS OGD indicated that a sample size of 5 slices would have 80% power for detecting a difference. No animal was excluded from the study. Slices from animals were randomly assigned to treatment and control groups without prior knowledge to the treatment conditions. Data are expressed as a fraction of baseline values. Baseline was calculated as the mean of the two samples preceding the onset of treatment. Data processing and statistical analyses were performed using Microsoft Office Excel 2010 and Prism6 (GraphPad, San Diego CA, USA). Data were analyzed with one-way or two-way ANOVA with repeated measures or t-test where indicated. Significant main effects or interactions were followed by t-tests with Bonferroni's correction. Data are expressed as mean ± SEM, and $P < 0.05$ was considered statistically significant.

4.4 Results

4.4.1 NO involvement in OGD injury

To illustrate that AGS tolerates OGD better than rat, hippocampal slices from a cohort of each species (rat and AGS) were exposed to 30 min OGD. Acute hippocampal slices from rat hippocampus exposed to OGD showed a significant increase in LDH release compared to control aCSF slices ($p<0.0001$, 2-way ANOVA, treatment x time, n= 10-12 slices) (Figure 4.1a). Slices from AGS showed less LDH release than rat in response to OGD ($p<0.0001$, 2-way ANOVA, species x time, n= 9-12 slices) (Supplementary Figure 4.1). Nonetheless, release of LDH in response to OGD exposure in AGS was significantly greater compared to the control aCSF slices ($p<0.0001$, 2-way ANOVA, treatment x time, n= 9-16 slices) (Figure 4.1d).

We next asked if NO is involved in OGD injury. The NOS inhibitor, 3-bromo-7-nitroindazole (IC50=17 μM), eliminated OGD induced cell death in rat ($p<0.0001$, 2-way ANOVA, treatment x time, n = 7-12 slices) (Figure 4.1a), and AGS ($p<0.0001$, 2-way ANOVA, treatment x time, n = 7-9 slices) (Figure 4.1d). In rat, a significant difference was also noted in total LDH release measured as the sum of LDH released from the start of insult to the end of the experiment ($p<0.0001$, 1-way ANOVA, n= 7-12 slices) (Figure 4.1b), however AGS showed no significant decrease in total LDH release in response to OGD ($p=0.34$, 1-way ANOVA, n= 7-9 slices) (Figure 4.1e).

Next, we ask if the NO donor spermine NONOate (10 μM, $T_{1/2}$= 39 min) alone caused LDH release in rat and AGS. Spermine NONOate alone did not increase total LDH release measured as the sum of LDH released from the start of insult to the end of the experiment in either rat (aCSF vs. NO donor, $p>0.0001$, 1-way ANOVA, n= 7-10

slices) (Figure 4.1b) or AGS (aCSF vs. NO donor, p=0.41, 1-way ANOVA, n= 7-16 slices) (Figure 4.1e). This indicates that NO donor alone is not sufficient to cause cell death. To test if exogenous NO would aggravate the OGD-induced injury, spermine NONOate was added to the OGD solution. Exogenous NO with OGD significantly increased total LDH release in rat compared to OGD alone ($p<0.0001$, 1-way ANOVA, n=7-12 slices). The response was concentration dependent with a plateau noted between 10 to 40 μM (Figure 4.1c). By contrast, no significant increase in total LDH release was observed in AGS slices at concentrations up to 40 μM ($p= 0.1$, 1-way ANOVA, n=7-9 slices) (Figure 4.1f). These results indicate that nitric oxide contributes to OGD-induced cell death in rat and that AGS resist NO-aggravated OGD-induced death.

We further analyzed the total LDH content per slice to ask if total LDH content limits the amount of LDH release following OGD. No difference in total LDH content was observed in slices from rat or AGS that were subjected to either aCSF or OGD treatment (Supplementary Figure 4.2). These results suggested that the difference in LDH release between rat and AGS not be due to a difference in total LDH content but is due to a difference in the injury associated with OGD exposure. As both males and females AGS were included in the study, we also compared LDH release between males and females to see if there is a significant sex difference on LDH release when subjected to OGD. No significant differences in LDH release were observed (Supplementary Figure 4.3).

4.4.2 $O_2^{\bullet-}$ involvement in OGD injury

To determine the role of $O_2^{\bullet-}$ mediated cell death at the tissue level, acute hippocampal slices from rat and AGS were subjected to $O_2^{\bullet-}$ donor (HX-XO system – 0, 15, 30, 45 mu/ml) with and without OGD exposure for 30 min. $O_2^{\bullet-}$ donor exposure alone

caused a slight increase in LDH release in both rat ($p<0.0001$, 2-way ANOVA, treatment x time, n= 7-10 slices) (Figure 4.2a) and AGS ($p<0.0001$, 2-way ANOVA, treatment x time, n= 5-16 slices) (Figure 4.2c), however, when OGD was introduced along with $O_2^{\bullet-}$ donor, significant increase in LDH release was observed in rat ($p<0.0001$, 2-way ANOVA, treatment x time, n= 7-12 slices) (Figure 4.2b), but not in AGS slices ($p=0.08$, 2-way ANOVA, treatment x time, n= 6-9 slices) (Figure 4.2d). This indicates that rat is more vulnerable to $O_2^{\bullet-}$ aggravated OGD-induced cell death than AGS.

Next, we ask whether $O_2^{\bullet-}$ causes OGD injury$^{\bullet-}$. Acute hippocampal slices from both rat and AGS were pretreated with the SOD mimetic (Tempol) along with OGD. The SOD mimetic significantly attenuates OGD mediated LDH release in the rat in a concentration-dependent manner ($p<0.0001$, 2-way ANOVA, treatment x time, n= 7-12 slices) (Figure 4.2e). In contrast, tempol pretreatment along with OGD had no significant effect on LDH release in AGS ($p=0.46$, 2-way ANOVA, treatment x time, n= 6-9 slices) (Figure 4.2f).

We next asked if OGD injury involves ROS-mediated lipid peroxidation, a marker of oxidative stress. Results show a significant increase in total 4-HNE adduct formation in slices from a rat that was exposed to OGD as compared to aCSF treatment ($p=0.02$, t-test, n = 3-6 slices). However, no significant increase in 4-HNE adduct was observed in AGS slices that were exposed to OGD ($p=0.4$, t-test, n= 3-7 slices) (Figure 4.2g).

4.4.3 AGS are better protected from $ONOO^-$ mediated injury than rats

Since NO is known to react with superoxide anion at a diffusion-limited rate to form the short-lived, potent oxidant peroxynitrite, we next examined whether $ONOO^-$ was involved in OGD mediated cell death. Pretreatment of peroxynitrite decomposition

catalyst 5,10,15,20-tetrakis (*N*-methyl-4′-pyridyl) porphyrinato iron III (FetMpyp, 5μM) caused a significant reduction in LDH release in rat acute hippocampal slices that were exposed to OGD ($p<0.0001$, 2-way ANOVA, treatment x time, n = 7-12 slices) (Figure 4.3a). By contrast, in AGS slices, pretreatment with the same concentration of FetMpyp had no influence on LDH release caused by OGD *(refer to Figure 4.1d)* ($p=0.11$, 2-way ANOVA, treatment x time, n = 7-12 slices) (**Figure 4.3b**). This suggests that AGS resist peroxynitrite-mediated OGD injury.

We further examined the levels of 3-NT, a marker of peroxynitrite-mediated injury. Our results show that NO donor along with OGD increases 3-NT levels in slices from rat ($p<0.0001$, 1-way ANOVA, n= 6 slices) (Figure 4.3c). However, AGS slices show no significant increase in 3-NT levels with increasing concentrations of NO donor along with OGD ($p=0.07$, 1-way ANOVA, n= 3-6 slices) (Figure 4.3d). Similarly, the increases in 3-NT levels were much greater in rat slices that were subjected to increasing concentrations of the $O_2^{\bullet-}$ donor along with OGD ($p<0.0004$, 1-way ANOVA, n= 3-6 slices) (Figure 4.3e). By contrast, no significant increase in 3-NT level was observed in AGS slices exposed to $O_2^{\bullet-}$ donor along with OGD ($p=0.34$, 1-way ANOVA, n = 3-5 slices) (Figure 4.3f).

4.5 Discussion

Here, we tested that tolerance to I/R injury modeled in an acute hippocampal slice preparation in AGS is due to protection from oxidative and nitrative stress associated with OGD. This study shows for the first time that in isolated acute hippocampal slices, AGS resist $ONOO^-$ induced lipid peroxidation and protein nitration injury during OGD. Moreover, we show that in rat both NO and $O_2^{\bullet-}$ are required for ischemia-modeled injury

since neither alone was sufficient to produce an increase in LDH release similar in time course and magnitude to what is seen with OGD.

AGS tolerate cerebral ischemia/reperfusion caused by cardiac arrest or mimicked by *in vitro* preparations (Dave et al. 2006, Christian et al. 2008, Ross et al. 2006, Bhowmick et al. 2017b). AGS hippocampus resists up to 2h of OGD (Christian et al. 2008), despite anoxic depolarization (Dave et al. 2009). Subsequent studies ruled out preservation of ATP levels or decreased excitatory amino acid release as mechanisms of tolerance (Bhowmick et al. 2017b). Until now, it was unclear what mechanisms, downstream of anoxic depolarization and glutamate release, contribute to AGS resistance to cerebral I/R. We now know that detoxification of $ONOO^-$ contributes to ischemia tolerance in AGS. We interpret the mechanism as detoxification because resistance to OGD coupled with NO was not lost at high concentrations of NO donor. We identify $ONOO^-$ as the damaging species in rat because both NO and $O_2^{\bullet-}$ were required for injury. NO and $O_2^{\bullet-}$ donors paired with OGD exacerbates cell death in rat, but neither one alone is sufficient to induce cell death in rat or AGS. We interpret results to indicate that OGD generates the endogenous NO and $O_2^{\bullet-}$ that when combined with exogenous NO or $O_2^{\bullet-}$ produces $ONOO^-$ and causes injury.

We know from prior studies in rat that one of the responses to cerebral ischemia is an increase in the production of NO, catalyzed by nitric oxide synthase (NOS) (Zhang et *al.* 1995). Recent studies demonstrated that excessive levels of NO generation due to NOS activation cause cell and tissue damage (Murphy 1999, Kader et al. 1993, Zhang et al. 1995, Zhang et *al.* 2008). Injury associated with NO can be related to either NO itself or be due to the interaction with $O_2^{\bullet-}$ forming $ONOO^-$ (Zielonka et al. 2010). Inhibition of

NOS has been reported to protect against ischemia mediated neurotoxicity (Hamada et *al.* 1994, Trifiletti 1992). Our results are in accord with previous studies that inhibition of NOS reduces production of NO during OGD and significantly decreases cell death in rat (Murphy 1999, Scorziello et *al.* 2004, Lu et *al.* 2015). There has been long debate as to whether NOS isoforms are activated during ischemia since the generation of NO via activation of NOS requires O_2 as a substrate (Forstermann & Sessa 2012). However, there are substantial evidences that NO increases at 2–6 min after middle cerebral artery occlusion and in the first 10 min of OGD in the cultured hippocampus (Zhang et al. 1995, Chan 1996). NO synthesized by different NOSs has controversial effects during cerebral ischemia. Previous studies have determined that NO derived from the endothelial NOS (eNOS) is beneficial in acute ischemia. In contrast, NO produced by the neuronal NOS (nNOS) and inducible NOS (iNOS) can be neurotoxic (Willmot et *al.* 2005). Our approach targeted nNOS as other results showed that use of selective nNOS inhibitors, or nNOS 'knock-out' mice, led to substantially lower infarct volumes during cerebral ischemia (Murphy 1999). By contrast, iNOS becomes upregulated from 12 hours after middle cerebral artery occlusion (MCAO) for up to 7 days (Niwa et *al.* 2001). For this reason, we used an inhibitor of nNOS 3-bromo-7-nitroindazol (0.17 μM) (IC50 = 0.17 μM). However, because 3-bromo-7-nitroindazol inhibits iNOS (IC50 = 0.29 μM) and eNOS (IC50 = 0.86 μM) (Babbedge et *al.* 1993) at slightly higher concentrations, we cannot rule out involvement of eNOS and iNOS isoforms. Resistance to OGD in AGS did not depend on lack of NOS activation since NOS inhibition eliminated the small amount of OGD-induced injury in AGS. Although this injury was much less in AGS than in rat, both were eliminated by NOS inhibition, so both involved NOS activation.

Increase in LDH release when exogenous NO is paired with OGD but not alone also reflects that NO combines with a reactive species generated during OGD that together contributes to cell death. In our study, a nitric oxide donor, spermine NONOate ((Z)-1-[N-[3-aminopropyl]-N-[4-(3-aminopropylammonio)butyl]-amino]diazen-1-ium-1,2-diolate) was chosen as an exogenous source of NO due to its simplicity in handling, storage stability and its convenient half-life in solution (about 39 min at 37°C). Spermine NONOate decomposes in solution producing 2 moles of NO per mole of the parent compound. In our microperfusion approach, the time taken for the perfusion solution containing spermine NONOate to reach the slice is 8 min. We therefore, do not know the actual concentration of NO in the slice, but are confident based on observations that spermine NONOate exacerbated OGD-induced injury in rats that the concentration and time of NONOate to reach the slice was sufficient to increase NO levels in the slice.

Generation of $O_2^{\bullet-}$ could be limited during OGD due to decreased availability of O_2. We do not think this is the case because other results support that $O_2^{\bullet-}$ generated and monitored during OGD in rat is cytotoxic (Lu et *al.* 2012) and cell death during OGD is attenuated by a SOD mimetic (Tempol) (Lahiani et *al.* 2016). Tempol is a membrane-permeable, SOD mimetic that catalyzes the reduction of $O_2^{\bullet-}$ to H_2O_2 (Salvemini et *al.* 2002). As an SOD mimetic, Tempol metabolizes $O_2^{\bullet-}$ generated in solutions of xanthine plus xanthine oxidase (Patel et *al.* 2006) and is neuroprotective against $O_2^{\bullet-}$ and $ONOO^-$ - induced inflammation (Khattab 2006). Recently the specificity of Tempol for $O_2^{\bullet-}$ has been questioned since it also reduces the formation of hydroxyl radicals (Mitchell et *al.* 1990, Monti et *al.* 1996) and attenuates the cytotoxic effects of H_2O_2 (Chatterjee et *al.* 2000). Tempol also inhibits $ONOO^-$-mediated nitration of tyrosine (Carroll et *al.* 2000).

The lack of specificity of tempol to reduce $O_2^{\bullet-}$ does not change our interpretation that $O_2^{\bullet-}$ alone is not the damaging species during OGD. We base this conclusion on the observation that the generation of $O_2^{\bullet-}$ by hypoxanthine plus xanthine oxidase produced a negligible increase in cell death. Only when combined with OGD did $O_2^{\bullet-}$ produce pronounced cell death and OGD-induced cell death was blocked by Tempol.

During I/R injury, three distinct mechanisms generate ROS contributing to cell death: mitochondrial ROS generation, xanthine oxidase (XO) system and the NADPH oxidase complex. The paradox of increased $O_2^{\bullet-}$ production during ischemia is counterintuitive since O_2 levels are decreased during ischemia, and ROS generation increases during the reperfusion phase when there is a high influx of O_2. However, the rate of $O_2^{\bullet-}$ generation is affected both by O_2 level and the availability of reduced flavins and quinones capable of acting as a source for univalent electron transfer. The tendency of reduced flavins to increase $O_2^{\bullet-}$ production at lower O_2 concentrations was previously described (Misra & Fridovich 1972). During ischemia, mitochondrial electron transport slows, augmenting the reduction state of electron carriers. This favors $O_2^{\bullet-}$ generation if some O_2 is still available. Our approach shows that an SOD mimetic (Tempol) attenuates OGD induced cell death suggesting that during OGD there is generation of $O_2^{\bullet-}$ which is in accord with previous work showing that increased mitochondrial ROS generation occurs only during the first few minutes of hypoxia (Abramov et *al.* 2007). Increase in LDH release in rat when $O_2^{\bullet-}$ donor was paired with OGD also support that $O_2^{\bullet-}$ contributes to $ONOO^-$ mediated cell death whereas AGS resist this scenario. In our study, HX-XO system was used to generate $O_2^{\bullet-}$ although under most conditions xanthine oxidase generates more H_2O_2 than $O_2^{\bullet-}$ (Cantu-Medellin & Kelley 2013). For this reason,

we cannot rule out that H_2O_2 may react with a species generated during OGD. This is less likely to be the fate of H_2O_2, however, because H_2O_2 is less reactive than $O_2^{\bullet-}$ (Kalogeris et *al.* 2014). $O_2^{\bullet-}$ generated during ischemia undergoes rapid dismutation to H_2O_2 by SOD. However, since NO is also generated during OGD, the presence of NO in close proximity to $O_2^{\bullet-}$ favors the formation of $ONOO^-$ over H_2O_2 since the rate constant of NO with $O_2^{\bullet-}$ is larger than with SOD and therefore NO outcompetes SOD for $O_2^{\bullet-}$ (Fridovich 1995, Ferrer-Sueta & Radi 2009). This mechanism explains why $O_2^{\bullet-}$ formation by xanthine oxidase is sufficient to mediate alterations in vascular function by reducing NO bioavailability via direct reaction ($NO + O_2^{\bullet-} \rightarrow ONOO^-$) (White et *al.* 1996).

Our results support a dominant role for $ONOO^-$ in OGD –induced injury because when FetMPyP, a peroxynitrite decomposition catalyst (PDCs) was used, LDH release was significantly reduced in rat. FetMPyP exhibits good specificity as a peroxynitrite decomposition catalyst with an EC50 value of 3.5 μM (Salvemini et *al.* 1999), and does not influence NO or $O_2^{\bullet-}$ action (Misko et *al.* 1998, Salvemini et *al.* 1998, Salvemini et al. 1999, Xie et *al.* 2002). We used FetMPyP at a concentration of 5 μM as this concentration is near the EC50 value and was shown previously to be efficacious in $ONOO^-$ decomposition (Jensen & Riley 2002, Stern et *al.* 1996). Furthermore, rat slices subjected to OGD in presence or absence of $NO/O_2^{\bullet-}$ increases 4-HNE adduct and 3-nitrotyrosine level. Both 4-HNE adduct and 3-nitrotyosine are generated in the presence of $ONOO^-$ (Hall et al. 2004, Xiong et al. 2007). Although the biomolecular modifications are not specific markers of $ONOO^-$ they are consistent with the presence of $ONOO^-$ and in light of other results discussed above support the interpretation that injury is due to $ONOO^-$.

Our results support that the increase in cell death is due to a direct bimolecular reaction of NO with $O_2^{\bullet-}$ generated during OGD which others have shown to yield $ONOO^-$ at almost diffusion-limited rates (rate constant (k)=6.7 – 19 × 10^9/M/s) (Jourd'heuil et al. 2001, Reiter et al. 2000). By rapidly consuming $O_2^{\bullet-}$, NO produces $ONOO^-$/ONOOH. $ONOO^-$ is a potent oxidant that plays a critical role in neurotoxicity of NO and $O_2^{\bullet-}$ (Pacher et al. 2007). $ONOO^-$ can easily cross the plasma membrane and oxidize many intracellular molecules including lipids, DNA and proteins (Szabo et al. 2007), subsequently inducing protein dysfunction and DNA damage, and cell death (Radi 2004). Previous studies also indicate that ischemia causes an increase in levels of NO, $O_2^{\bullet-}$ and $ONOO^-$ concentrations in the brain from basal levels of 1-10 nM (Halliwell et al. 1999) to the low μM range (Lipton 1999) with subsequent protein nitration and cellular injury (Eliasson et al. 1999). Our results are consistent with other studies suggesting that excess NO radical in the presence of $O_2^{\bullet-}$ is neurodestructive (Dawson et *al.* 1993). Other studies in human neuroblastoma cells also reported that when NO donor was applied along with nontoxic concentrations of H_2O_2 (an oxidative stress), neurotoxicity due to the formation of $ONOO^-$ was observed (Tajes et al. 2013). Resistance to cell death in AGS associated with NO or $O_2^{\bullet-}$ donor with OGD suggests that AGS avoids this mechanism of injury that is deleterious in rat. Pretreatment with FetMPyP during OGD further confirms that $ONOO^-$ is generated during OGD (Thiyagarajan et *al.* 2004) causing lipid peroxidation and protein nitration, markers of $ONOO^-$ mediated cell death (Hall et al. 2004). Lower levels of lipid peroxidation and protein nitration in AGS suggest that AGS resist $ONOO^-$ induced cell death.

The microperfusion technique (Kirschner et al. 2009) used in the present study was developed specifically for the study of OGD in adult brain slices. Constant perfusion of slices with aCSF maintains slice integrity for ~8 hours. This approach was used previously to monitor glutamate and adenosine release in rat slices during OGD (Bhowmick et al. 2017a). We acknowledge that the *in vitro* approach used for our study might not apply to the *in vivo* scenario wherein whole animal mechanisms such as pH, buffering capacity and limited inflammatory response contribute to tolerance to ischemia reperfusion injury (Bogren et al. 2014b). However, this approach isolates mechanisms intrinsic to hippocampus and allows for each component to be manipulated in the ischemic cascade to study mechanisms at the tissue level. The approach allows for the study of cell death in adult AGS tissue. Although the time constraint in tissue viability in our approach limits the study of apoptotic cell death that is possible with organotypic brain slice culture, capacity to study adult tissue is an important advantage since AGS are seasonal breeders which limits availability of neonatal tissue for organotypic culture (Fukuda et al. 1995). Another advantage with this approach is that cell death can be monitored by capturing LDH release (Chan et al. 2013) from the entire slice and thus overcomes the limitations of methods used in prior studies where high baseline cell death could have compromised interpretation (Ross et al. 2006, Christian et al. 2008). Finally, the method provides some temporal resolution to study the time course of cell death.

Our experimental approach reduces animal numbers and refines techniques as per the ARRIVE guidelines. We have chosen the slice model for our study because brain tissue is a complex collection of neurons and glia that cannot be modeled entirely using cell culture. Cell and tissue culture differ from adult brain slices in several ways such as

the influence of age (adult vs. neonatal) on the mechanisms of resistance, the proportion of neurons to glia, synaptic connections between neurons, neural circuitry that affects metabolic demand of the tissue and maturity of the neurons studied. However, the slice model reduces the number of animals used and refines the experimental approach to minimize animal pain and suffering associated with whole animal studies. The microperfusion technique also refines the approach to the study of brain injury by providing a time course of acute injury that has not been possible to date with cell and tissue culture.

4.6 Conclusions

In summary, our data supports that NO and $O_2^{\bullet-}$ alone are not causing injury in rat or AGS because neither produced significant injury except when paired with OGD. OGD injury is caused by the release of both NO and $O_2^{\bullet-}$ and one without the other is not sufficient to induce cell death. Our data suggests that the injury is due to the combination of NO and $O_2^{\bullet-}$ together forming $ONOO^-$ leading to cell death. We interpret these findings to mean that resistance to injury in AGS is associated with reduced susceptibility to highly reactive $ONOO^-$ generated during I/R injury.

4.7 Acknowledgements

This work was supported by the US Army Medical research and Material Command, No 0517800; the National Institute of Neurological Disorder and Stroke, Nos. NS041069-06 and R15NS070779; Institutional Development Award (IDeA) from the National Institute of General Medical Sciences of the National Institutes of Health under grant number P20GM103395.

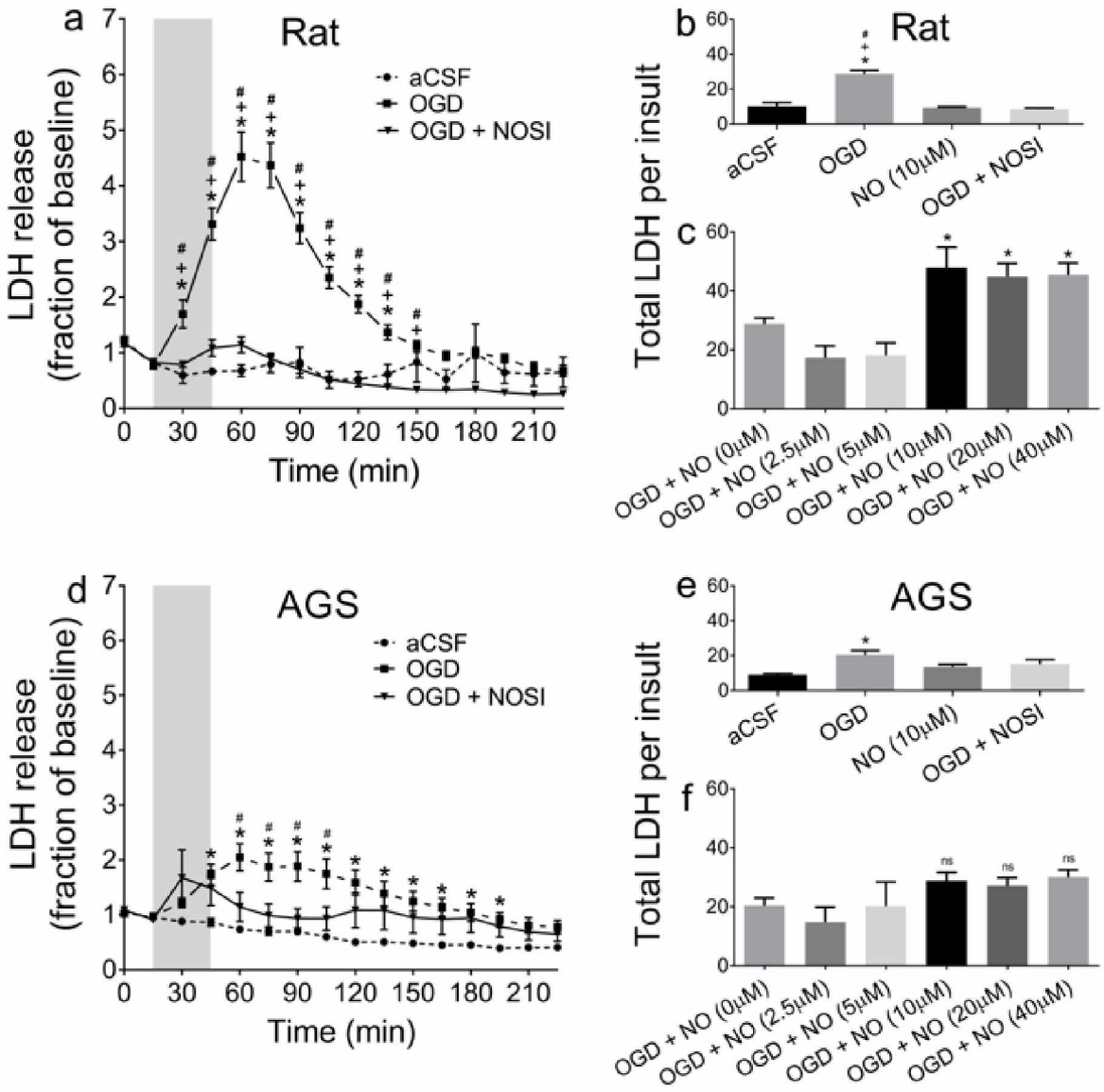

Figure 4.1: AGS resist nitric oxide mediated LDH release.

(a, d) Slices from rats and AGS were subjected to 30 min of aCSF, OGD, and OGD + NOSI. The time course of LDH release is shown. $^{*}p< 0.05$ (aCSF vs. OGD), $^{\#}p<0.05$ (OGD vs. OGD + NOSI). (b, e) Total LDH (the sum of LDH released from the start of insult to the end of the experiment) is shown in a and b. $^{*}p< 0.05$ vs. aCSF, $^{+}p<0.05$ vs. NO (10 μM), $^{\#}p<0.05$ vs. OGD + NOSI. (c, f) Total LDH release from additional experiments in which NO donor was included with OGD. *p< 0.05 vs. OGD. Grey bar indicates insult period.

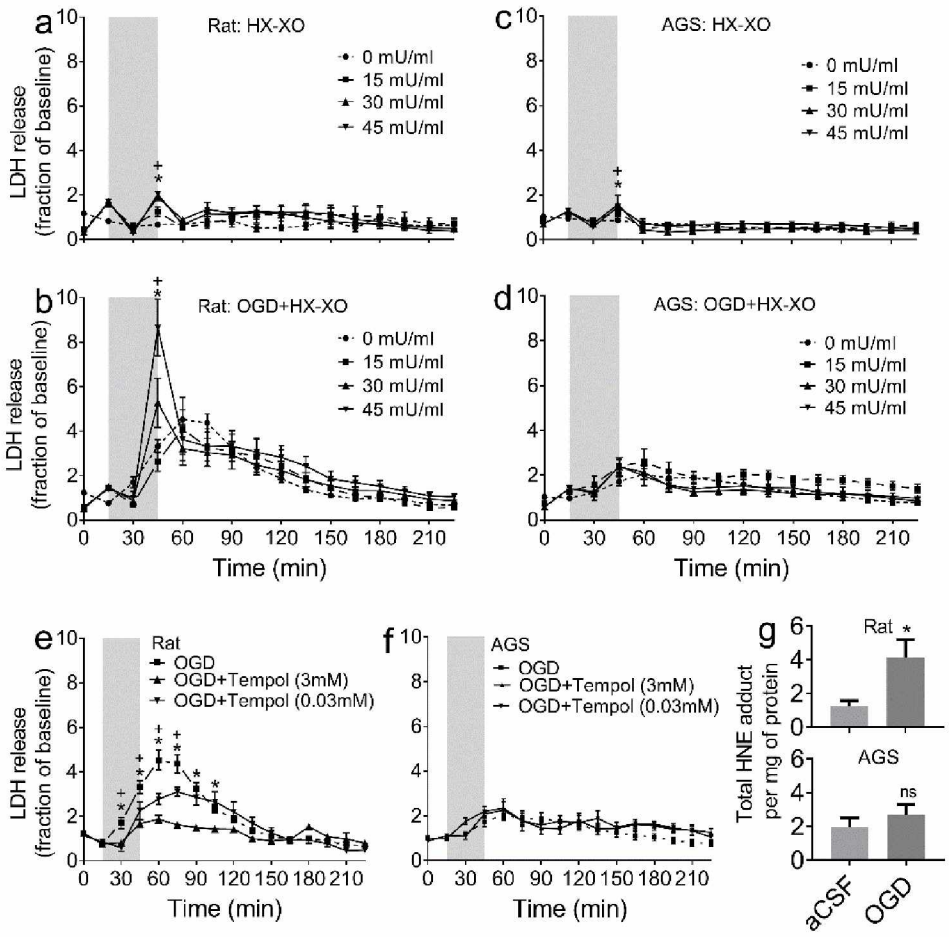

Figure 4.2: AGS show better tolerance to $O_2^{\bullet-}$ mediated cell death.

(a, c) Acute hippocampal slices from both rat and AGS were subjected to different concentrations of $O_2^{\bullet-}$ donor (HX-XO: 0, 15, 30, 45 mU/ml) and LDH release over a course of time was monitored. *p< 0.05 (0mU/ml vs. 45mU/ml), $^{+}$p<0.05 (0mU/ml vs. 30mU/ml). (b, d) Time course of LDH release was monitored in rat and AGS slices exposed to different concentrations of $O_2^{\bullet-}$ donor (HX-XO: 0, 15, 30, 45 mU/ml) along with OGD. *p< 0.05 (OGD+0mU/ml vs. OGD+45mU/ml), $^{+}$p<0.05 (OGD+0mU/ml vs. OGD+30mU/ml). (e, f) Acute hippocampal slices from rat and AGS pretreated with SOD mimetic (tempol) followed by OGD. *p<0.05 (OGD vs OGD+Tempol (3mM)), $^{+}$p<0.05 (OGD vs OGD+Tempol (0.03mM)) (g) shows total 4-HNE–Protein adduct formation in rat and AGS slices exposed to OGD *p< 0.05 vs. aCSF.

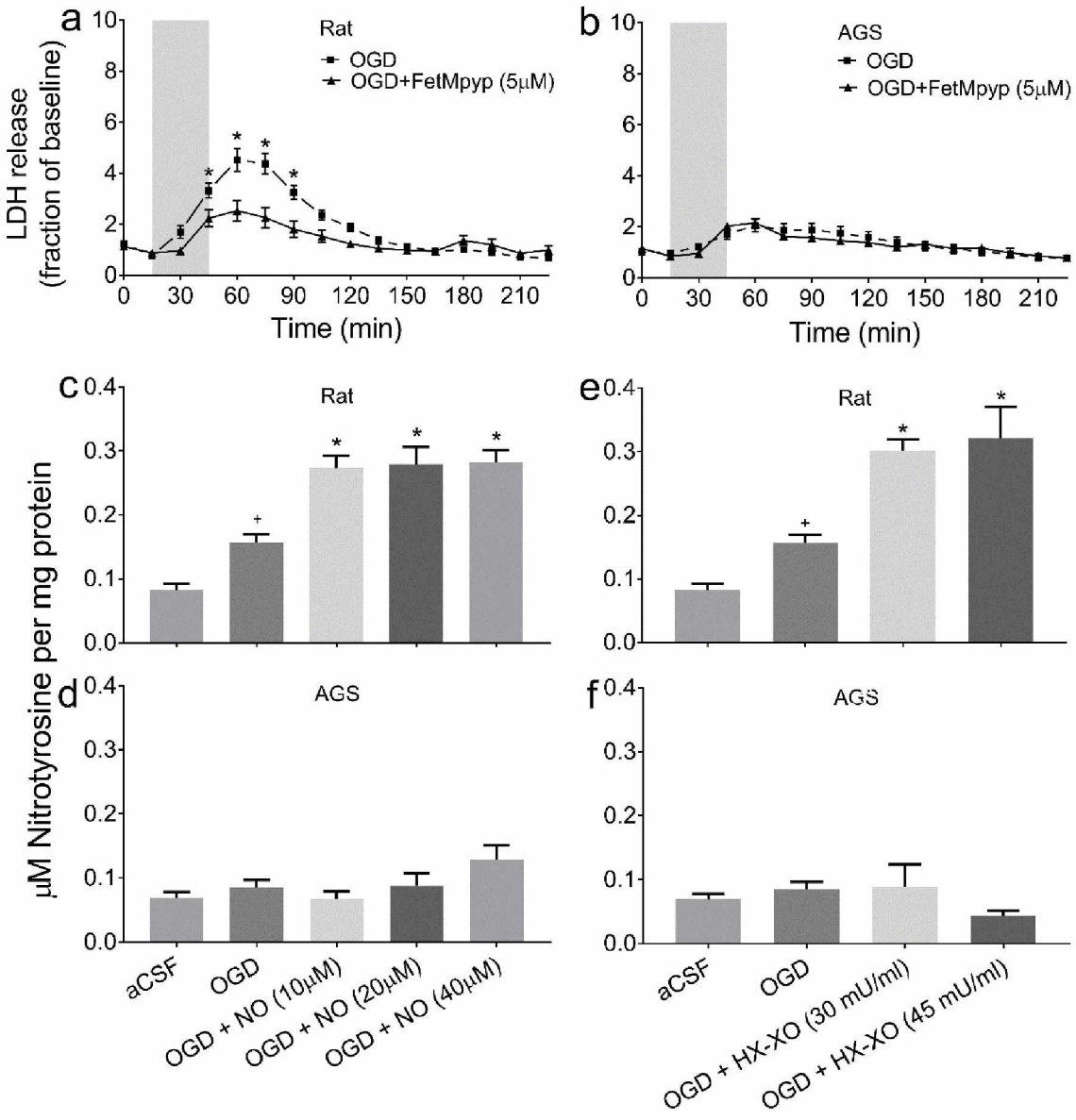

Figure 4.3: AGS tolerate peroxynitrite mediated OGD injury.

(a, b) rat and AGS slices were preincubated with FetMpyp (peroxynitrite decomposition catalyst) and LDH release was monitored. *p< 0.05 vs. OGD. (c, d) 3-NT was measured in rat and AGS slices subjected to NO donor along with OGD. *p< 0.05 vs. OGD, +p< 0.05 vs. aCSF. (e, f) 3-NT was measured in rat and AGS slices when subjected to $O_2^{\bullet-}$ donor along with OGD. *p< 0.05 vs. OGD.

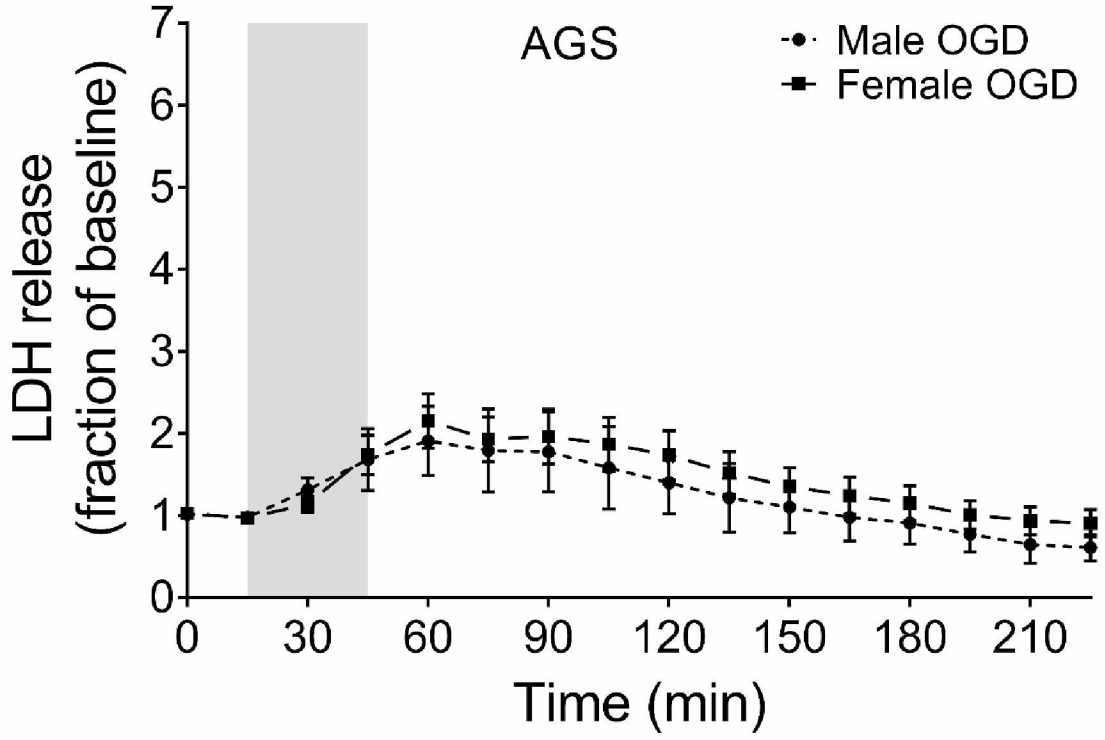

Supplementary Figure 4.1: Comparison of OGD injury in male and female AGS

Slices from rats and AGS were subjected to 30 min OGD. The time course of injury (LDH release) is shown. *p< 0.05 vs. OGD, 2-way ANOVA, species x time, n= 9-12 slices. Grey bar indicates insult period. Data shown are means ± SEM.

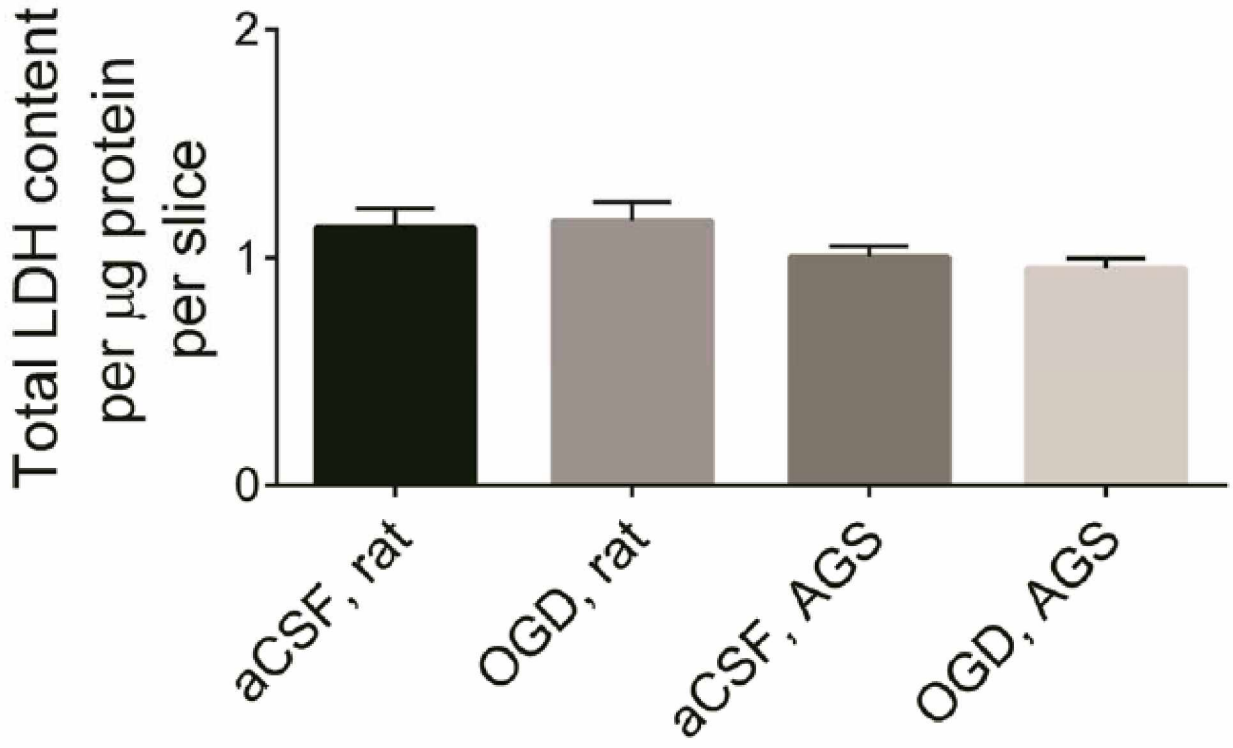

Supplementary Figure 4.2: Measurement of total LDH content in rat and AGS

Total LDH content per slice from rat and AGS were subjected to 30 min of either aCSF or OGD treatment. At the end of each experiment, slices were homogenized and total LDH content per slice was measured. Data shown are means ± SEM.

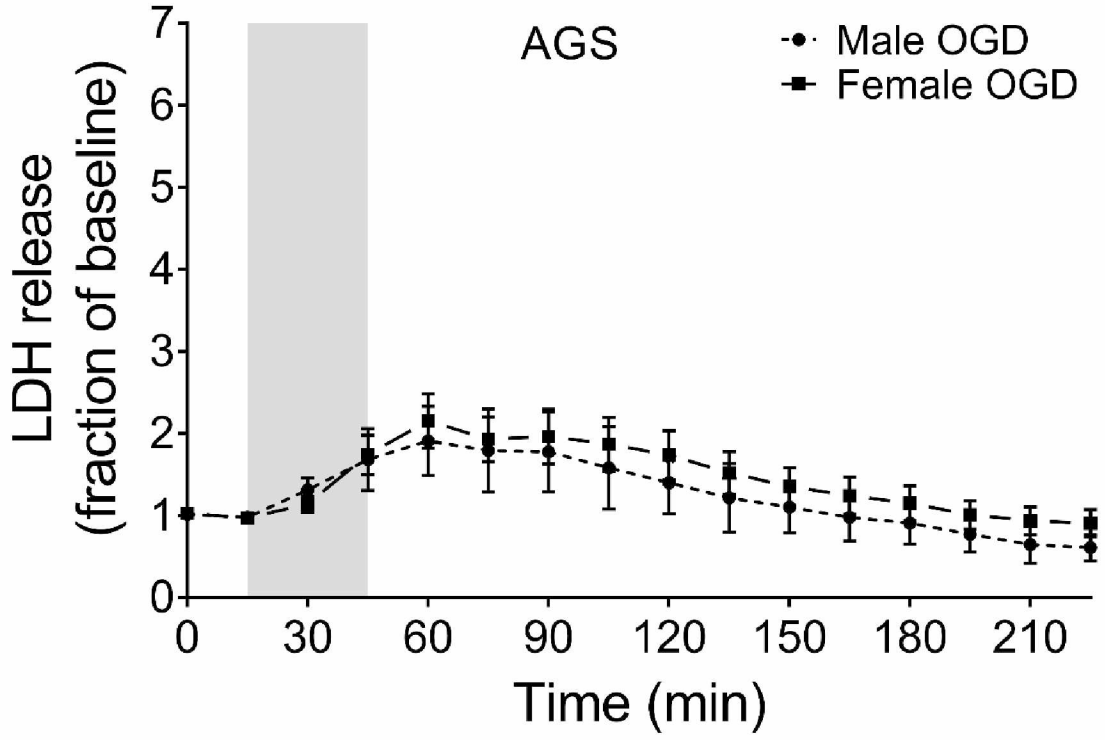

Supplementary Figure 4.3: LDH release monitored in male and female AGS subjected to OGD

Male and female AGS hippocampal slices were subjected to 30 min No significant differences in LDH release was observed ($p>0.9999$, 2-way ANOVA, Sex vs. time). Grey bar indicates insult period. Data shown are means ± SEM.

4.8 References

Abramov, A. Y., Scorziello, A. and Duchen, M. R. (2007) Three distinct mechanisms generate oxygen free radicals in neurons and contribute to cell death during anoxia and reoxygenation. *The Journal of neuroscience : the official journal of the Society for Neuroscience,* **27,** 1129-1138.

Babbedge, R. C., Bland-Ward, P. A., Hart, S. L. and Moore, P. K. (1993) Inhibition of rat cerebellar nitric oxide synthase by 7-nitro indazole and related substituted indazoles. *Br J Pharmacol,* **110,** 225-228.

Beckman, J. S., Beckman, T. W., Chen, J., Marshall, P. A. and Freeman, B. A. (1990) Apparent hydroxyl radical production by peroxynitrite: implications for endothelial injury from nitric oxide and superoxide. *Proceedings of the National Academy of Sciences of the United States of America,* **87,** 1620-1624.

Bhowmick, S., Moore, J. T., Kirschner, D. L., Curry, M. C., Westbrook, E. G., Rasley, B. T. and Drew, K. L. (2017a) Acidotoxicity via ASIC1a Mediates Cell Death during Oxygen Glucose Deprivation and Abolishes Excitotoxicity. *ACS Chem Neurosci*.

Bhowmick, S., Moore, J. T., Kirschner, D. L. and Drew, K. L. (2017b) Arctic ground squirrel hippocampus tolerates oxygen glucose deprivation independent of hibernation season even when not hibernating and after ATP depletion, acidosis and glutamate efflux. *Journal of neurochemistry*.

Bogren, L. K., Olson, J. M., Carpluk, J., Moore, J. M. and Drew, K. L. (2014) Resistance to systemic inflammation and multi organ damage after global ischemia/reperfusion in the arctic ground squirrel. *PloS one,* **9,** e94225.

Calabrese, V., Mancuso, C., Calvani, M., Rizzarelli, E., Butterfield, D. A. and Stella, A. M. (2007) Nitric oxide in the central nervous system: neuroprotection versus neurotoxicity. *Nat Rev Neurosci,* **8,** 766-775.

Cantu-Medellin, N. and Kelley, E. E. (2013) Xanthine oxidoreductase-catalyzed reactive species generation: A process in critical need of reevaluation. *Redox Biol,* **1,** 353-358.

Carroll, R. T., Galatsis, P., Borosky, S., Kopec, K. K., Kumar, V., Althaus, J. S. and Hall, E. D. (2000) 4-Hydroxy-2,2,6,6-tetramethylpiperidine-1-oxyl (Tempol) inhibits peroxynitrite-mediated phenol nitration. *Chem Res Toxicol,* **13,** 294-300.

Chan, F. K., Moriwaki, K. and De Rosa, M. J. (2013) Detection of necrosis by release of lactate dehydrogenase activity. *Methods Mol Biol,* **979,** 65-70.

Chan, P. H. (1996) Role of oxidants in ischemic brain damage. *Stroke; a journal of cerebral circulation,* **27,** 1124-1129.

Chatterjee, P. K., Cuzzocrea, S., Brown, P. A., Zacharowski, K., Stewart, K. N., Mota-Filipe, H. and Thiemermann, C. (2000) Tempol, a membrane-permeable radical scavenger, reduces oxidant stress-mediated renal dysfunction and injury in the rat. *Kidney Int,* **58,** 658-673.

Christian, S. L., Ross, A. P., Zhao, H. W., Kristenson, H. J., Zhan, X., Rasley, B. T., Bickler, P. E. and Drew, K. L. (2008) Arctic ground squirrel (Spermophilus parryii) hippocampal neurons tolerate prolonged oxygen-glucose deprivation and maintain baseline ERK1/2 and JNK activation despite drastic ATP loss. *Journal of cerebral blood flow and metabolism : official journal of the International Society of Cerebral Blood Flow and Metabolism,* **28,** 1307-1319.

Cudd, A. and Fridovich, I. (1982) Electrostatic interactions in the reaction mechanism of bovine erythrocyte superoxide dismutase. *The Journal of biological chemistry,* **257,** 11443-11447.

Cuzzocrea, S., Riley, D. P., Caputi, A. P. and Salvemini, D. (2001) Antioxidant therapy: a new pharmacological approach in shock, inflammation, and ischemia/reperfusion injury. *Pharmacol Rev,* **53,** 135-159.

Dave, K. R., Anthony Defazio, R., Raval, A. P., Dashkin, O., Saul, I., Iceman, K. E., Perez-Pinzon, M. A. and Drew, K. L. (2009) Protein kinase C epsilon activation delays neuronal depolarization during cardiac arrest in the euthermic arctic ground squirrel. *Journal of neurochemistry,* **110,** 1170-1179.

Dave, K. R., Prado, R., Raval, A. P., Drew, K. L. and Perez-Pinzon, M. A. (2006) The arctic ground squirrel brain is resistant to injury from cardiac arrest during euthermia. *Stroke; a journal of cerebral circulation,* **37,** 1261-1265.

Dawson, V. L., Dawson, T. M., Bartley, D. A., Uhl, G. R. and Snyder, S. H. (1993) Mechanisms of nitric oxide-mediated neurotoxicity in primary brain cultures. *The Journal of neuroscience : the official journal of the Society for Neuroscience,* **13,** 2651-2661.

El Kossi, M. M. and Zakhary, M. M. (2000) Oxidative stress in the context of acute cerebrovascular stroke. *Stroke; a journal of cerebral circulation,* **31,** 1889-1892.

Eliasson, M. J., Huang, Z., Ferrante, R. J., Sasamata, M., Molliver, M. E., Snyder, S. H. and Moskowitz, M. A. (1999) Neuronal nitric oxide synthase activation and peroxynitrite formation in ischemic stroke linked to neural damage. *The Journal of neuroscience : the official journal of the Society for Neuroscience,* **19,** 5910-5918.

Erecinska, M. and Silver, I. A. (2001) Tissue oxygen tension and brain sensitivity to hypoxia. *Respir Physiol,* **128,** 263-276.

Faul, F., Erdfelder, E., Lang, A. G. and Buchner, A. (2007) G*Power 3: a flexible statistical power analysis program for the social, behavioral, and biomedical sciences. *Behavior research methods,* **39,** 175-191.

Ferrer-Sueta, G. and Radi, R. (2009) Chemical biology of peroxynitrite: kinetics, diffusion, and radicals. *ACS Chem Biol,* **4,** 161-177.

Forstermann, U. and Sessa, W. C. (2012) Nitric oxide synthases: regulation and function. *Eur Heart J,* **33,** 829-837, 837a-837d.

Fridovich, I. (1995) Superoxide radical and superoxide dismutases. *Annu Rev Biochem,* **64,** 97-112.

Fukuda, A., Czurko, A., Hida, H., Muramatsu, K., Lenard, L. and Nishino, H. (1995) Appearance of deteriorated neurons on regionally different time tables in rat brain thin slices maintained in physiological condition. *Neuroscience letters,* **184,** 13-16.

Guix, F. X., Uribesalgo, I., Coma, M. and Munoz, F. J. (2005) The physiology and pathophysiology of nitric oxide in the brain. *Prog Neurobiol,* **76,** 126-152.

Hall, E. D., Detloff, M. R., Johnson, K. and Kupina, N. C. (2004) Peroxynitrite-mediated protein nitration and lipid peroxidation in a mouse model of traumatic brain injury. *J Neurotrauma,* **21,** 9-20.

Halliwell, B., Evans, P. and Whiteman, M. (1999) Assessment of peroxynitrite scavengers in vitro. *Methods in enzymology,* **301,** 333-342.

Hamada, Y., Hayakawa, T., Hattori, H. and Mikawa, H. (1994) Inhibitor of nitric oxide synthesis reduces hypoxic-ischemic brain damage in the neonatal rat. *Pediatr Res,* **35,** 10-14.

Huie, R. E. and Padmaja, S. (1993) The reaction of no with superoxide. *Free Radic Res Commun,* **18,** 195-199.

Jensen, M. P. and Riley, D. P. (2002) Peroxynitrite decomposition activity of iron porphyrin complexes. *Inorg Chem,* **41,** 4788-4797.

Jourd'heuil, D., Jourd'heuil, F. L., Kutchukian, P. S., Musah, R. A., Wink, D. A. and Grisham, M. B. (2001) Reaction of superoxide and nitric oxide with peroxynitrite. Implications for peroxynitrite-mediated oxidation reactions in vivo. *The Journal of biological chemistry,* **276,** 28799-28805.

Kader, A., Frazzini, V. I., Solomon, R. A. and Trifiletti, R. R. (1993) Nitric oxide production during focal cerebral ischemia in rats. *Stroke; a journal of cerebral circulation,* **24,** 1709-1716.

Kalogeris, T., Bao, Y. and Korthuis, R. J. (2014) Mitochondrial reactive oxygen species: a double edged sword in ischemia/reperfusion vs preconditioning. *Redox Biol,* **2,** 702-714.

Khattab, M. M. (2006) TEMPOL, a membrane-permeable radical scavenger, attenuates peroxynitrite- and superoxide anion-enhanced carrageenan-induced paw edema and hyperalgesia: a key role for superoxide anion. *Eur J Pharmacol,* **548,** 167-173.

Kilkenny, C., Browne, W. J., Cuthill, I. C., Emerson, M. and Altman, D. G. (2010) Improving bioscience research reporting: the ARRIVE guidelines for reporting animal research. *PLoS biology,* **8,** e1000412.

Kirschner, D. L., Wilson, A. L., Drew, K. L. and Green, T. K. (2009) Simultaneous efflux of endogenous D-ser and L-glu from single acute hippocampus slices during oxygen glucose deprivation. *Journal of neuroscience research,* **87,** 2812-2820.

Lahiani, A., Hidmi, A., Katzhendler, J., Yavin, E. and Lazarovici, P. (2016) Novel Synthetic PEGylated Conjugate of alpha-Lipoic Acid and Tempol Reduces Cell Death in a Neuronal PC12 Clonal Line Subjected to Ischemia. *ACS Chem Neurosci,* **7,** 1452-1462.

Larson, J., Peterson, B. L., Romano, M. and Park, T. J. Buried Alive! Arrested Development and Hypoxia Tolerance in the Naked Mole-Rat. *Frontiers in Behavioral Neuroscience*, 10.3389/conf.fnbeh.2012.27.00047.

Lipton, P. (1999) Ischemic cell death in brain neurons. *Physiological reviews,* **79,** 1431-1568.

Lu, Q., Harris, V. A., Rafikov, R., Sun, X., Kumar, S. and Black, S. M. (2015) Nitric oxide induces hypoxia ischemic injury in the neonatal brain via the disruption of neuronal iron metabolism. *Redox Biol,* **6,** 112-121.

Lu, Q., Wainwright, M. S., Harris, V. A., Aggarwal, S., Hou, Y., Rau, T., Poulsen, D. J. and Black, S. M. (2012) Increased NADPH oxidase-derived superoxide is involved in the neuronal cell death induced by hypoxia-ischemia in neonatal hippocampal slice cultures. *Free radical biology & medicine,* **53,** 1139-1151.

Misko, T. P., Highkin, M. K., Veenhuizen, A. W., Manning, P. T., Stern, M. K., Currie, M. G. and Salvemini, D. (1998) Characterization of the cytoprotective action of peroxynitrite decomposition catalysts. *The Journal of biological chemistry,* **273,** 15646-15653.

Misra, H. P. and Fridovich, I. (1972) The univalent reduction of oxygen by reduced flavins and quinones. *The Journal of biological chemistry,* **247,** 188-192.

Mitchell, J. B., Samuni, A., Krishna, M. C., DeGraff, W. G., Ahn, M. S., Samuni, U. and Russo, A. (1990) Biologically active metal-independent superoxide dismutase mimics. *Biochemistry,* **29,** 2802-2807.

Monti, E., Cova, D., Guido, E., Morelli, R. and Oliva, C. (1996) Protective effect of the nitroxide tempol against the cardiotoxicity of adriamycin. *Free radical biology & medicine,* **21,** 463-470.

Murphy, M. P. (1999) Nitric oxide and cell death. *Biochimica et biophysica acta,* **1411,** 401-414.

Niwa, M., Inao, S., Takayasu, M., Kawai, T., Kajita, Y., Nihashi, T., Kabeya, R., Sugimoto, T. and Yoshida, J. (2001) Time course of expression of three nitric oxide synthase isoforms after transient middle cerebral artery occlusion in rats. *Neurol Med Chir (Tokyo),* **41,** 63-72; discussion 72-63.

Pacher, P., Beckman, J. S. and Liaudet, L. (2007) Nitric oxide and peroxynitrite in health and disease. *Physiological reviews,* **87,** 315-424.

Patel, K., Chen, Y., Dennehy, K. et al. (2006) Acute antihypertensive action of nitroxides in the spontaneously hypertensive rat. *American journal of physiology. Regulatory, integrative and comparative physiology,* **290,** R37-43.

Radi, R. (2004) Nitric oxide, oxidants, and protein tyrosine nitration. *Proceedings of the National Academy of Sciences of the United States of America,* **101,** 4003-4008.

Reiter, C. D., Teng, R. J. and Beckman, J. S. (2000) Superoxide reacts with nitric oxide to nitrate tyrosine at physiological pH via peroxynitrite. *The Journal of biological chemistry,* **275,** 32460-32466.

Ross, A. P., Christian, S. L., Zhao, H. W. and Drew, K. L. (2006) Persistent tolerance to oxygen and nutrient deprivation and N-methyl-D-aspartate in cultured hippocampal slices from hibernating Arctic ground squirrel. *Journal of cerebral blood flow and metabolism : official journal of the International Society of Cerebral Blood Flow and Metabolism,* **26,** 1148-1156.

Rossi, D. J., Oshima, T. and Attwell, D. (2000) Glutamate release in severe brain ischaemia is mainly by reversed uptake. *Nature,* **403,** 316-321.

Salvemini, D., Riley, D. P. and Cuzzocrea, S. (2002) SOD mimetics are coming of age. *Nat Rev Drug Discov,* **1,** 367-374.

Salvemini, D., Riley, D. P., Lennon, P. J., Wang, Z. Q., Currie, M. G., Macarthur, H. and Misko, T. P. (1999) Protective effects of a superoxide dismutase mimetic and peroxynitrite decomposition catalysts in endotoxin-induced intestinal damage. *Br J Pharmacol,* **127,** 685-692.

Salvemini, D., Wang, Z. Q., Stern, M. K., Currie, M. G. and Misko, T. P. (1998) Peroxynitrite decomposition catalysts: therapeutics for peroxynitrite-mediated pathology. *Proceedings of the National Academy of Sciences of the United States of America,* **95,** 2659-2663.

Scorziello, A., Pellegrini, C., Secondo, A. et al. (2004) Neuronal NOS activation during oxygen and glucose deprivation triggers cerebellar granule cell death in the later reoxygenation phase. *Journal of neuroscience research,* **76,** 812-821.

Soler, E. P. and Ruiz, V. C. (2010) Epidemiology and risk factors of cerebral ischemia and ischemic heart diseases: similarities and differences. *Current cardiology reviews,* **6,** 138-149.

Stern, M. K., Jensen, M. P. and Kramer, K. (1996) Peroxynitrite Decomposition Catalysts. *Journal of the American Chemical Society,* **118,** 8735-8736.

Suh, S. W., Shin, B. S., Ma, H., Van Hoecke, M., Brennan, A. M., Yenari, M. A. and Swanson, R. A. (2008) Glucose and NADPH oxidase drive neuronal superoxide formation in stroke. *Ann Neurol,* **64,** 654-663.

Szabo, C., Ischiropoulos, H. and Radi, R. (2007) Peroxynitrite: biochemistry, pathophysiology and development of therapeutics. *Nat Rev Drug Discov,* **6,** 662-680.

Tajes, M., Ill-Raga, G., Palomer, E. et al. (2013) Nitro-oxidative stress after neuronal ischemia induces protein nitrotyrosination and cell death. *Oxid Med Cell Longev,* **2013,** 826143.

Tang, X. N., Cairns, B., Kim, J. Y. and Yenari, M. A. (2012) NADPH oxidase in stroke and cerebrovascular disease. *Neurol Res,* **34,** 338-345.

Thiyagarajan, M., Kaul, C. L. and Sharma, S. S. (2004) Neuroprotective efficacy and therapeutic time window of peroxynitrite decomposition catalysts in focal cerebral ischemia in rats. *Br J Pharmacol,* **142,** 899-911.

Toda, N., Ayajiki, K. and Okamura, T. (2009) Cerebral blood flow regulation by nitric oxide: recent advances. *Pharmacol Rev,* **61,** 62-97.

Trifiletti, R. R. (1992) Neuroprotective effects of NG-nitro-L-arginine in focal stroke in the 7-day old rat. *Eur J Pharmacol,* **218,** 197-198.

Uttara, B., Singh, A. V., Zamboni, P. and Mahajan, R. T. (2009) Oxidative stress and neurodegenerative diseases: a review of upstream and downstream antioxidant therapeutic options. *Current neuropharmacology,* **7,** 65-74.

White, C. R., Darley-Usmar, V., Berrington, W. R., McAdams, M., Gore, J. Z., Thompson, J. A., Parks, D. A., Tarpey, M. M. and Freeman, B. A. (1996) Circulating plasma xanthine oxidase contributes to vascular dysfunction in hypercholesterolemic rabbits. *Proceedings of the National Academy of Sciences of the United States of America,* **93,** 8745-8749.

Willmot, M., Gibson, C., Gray, L., Murphy, S. and Bath, P. (2005) Nitric oxide synthase inhibitors in experimental ischemic stroke and their effects on infarct size and cerebral blood flow: a systematic review. *Free radical biology & medicine,* **39,** 412-425.

Xie, Z., Wei, M., Morgan, T. E., Fabrizio, P., Han, D., Finch, C. E. and Longo, V. D. (2002) Peroxynitrite mediates neurotoxicity of amyloid beta-peptide1-42- and lipopolysaccharide-activated microglia. *The Journal of neuroscience : the official journal of the Society for Neuroscience,* **22,** 3484-3492.

Xiong, Y., Rabchevsky, A. G. and Hall, E. D. (2007) Role of peroxynitrite in secondary oxidative damage after spinal cord injury. *Journal of neurochemistry,* **100,** 639-649.

Zhang, L., Deng, T., Sun, Y., Liu, K., Yang, Y. and Zheng, X. (2008) Role for nitric oxide in permeability of hippocampal neuronal hemichannels during oxygen glucose deprivation. *Journal of neuroscience research,* **86,** 2281-2291.

Zhang, Z. G., Chopp, M., Bailey, F. and Malinski, T. (1995) Nitric oxide changes in the rat brain after transient middle cerebral artery occlusion. *J Neurol Sci,* **128,** 22-27.

Zielonka, J., Sikora, A., Joseph, J. and Kalyanaraman, B. (2010) Peroxynitrite is the major species formed from different flux ratios of co-generated nitric oxide and superoxide: direct reaction with boronate-based fluorescent probe. *The Journal of biological chemistry,* **285,** 14210-14216.

Chapter 5: General conclusion

Cardiovascular accidents characterized by ischemia/reperfusion (I/R) injury such as stroke and, cardiac arrest pose severe medical complications. Mammals capable of hibernation represents a robust example of tolerance to I/R injury that is unmatched by any other model of ischemia tolerance. Obligate hibernators such as arctic ground squirrel may hold insight into possible interventions to ameliorate disorders characterized by I/R injury. To date, researchers have explored several factors associated with hibernation such as hypothermia, hypometabolism, high base excess that might contribute to I/R tolerance in hibernating animals. However, in the whole animal model, it is difficult to isolate neuroprotective factors at the tissue level that provides tolerance to I/R injury.

Through this thesis work, I have demonstrated that a microperfusion approach provides better temporal resolution of I/R injury that leads to decipher the complex interactions of glutamate-mediated excitotoxicity with acidosis-mediated acidotoxicity and to understand the role of acid-sensing ion channels (ASIC1a) and pH in mediating cellular injury during ischemia. In addition, the thesis demonstrates that hibernation season or state is not essential for resistance to ischemic injury in AGS. Rather, resistance is associated with reduced susceptibility to highly reactive $ONOO^-$ generated during I/R injury.

Herein, in chapter 2, I validate a novel *in vitro* microperfusion approach to study I/R injury and demonstrate that oxygen glucose deprivation (OGD) injury modeled in rat acute hippocampal slice mimics *in vivo* I/R conditions such as ATP depletion and the overflow of neurotransmitters and neuromodulators such as glutamate, aspartate and adenosine. This approach also validates that injury associated with low pH or OGD occurs

during the insult phase and not during the reperfusion phase which is not possible to decipher *in vivo*. Under *in vivo* cerebral I/R, as the multiple events occur concomitantly, it is not possible to evaluate the role of each component of the ischemic cascade and their interaction during the event of I/R injury. Traditional *in vitro* slice preparations do not produce the same changes in the extracellular milieu as what occurs *in vivo* because of rapid washing with a highly-diluted bath solution. In the present study, the microperfusion approach provides a better tool for monitoring temporal resolution of injury as well as the overflow of metabolites and neurotransmitters and allows for manipulation of each component of the ischemic cascade to better understand interaction during I/R injury.

During a stroke or cardiac arrest, tissue acidosis (low pH) and excitotoxicity (glutamate receptor-mediated cell death), both occur concomitantly. However, in the whole animal model, it has not been possible to separate the effects of low pH from glutamate mediated excitotoxicity. In chapter 2, I, therefore, investigated the effect of acidosis on glutamate-mediated excitotoxicity in acute hippocampal slices to resolve the controversy regarding the relative importance of acidotoxicity and NMDAR mediated excitotoxicity. Using a novel microperfusion technique, I separated the effects of pH and oxygen glucose deprivation and showed that injury caused by oxygen glucose deprivation without low pH is caused by stimulation of NMDA glutamate receptors. However, when low pH was added to the insult, as would occur during a stroke or cardiac arrest, low pH abolished the injury caused by stimulation of glutamate receptors but produced its own type of injury. Furthermore, I show that damage resulting from low pH was due to activation of acid sensing ion channels (type 1a). These findings argue that activation of acid sensing ion channels produce brain injury during cerebral I/R and help to explain

why clinical trials using drugs that block glutamate NMDA receptors failed to protect stroke patients.

In chapter 3, I show that tolerance persists in AGS hippocampal slices obtained from summer and winter (hibernating and interbout arousal) animals subjected to OGD at 36°C. This reflects that tolerance persists independently of the hibernation season or state as well as cold tissue temperature. This suggests that AGS exhibit tolerance at the tissue level and may be unique compared to other hibernating species in the lack of seasonal dependence on ischemic tolerance. Moreover, AGS are highly tolerant to OGD compared to ischemic susceptible Sprague-Dawley rat despite the loss of ATP, excitatory amino acid release, and acidosis and persists during conditions that mimic acidosis and ischemic shift characteristics of cerebral I/R injury. Taken together, this study suggests that tolerance to I/R injury in AGS resides downstream of or is independent of glutamate release.

Oxidative and nitrative stress has long been associated with I/R injury. Chapter 4, shows for the first time that at the tissue level, during modeled ischemia in rat hippocampus, injury is caused by peroxynitrite ($ONOO^-$) that requires both nitric oxide (NO) and superoxide ($O_2^{\bullet -}$); neither species was injurious alone, but both exacerbated injury caused by oxygen glucose deprivation. My data suggest that the injury is due to the combination of NO and $O_2^{\bullet -}$ together forming $ONOO^-$ leading to cell death. This work identifies for the first time a mechanism that is absent in the I/R cascade that can explain resistance to injury in the arctic ground squirrel and will provide novel avenues for translating protection from $ONOO^-$ injury in humans.

Unlike mammalian hibernators, humans suffer consequences in response to limited blood flow where they experience significant injury in response to ischemia and reperfusion. Currently, much is known about these mechanisms, however, no therapeutic has emerged from this understanding. A clear understanding of the degree of ischemia tolerance hibernating animals display opens the door for further in depth mechanistic studies. A better understanding of regulatory mechanisms will guide discovery of therapeutics designed to mimic natural means of ischemia tolerance.

Appendices

Appendix A 1: IACUC approval letter for research protocol

(907) 474-7800
(907) 474-5993 fax
fyiacuc@uaf.edu
www.uaf.edu/iacuc

Institutional Animal Care and Use Committee
909 N Koyukuk Dr. Suite 212, P.O. Box 757270, Fairbanks, Alaska 99775-7270

April 15, 2013

To: Kelly Drew, PhD
Principal Investigator

From: University of Alaska Fairbanks IACUC

Re: [443309-2] Ischemia Resistance

The IACUC reviewed and approved the Revision referenced above by Designated Member Review.

Received:	March 27, 2013
Approval Date:	April 15, 2013
Initial Approval Date:	April 15, 2013
Expiration Date:	April 15, 2014

This action is included on the April 18, 2013 IACUC Agenda.

Applicant was asked to:

1. In the Objectives section, please state why additional slices are needed based on previous work.

-The objectives are now clarified, justifying the additinal work.

2. Specify the needle gauge for heart puncture.

-21-25 ga 1 to 1.5 inch needles are now specified, and appear appropriate for cardiac puncture in animals to be euthanized.

PI responsibilities:

- *Acquire and maintain all necessary permits and permissions prior to beginning work on this protocol. Failure to obtain or maintain valid permits is considered a violation of an IACUC protocol and could result in revocation of IACUC approval.*
- *Ensure the protocol is up-to-date and submit modifications to the IACUC when necessary (see form 006 "Significant changes requiring IACUC review" in the IRBNet Forms and Templates)*
- *Inform research personnel that only activities described in the approved IACUC protocol can be performed. Ensure personnel have been appropriately trained to perform their duties.*
- *Be aware of status of other packages in IRBNet; this approval only applies to this package and the documents it contains; it does not imply approval for other revisions or renewals you may have submitted to the IACUC previously.*

Appendix A 2: Neuroglobin expression in Arctic ground squirrel

Western blots were performed to compare the expression of Ngb in cortex and hippocampus of Rats and AGS. Results showed that in the cortex, Ngb expression in AGS is higher as compared to rat (n=6, $p<0.003$); cortex of winter AGS (wAGS) shows higher level of Ngb expression than summer AGS (sAGS) (n=4, $p<0.0045$); no significant difference in Ngb expression in hippocampus of winter AGS versus summer AGS (n=6, $p<0.24$).

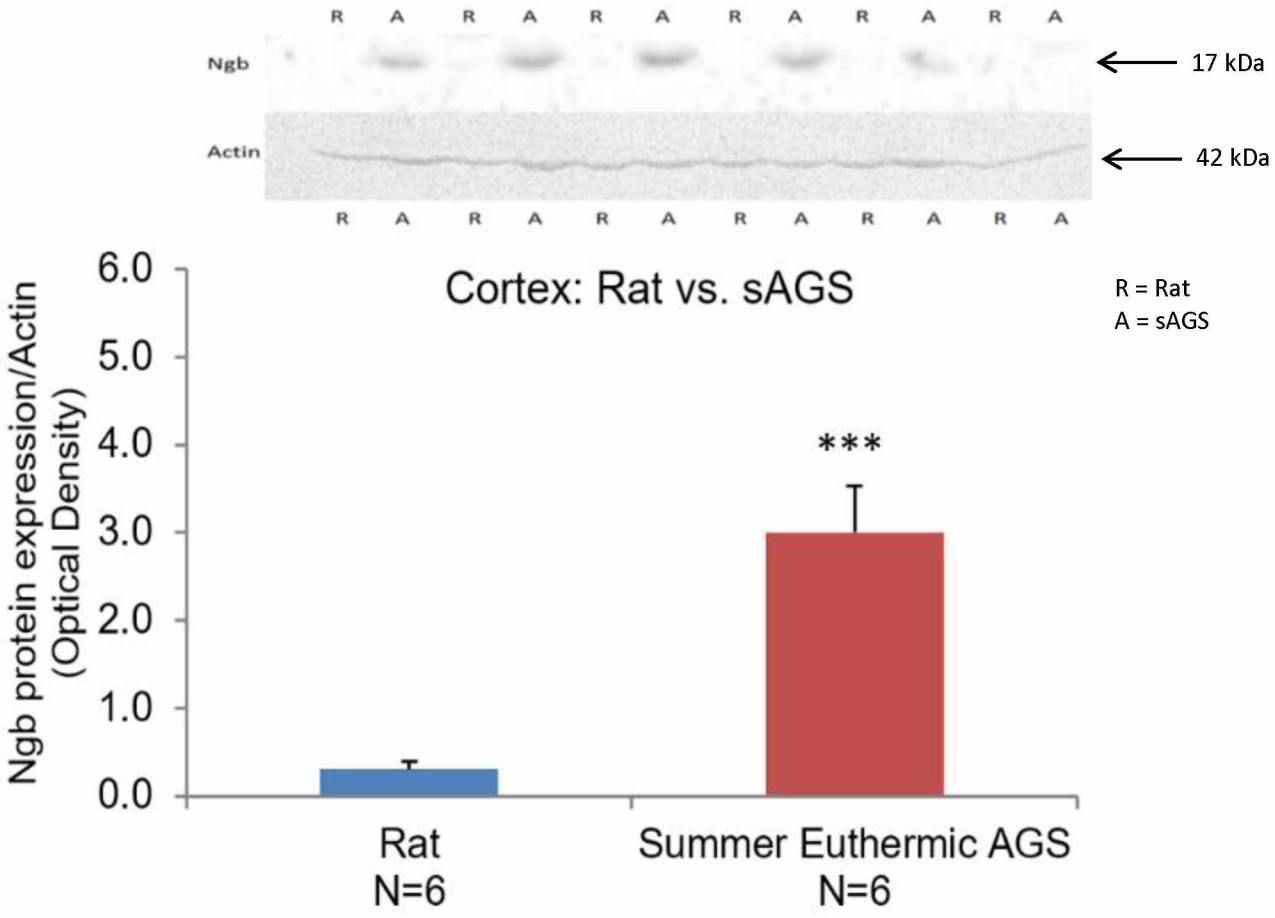

Figure A1. Ratio of Ngb density to actin is significantly greater in cortex of sAGS versus Rat ($P<0.0003$). Ngb antibody (FL-151): sc-30144 (Santa Cruz Biotechnology).

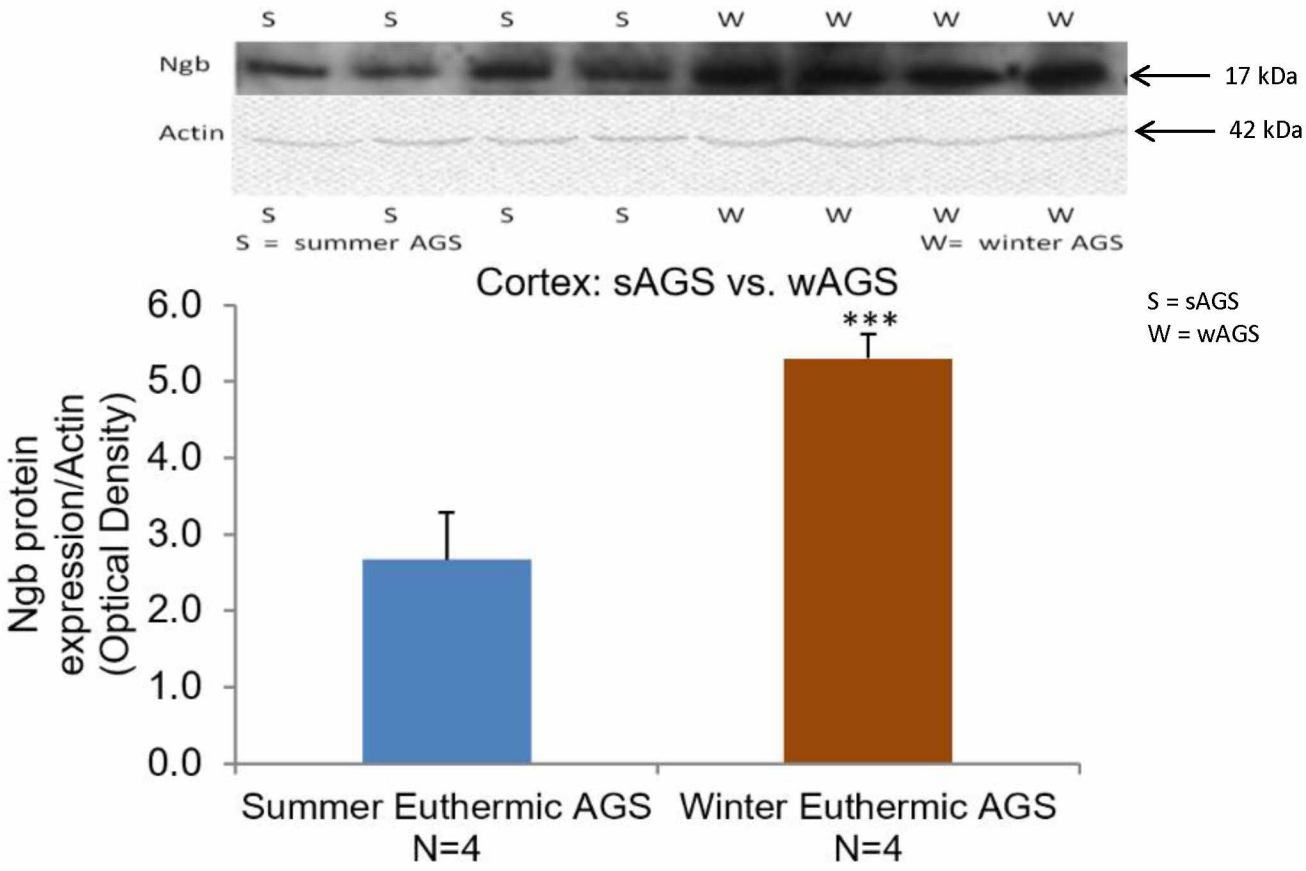

Figure A2. Ratio of Ngb density to actin is significantly greater in cortex of wAGS versus summer euthermic AGS ($P<0.0045$). Ngb antibody (FL-151): sc-30144 (Santa Cruz Biotechnology)

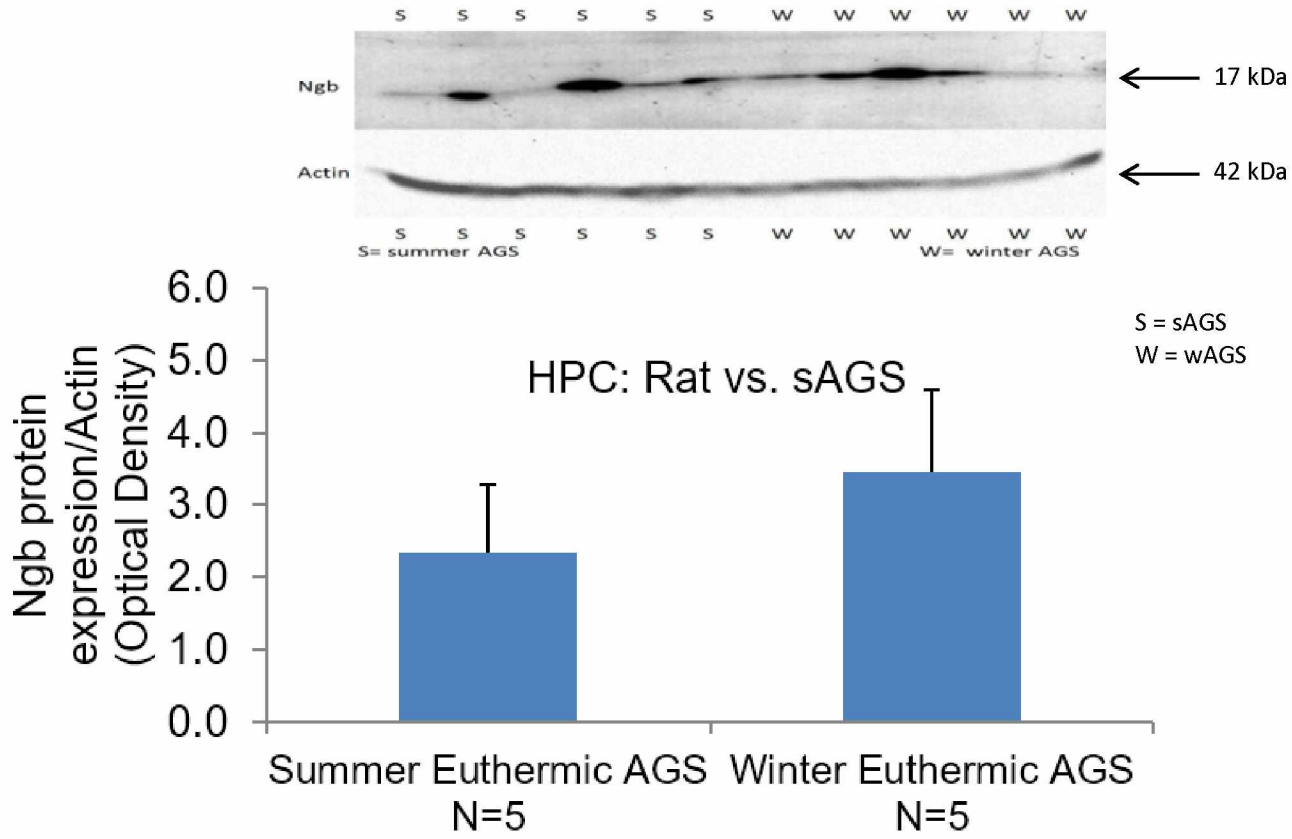

Figure A3. No significant difference in Ngb in hippocampus of summer euthermic AGS versus winter AGS ($P<0.24$). Ngb antibody (FL-151): sc-30144 (Santa Cruz Biotechnology)

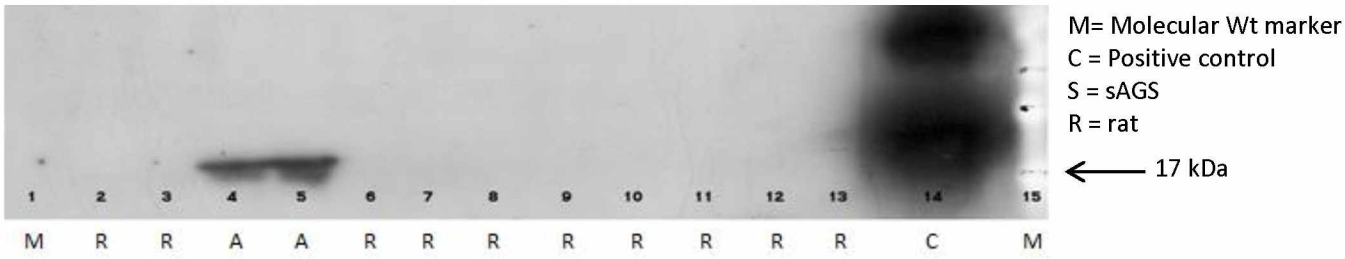

Figure A4. Validation of Ngb in AGS using Anti-Ngb [13C8]- Azide free (ab37258) Antibody.

Conclusion: The objective of the research is to identify the role and mechanism of Ngb in increasing resistance to cerebral I/R injury by using a natural model of high tolerance to ischemia. Results show that ischemic tolerant species, AGS constitutively express high Ngb level as compared to susceptible species, rats. However, I could not proceed with the experiments to decipher the role of Ngb in ischemia tolerance in AGS because the antibody (sc-30144) was discontinued. Another antibody 13c8-Azide free (ab37258) from Abcam showed bands at 17 kDa, but positive control produced two large bands and experts in the field questioned the specificity of this antibody. I did not have resources to validate specificity so did not pursue further investigation of Ngb.

Appendix A 3: Western blot protocol

I. Assembling Plate:

1. Wash and clean the plates with 70% ethanol and with detergent if needed.
2. Place into casting tray in upwards direction and close the notch.
3. Add distilled water to check leakage for 10 Sec.
4. Pour off the water and wipe at the corner by Kim wipe or by using a vacuum pipette.
5. Mark 1cm below comb = height of separating gel (a scale with mark is already there)

II. Preparation and pouring of gel:

1. Separating gel/ Resolving gel:

a. While assembling the plate, take the acrylamide out of the fridge and let it warm up. Also, get an aliquot of APS from the freeze and let it thaw.

b. Recipe for gels with different % acrylamide is listed in reagent section. Add the reagent in the ordered list.

c. Pour the separating gel mix using a pipet between the plates up to the mark plus some to allow for shrinkage. Touching the pipet to the back plate will ensure smooth pouring and avoid bubbles.

d. Using a pasteur pipette, gently but quickly overlay the acrylamide mix with ~ 0.5-1 ml of isopropanol.

e. Allow it to solidify for 15- 20 Min. and check by looking at the remaining gel in the tube. N.B. Keep the cap open.

f. Once the gel is polymerized, rinse the isopropanol gently with milliQ H20 using a P-200 tip attached to the suction tube and ensure all the isopropanol is removed.

2. Stacking gel:

a. While separating gel is solidifying, make 4.5% stacking gel in a 50ml centrifuge tube. Combine all reagents for stacking gel in the order the ordered list except APS and TEMED.
b. Find the appropriate comb to make the wells for the gel and rinse it off.
c. Pour the gel and quickly insert the comb, trying not to get any bubble beneath the comb. It is OK if extra acrylamide spills over the edge. Do this on a paper towel. Work quickly because the stacking gel will polymerize within a few minutes.
d. Wait 10 Min. for the gel to solidify and check by looking at the remaining gel in the tube. N.B. Keep the cap open.

III. Preparing sample: (Sample + sample buffer + dH2O)

1. While the stacking gel is polymerizing, turn on the boiling water bath.
2. Thaw the sample if previously frozen.
3. Make up gel standards (same volume of sample buffer + 1 µl of either high or low unstained MW standards).
4. Boil all samples for 5 minutes. Do not boil positive control -- 30 sec only.
5. Let samples cool for a minute, and then do quick spin in centrifuge to get liquid to bottom of tube.

IV. Setting up Gels and Loading samples

1. Wipe the plates and load onto the electrophoresis unit along with the Dam Plate or 2nd plate, if available, by holding the plates down and clamping it.
2. Pour 1X running buffer into upper and lower (just above lower screws) chambers

3. Carefully remove comb, running buffer will flow into wells and rinse out unpolymerized acrylamide.
4. Using a pasteur pipette and gel loading tip, get rid of any air bubble and unpolymerized acrylamide inside the well.
5. Load the samples using P-200 and gel loading tips. Place the tip close to the bottom of the well. the sample is denser the running buffer and will sink to the bottom of the well. Be careful not to expel a big air bubble at the end and avoid forcing sample out of the well.
6. When all samples are loaded, place the cover on the gel box.
7. Turn ON the power supply.

V. Gel Running Conditions: (Choose one of the following)

1. Run sample into gel at 100V, then turn upto 150 if hooked to a cooling system. Check to make sure samples are running down. At 150 V, running takes about 1-1/4 hours

2. For overnight, run at 20-30 V. In the morning, turn up the power to 200 V for a while to refocus the bands.

Gel running continued.....

a. Run gel until dye front is near the bottom
b. Turn off the power supply
c. Place the gel box in a pan and remove the connection to the water circulation.
d. Undo the clamps and remove the gel plates
e. Using a spacer, pry apart the plates. the gel should stick to one plate or the other. keeping gels on shorter plate gives membrane orientation with broad standard on left.
f. Gently remove the stacking gel using the spacer.
g. If you are going to dry the gel, place the gel into Coomassie blue stain. If you are going to do a transfer, you should have already set up the transfer cassette.
h. Turn the plate upside down over the transfer cassette, prod the gel with the spacer and let it fall into the buffer.

VI. Mini-gel transfers to nitrocellulose:

1. While gel is running:

a. Make sure there is enough transfer buffer or make more.
b. Get pan for assembling sandwich and rinse with distilled water.
c. Get transfer box, cassettes, sponges and rinse with distilled water.
d. Get filter forceps and rinse.
e. Cut 4 pieces of 3MM filter paper per gel to 6 x 9 cm
f. Cut nitrocellulose to 5.5 x 8 cm. Equilibrate in transfer buffer for 30 min before transfer.

2. Assemble sandwich - wear gloves!

a. Take the transfer cassette and arrange in the following order....

Black Side < Sponges < Filter Paper < Gel || Membrane > Filter Paper > Sponges > Transparent Side.

b. Place gel on 3MM filter paper. Gel should be placed down so that blot comes out with same orientation as loaded. Smooth out with fingers.

c. Label upper right hand side of nitrocellulose to maintain orientation. Use forceps to place nitrocellulose on gel. Run spacer over it to get rid of bubbles.

d. Close cassette and put in transfer box with black side of cassette facing the black side of the transfer box insert.

e. Put white plastic insert with ice into transfer box.

f. Fill transfer box with transfer buffer.

3. Transfer parameters:

a. Run at 70 volts for 75 min. Starting current =190 mA for 2 gels. Equipment can also be set to run by amps. Check to make sure current is flowing.

b. To transfer overnight, run at 20-30 V. Omit ice insert.

c. Take out the cast and look for the ladder.

VII. Protein Identification:

1. Take the blocking buffer (5%milk/ TBS) in a box and incubate the membrane in it for 1 Hr. at room temperature on orbital shaker.
2. Pour off the blocking buffer and incubate the membrane with primary antibody overnight at 4^0C.
3. Remove the primary antibody by pipette and micro syringe and keep in the original tube for future use.
4. Rinse with TBS-Tween (TBST) .....X 2.

5. Wash with TBST.....X 4, 15 min each (shaker).
6. Incubate with secondary antibody at room temperature for 1Hr. in shaker.
7. Rinse with TBS-Tween (TBST) .....X 2.
8. Wash with TBST.....X 4, 15 min each (shaker).
9. Discard the washing buffer and add chemiluminescense Compound for HRP by spraying enough to cover the membrane.
10. Take the membrane out, wipe off the extra substrate by wrapping in Kimwipe, and wrap in a plastic film.
11. Take the autoradiography cassette, stick a ruler to it, and charge it by keeping in light.
12. Put the membrane on one corner of the autoradiography cassette by sticking to a tape and take to dark room for development along with the films.
13. In the dark room activate the machine first and keep the film in the autoradiography cassette for varying periods of time and develop the autoradiograph.
14. A molecular marker (Biorad Precision Plus Protein™ Kaleidoscope™ Prestained Protein Standards) and positive control (Ab63278) is used to determine the molecular weight of the target protein (Ngb).

Appendix A 4: Acute slice preparation and microperfusion procedure

1. Identify animal to be used – Rat #_____
2. Calibrate **pH meter** using fresh standards.
3. Prepare **1 L HEPES-aCSF*,** bubble vigorously with 95% O_2/5%CO_2 at RT until pH is 7.3-7.4, at least 30 minutes.
4. Turn on one **hot water bath** to 36˚C.
5. Prepare **2 L aCSF*** to fill microperfusion water bath. Bubble vigorously with 95% O_2/5%CO_2 at 36˚C.
6. Prepare **100 mL aCSF * and 100 mL low pH aCSF***. Filter, bubble vigorously with 95% O_2/5%CO_2 at 36˚C. Record pH when stable.
7. Prepare **100 mL OGD ***. Filter, bubble vigorously with 95% N_2/5%CO_2 at 36˚C. Record pH when stable.
8. Turn on **cooling bath for vibratome** (-7.7˚C).
9. Set up for **dissection**. Prepare slice chamber for Hepes recovery at RT, bubble with 95%O_2/5%CO_2.
10. Prepare 2 ml **homogenization buffer****.
11. Pour Hepes-aCSF into vibratome bath (add blade!), beaker for brain rinse, and petri dish for hippocampus. Allow to **cool for 30 minutes**.
12. Set up oxygen electrode. Calibrate using dH_2O for gain, dH_2O+sodium dithionite for zero. Keep in dH_2O at RT.
13. Weigh out 1.25g **Agar**, add 50ml of HEPES-aCSF. Add stir bar, place in water on hot plate and cover with foil. Start hot plate at setting 4 and stir when vibratome bath is at 3˚C.

14. When vibratome bath temperature reaches 2˚C, **anaesthetize animal** with Isoflurane. Weigh animal and record body/temporalis temperatures.
15. Decapitate animal. **Extract brain** on ice, place in cold HEPES-aCSF for 40 seconds.
16. Pour heated agar into a Petri dish.
17. Dissect brain on ice. Place 1 **hippocampus** in a covered Petri dish with cold HEPES-aCSF while agar cools to 40˚C.
18. **Embed one hippocampus in agar**, lined up, cool on ice until agar solidifies. Cut agar/hippocampus block to mount on vibratome block with tissue adhesive. Adjust Hepes-aCSF volume in vibratome. Adjust bubbling in vibratome and slice chambers. Slice 400um thick sections at speed setting 6, amplitude max (10).
19. Remove agar from slices and transfer slices to RT **Hepes brain slice chamber**.
20. Allow slices to **recover for 1 hour 20 min at RT**, bubbling continually.
21. Transfer and load the slices into micro perfusion chambers for treatment

*** Solutions**

Add to Graduated Cylinder	100 mL Low-pH OGD	100 mL Low-pH aCSF	100 mL aCSF	2L aCSF For LDH	1 L HEPES-aCSF (on ice)
Milli-Q H2O	~80 mL	~80 mL	~80 mL	1600 ml	~800 ml
Buffer	10 mL 10X low pH aCSF	10 mL 10X low pH aCSF	10 ml 10xaCSF	200 ml 10x aCSF	100 ml 10x Hepes
0.5M CaCl2	360 ul	360 ul	360 ul	7.2 ml	4 ml
100X (anhydrous 2.4M MgSO4)	1 ml	1 ml	1 ml	20 ml	
100X Dextrose		1 ml	1 ml	20 ml	10 ml
QS to final volume:	100 ml	100 mL	100 mL	2 L	1 L

****Homogenization Buffer Recipe (*keep on ice*):**

Preliminary Buffer	Volume	2xVolume
1% NP-40 Lysis Buffer	958 ul	2*958 ul
PMSF	10 ul	20 ul
Orthovanadate	10 ul	20 ul
Leupeptin	10 ul	20 ul
B-glycerolphosphate	10 ul	20 ul
Aprotinin	1 ul	2 ul
Antipain	1 ul	2 ul

aCSF Normoxia pH (7.4) solution

Compound	FWt	wt for 500ml of 10x aCSF	Final 10X concentration(M)
NaCl	58.44	35.05 g	1.20
$NaHCO_3$	84.01	19.20 g	0.4570
KCl	74.55	1.23 g	0.033
NaH_2P0_4-H_2O	138	830 mg	0.012

HEPES buffer aCSF

Compound	FWt	g for 500 mL of 10x HEPES	g for 2L of 5x HEPES	Final working concentration(mM)
NaCl	58.44	35.06	70.12	120
$NaHCO_3$	84.01	8.40	16.8	20
HEPES acid	238.3	7.96	15.92	6.68
HEPES salt	260.3	4.29	8.58	3.30
KCl	74.55	1.86	3.72	5.00
Anhydrous $MgSO_4$	120.30	1.20	2.40	2.00

Other stock solutions used

Compound (Final concentration)	Grams/volume
MgSO4 *anhydrous* (2.4 M)	2.96g/100ml
$CaCl2{\cdot}2H_20$ (0.5 M)	7.35g/100ml
Glucose (1.0 M)	18.02/100ml